



Technical University of Crete

School of Mineral Resources

Miscible Flooding Simulation Feasibility Study for the Libyan Oil

Reservoir Sarir Oil Field

Master of Science Thesis

By:

Hassan A Hashem Mohamed

Supervisor:

Professor Nikolaos Varotsis

CHANIA – GREECE

March 2018

ACKNOWLEDGEMENT

First and foremost I offer my sincerest gratitude to my supervisor, **Professor Nikolaos Varotsis**, who has supported me throughout my thesis with his patience and knowledge whilst allowing me the room to work in my own way. I attribute the level of my Master degree to his encouragement and effort and without him this thesis would not have been completed or written. One simply could not wish for a better or friendlier supervisor.

I am deeply indebted to **Dr. Gaganis Vasileios** without his guidance, support and good nature; I would never have been able to finish this work.

I would also like to thank all the professors and staff members of the MSc Petroleum Engineering program for their unrelenting attitude to teach, inspire and mold students to be able to succeed in the petroleum industry and various aspects of life. It was such a great honor to be taught by **Professor Pasadakis, Dr. Marinakis, Dr. Kourounis Dr. Maravelis, Mr. Skerletis** and all the people from the industry who came to provide us with expertise knowledge and of course friends and classmates for their care and support.

I am also hugely appreciative to **Dr. Adel Elzwi** for his effort in collecting the data and getting it to me so quickly to use it as part of my thesis and for being so dedicated to his role as my external supervisor.

I also want to thank **Dr. Yasin Ellabad** and **Mr. Abduladim Wanis** for their help and support during writing up my thesis.

And finally, special and profound thanks to: 1) My brother **Dr. Atef A Hahem** who offered invaluable support and humor during my studies ; 2) My mother (**Gamila**) who constantly reminded me and demonstrated that all I had to do was say the word and she would be here, if for nothing else than to just make me a dinner ; 3) my father (**Abdulrahman**) who helped me find the strength to finish my studies here and helped me come to the decision, once and for all, that obtaining this degree would not be the first challenge in my life that I would not rise to meet and ; 4) The rest of my family. Words can't express how much I love you all and how grateful I am for your support. Without you I most certainly would not be where I am today.

ABSTRACT

This work aims to study whether CO₂ Miscible flooding could enhance the oil recovery in Sarir oil Field. The Peng-Robinson equation is tuned and validated against experimental data. The PVT data that was used in the study includes compositional analysis, differential liberation test data, constant composition expansion test data, separator test data and viscosity data. The Actions that have been taken to build a reliable EOS are as the following:

1. An EoS model was tuned against the PVT data. Several approaches were tried until the best possible match was achieved....., etc
2. The Miscibility option of the Winprop software was tried
3. The slim tube option of the PVTP software was tried
4. The 1-D reservoir model was built using the Reveal simulator

The critical properties of the heavy end PC, T_c, AC, MW+ volume of shift and K_{ij} values between methane CH₄ and heavy ends were the best candidates for tuning the developed Eos models against experimental data.

Cell to cell simulation calculation was performed to asses and estimate the minimum miscibility pressure by using the EOS and these results were compared against actual experimental value of MMP. The results have shown that the CO₂ is immiscible with Sarir Oil at reservoir condition 225F and 3300Psig. The MMP was estimated to be at 5047 Psig with an error of 37% from the experimental value. The Slim tube option in PVTP has shown unrealistic results therefore this option has been evaluated in terms of both limitations and accuracies. This has been done by building 1-D slimtube model using Reveal.

The simulation of the slimtube experiment using 1-D model has been developed to validate the laboratory experiment and used EOS as well as to investigate the possibility of serving as a fast and reliable tool for MMP determination. Sensitivity analyses were performed by testing different grid block sizes (a different number of cells). A model with 150 cells has been chosen as the optimum model. The results of slim tube model has shown a comparable results with lab experiment results for both minimum miscibility pressure MMP calculation and Oil Recovery Where the marginal Error between the two data was about 9% for the MMP and 2% for Oil Recovery .

Περίληψη

Ο ταμειυτήρας Sarir της Λιβύης με το σχετικά ελαφρύ πετρέλαιο που περιέχει και την έντονα παραφινική του σύσταση διαθέτει ενδεχομένως τις προϋποθέσεις για επιτυχή εφαρμογή της μεθόδου έγχυσης CO₂ υπό υψηλή πίεση για την μεγιστοποίηση της αποληψιμότητας του αν θα μπορούσε να επιτευχθεί πλήρης αναμειξιμότητα του αερίου με το πετρέλαιο. Θα χρησιμοποιηθούν τα εργαστηριακά δεδομένα PVT του ταμειυτήρα αυτού καθώς και τα διαθέσιμα θεωρητικά εργαλεία προσομοίωσης για να εκτιμηθεί κατά πόσον εμφανίζεται πιθανή η επίτευξη πλήρους αναμειξιμότητας. Στόχος της εργασίας είναι να αναδείξει τυχόν διαφορές στα αποτελέσματα των διαφόρων προσεγγίσεων και να επιχειρηθεί η ερμηνεία και ο σχολιασμός τους.

Table of Contents

ACKNOWLEDGEMENT	3
ABSTRACT.....	4
List of Figures	10
List of Tables	13
Nomenclature.....	14
1.1 Enhanced Oil Recovery (EOR).....	17
1.2 Introduction	17
1.2.1 Definition of EOR.....	17
1.3 Classification of Enhanced Oil Recovery (EOR) Methods.....	17
1.3.1 Thermal	17
1.3.2 Chemical	18
1.3.3 Miscible or Solvent Injection.....	18
Hydrocarbon Miscible Injection	18
Carbon Dioxide Injection	18
Nitrogen and Flue Gas Injection.....	18
1.4 General EOR Screening Criteria	19
1.5 Miscible Displacement Processes	20
1.5.1 Introduction.....	20
1.5.2 History.....	20
1.6 Screening Criteria Ranges for CO ₂ Miscible Projects.....	22
1.7 The Potential of Unconventional Oil Reservoir in Libya (Shale Oil).....	23
1.8 The CO ₂ is the future candidate for Shale Oil.....	25
1.8.1 Some Considerations of Using the CO ₂ in Unconventional Reservoirs	26
1.9 Some Selective Successful Miscible Gas and CO ₂ Injection Projects	28
1.9.1 Miscible Gas Injection in Rhourde El Krouf Field, Algeria.....	28
1.9.2 Miscible Gas Injection in a Mature U.K. North Sea Field.....	28
1.9.3 Miscible Gas Injection in Harweel Field Oman.	28
1.9.4 CO ₂ Injection in Rumaita Field, UAE.....	29
1.9.5 Immiscible-CO ₂ Injection in Bati Raman Field, Turkey.....	29
2. Literature Review	30

2.1	General Description of Miscible Displacement	30
2.2	Miscible Displacement.....	32
2.3	Principles of Phase Behavior Related to Miscibility.....	33
2.3.1	Phase Rule.....	33
2.3.2	Pressure/Temperature Diagram for Two-Component System.....	34
2.3.3	Pressure/Composition Diagram “P-X” for Binary Systems	37
2.4	Principle of Using Ternary Diagram.....	40
2.4.1	Hypothetical System with Three Components	40
2.4.2	Multi Components System (Pseudo-ternary Diagram).....	42
2.5	Miscible Gas Injection Mechanisms	44
2.5.1	First Contact Miscibility (FCM) Process.....	44
2.5.2	Minimum Miscibility pressure (MMP).....	46
2.6	MCM processes.....	46
2.6.1	Vaporizing Gas (Lean Gas) Displacement	47
2.6.2	Condensing gas drive (or enriched gas drive).....	50
2.6.3	Critical Displacement (stair-stepping)	52
2.6.4	CO2 Miscible displacement processes.....	53
2.7	Summary of the Classification of Solvent Displacement.....	59
2.8	Methods of Assessing and Evaluating Miscible Gas Injection Projects	60
2.9	Solvent Phase Behavior Experiments	60
2.9.1	Single Contact.....	60
2.9.2	Multiple Contact Experiment.....	60
2.9.3	Swelling Test	63
2.9.4	CO2 Core Floods	63
2.9.5	Slim-tube experiment.....	65
2.9.6	Rising Bubble Apparatus (RBA)	67
2.10	Simulation (Mathematical Modeling)	69
2.11	The Equation of State (EOS).....	70
2.12	Simulation Methods for Assessing Gas Injection Processes.....	71
3.	PVT Modeling.....	73
3.1	Sarir Field: A Proposed CO2 Injection Site.....	73

3.1.1	Description	73
3.1.2	Location	74
3.1.3	Reservoir and Production Data	75
3.2	Purpose of The Gas Injection Feasibility Study	76
3.3	Methodology of the Present Study	76
3.3.1	CMG (winprop)Program.....	76
3.3.2	Petroleum Expert (PETEX) (PVTP).....	77
3.3.3	Reveal	77
3.4	Equation of State Generation	77
3.4.1	Base Model C7+	78
3.4.2	Splitting the EOS C7+ Fraction into EOS C31+	78
3.4.3	Lumping of EOS C31+ into EOS15	82
3.5	The Results of the Tuned EOS Models.....	86
3.5.1	EOSC7+ Model.....	87
3.5.2	EOS C31+ Model.....	89
3.5.3	The lumped EOS C15	91
3.6	Multiple Contact Miscibility Calculation (Cell to cell simulation)	94
3.6.1	Methodology.....	95
3.7	Multiple Contacts Miscibility Results.....	99
3.7.1	EOS C7+	99
4.	Slimtube Simulation	103
4.1	Simulating Slim-Tube Experiment Using Slimtube Calculation Option in PVTP.....	103
4.2	Methodology	103
4.3	Simulation Results.....	104
4.3.1	Case 1: Conducting slim- tube simulation using 100% CO2 solvent.....	104
4.3.2	Case 2: Conducting Slim-tube Simulation Using Separator Gas.....	105
4.3.3	Case 3: Conducting Slimtube Simulation Using 100% CO2 for Light Oil ...	107
5.	1-D Slimtube Simulation Model.....	110
5.1	Building 1-D Slimtube Model by Using Reveal	110
5.2	Steps Followed to Build the 1-D model.....	111
5.3	1-D Model Simulation Results.....	116

5.3.1	Miscibility Investigation at Pressure of 3300 psig.....	117
5.3.2	Miscibility Investigation at Pressure of 4010Psig	121
5.3.3	Comparison of the Estimation of MMP Using Two Different Methods	123
6.	Conclusion and Discussion.....	125
6.1	Equation of state Model	125
6.2	Minimum Miscibility Pressure MMP Calculation	127
6.3	The 1-D Slimube Simulation Model	130
	Recommendation	132
	References.....	132
	Appendix A:(Sarir Oil Field Data)	137
	Appendix B: (PVT Data)	139
	Appendix C: (Slim-Tube Data).....	143
	Appendix D:(EOSs Tuning Results).....	147
	Appendix E	153

List of Figures

FIGURE 1.1: OIL RECOVERY CLASSIFICATIONS (ADAPTED FROM THE OIL AND GAS JOURNAL..	19
FIGURE 1.2: NUMBER OF FIELD MISCIBLE SLUG DRIVES INITIATED BETWEEN A PERIOD OF ...	22
FIGURE 1.3: EOG’S PREDICTION FOR HOW GAS INJECTION EOR WILL INCREASE OUTPUT.....	25
FIGURE 1.4: REPEATED GAS INJECTION CYCLES INCREASED THE HYDROCARBON OUTPUT	26
FIGURE 1.5: AN OLD VERTICAL WELL WAS USED TO INJECT CO ₂	27
FIGURE 1.6: NATURAL GAS AND CO ₂ RECOVERED MOST OF THE OIL IN A ROCK SAMPLE	27
FIGURE 2.1: IMMISCIBILITY OF METHANE (GAS) AND OIL (LIQUID) AT RESERVOIR CONDITION .	30
FIGURE 2.2: MISCIBILITY OF METHANE AND PROPANE LIQUID AT RESERVOIR CONDITIONS .	31
FIGURE 2.3: MISCIBILITY OF METHANE AND PROPANE LIQUID AT RESERVOIR CONDITIONS ...	31
FIGURE 2.4: MISCIBLE DISPLACEMENT	32
FIGURE 2.5: TYPICAL P-T DIAGRAM FOR 2-COMPONENTS SYSTEM	34
FIGURE 2.6: THE EFFECT OF COMPOSITION CHANGE ON THE TWO-PHASE ENVELOPE	36
FIGURE 2.7 P-X DIAGRAM	38
FIGURE 2.8: P-X DIAGRAM	39
FIGURE 2.9: TERNARY DIAGRAM	41
FIGURE 2.10 : PROPERTIES OF THE TERNARY DIAGRAM	42
FIGURE 2.11: PSEUDO-TERNARY DIAGRAM.....	43
FIGURE 2.12: SCHEMATIC OF THE FIRST-CONTACT MISCIBLE PROCESS.....	45
FIGURE 2.13: ILLUSTRATION OF MISCIBLE DISPLACEMENT (HIGH-PRESSURE GAS INJECTION) ..	48
FIGURE 2.14: VAPORIZING GAS DRIVE PROCESS	49
FIGURE 2.15: CONDENSING GAS DRIVE PROCESS	52
FIGURE 2.16: CONDENSING GAS-DRIVE CRITICAL DISPLACEMENT ON TRIANGULAR GRAPH	53
FIGURE 2.17: COMPRESSIBILITY FACTOR FOR CO ₂	54
FIGURE 2.18: CO ₂ PROCESS.....	55
FIGURE 2.19: CO ₂ /HYDROCARBON SYSTEM AT TEMPERATURE ABOVE 120F	56
FIGURE 2.20: CO ₂ /HYDROCARBON SYSTEM AT TEMPERATURE BELOW 120F	57
FIGURE 2.21: CASE 1	57
FIGURE 2.22: CASE 2	58
FIGURE 2.23: CASE 3	58
FIGURE 2.24: CLASSIFICATION OF SOLVENT DISPLACEMENT	59
FIGURE 2.25: A SCHEMATIC DIAGRAM OF MULTIPLE CONTACT EXPERIMENT.....	61
FIGURE 2.26: PICTURE DIAGRAM FOR FORWARD AND BACKWARD MULTIPLE CONTACTS	62
FIGURE 2.27: SCHEMATIC OF A TYPICAL CORE FLOODING EXPERIMENTAL SETUP	65
FIGURE 2.28: A SCHEMATIC DIAGRAM OF SLIM-TUBE EXPERIMENT	67
FIGURE 2.29: SLIM-TUBE EXPERIMENT SETUP	67
FIGURE 2.30: GAS BUBBLE VISUALIZING IN THE RBA EXPERIMENT.....	68
FIGURE 2.31: A SCHEMATIC DIAGRAM FOR RBA SYSTEM	69
FIGURE 2.32: AN ACTUAL EXPERIMENT SETUP OF RBA SYSTEM	69
FIGURE 2.33: EOS FORMULAS	71

FIGURE 3.1: SARIR FIELD LOCATION MAP.....	73
FIGURE 3.2: MAP OF SIRTE BASIN, LIBYA.....	74
FIGURE 3.3: STRUCTURE MAP OF SARIR FIELD COMPLEX (AFTER SANFORD, 1970).....	75
FIGURE 3.4: THE COMPOSITIONAL DISTRIBUTION OF EOS C31+	81
FIGURE 3.5: THE COMPOSITIONAL DISTRIBUTION THE LUMPED EOS C15.....	85
FIGURE 3.6: CCE DATA (RELATIVE VOLUME VERSUS PRESSURE)	87
FIGURE 3.10: DV DATA (GAS OIL RATIO VERSUS PRESSURE).....	87
FIGURE 3.7: DV DATA (FORMATION VOLUME FACTOR VERSUS PRESSURE)	88
FIGURE 3.8:DV DATA(OIL DENSITY VERSUS PRESSURE).....	88
FIGURE 3.9: VISCOSITY VERSUS PRESSURE	89
FIGURE 3.11:CCE DATA(RELATIVE VOLUME VERSUS PRESSURE).....	89
FIGURE 3.15:DV DATA(GAS OIL RATIO VERSUS PRESSURE)	90
FIGURE 3.12: DV DATA(FORMATION VOLUME FACTOR VERSUS PRESSURE)	90
FIGURE 3.13: DV DATA (OIL DENSITY VERSUS PRESSURE)	91
FIGURE 3.14: VISCOSITY VERSUS PRESSURE	91
FIGURE 3.16: CCE DATA (RELATIVE VOLUME VERSUS PRESSURE)	92
FIGURE 3.18:DV DATA(GAS OIL RATIO VERSUS PRESSURE)	92
FIGURE 3.17: DV DATA (FORMATION VOLUME FACTOR VERSUS PRESSURE)	93
FIGURE 3.19: DV DATA (OIL DENSITY VERSUS PRESSURE)	93
FIGURE 3.20: VISCOSITY VERSUS PRESSURE.....	94
FIGURE 3.21:PSEUDO-TERNARY DIAGRAM.....	99
FIGURE 3.22: PSEUDO TERNARY DIAGRAM (SEPARATOR GAS)	100
FIGURE 3.23: PSEUDO TERNARY DIAGRAM CO2	100
FIGURE 3.24: PSEUDO TERNARY DIAGRAM (SEPARATOR GAS).....	101
FIGURE 3.25: PSEUDO TERNARY DIAGRAM CO2	102
FIGURE 4.1:OIL RECOVERY FROM SLIMTUBE AT 5300PSIG.....	104
FIGURE 4.2: OIL RECOVERY FROM SLIMTUBE AT 3300.....	105
FIGURE 4.3: OIL RECOVERY FROM SLIMTUBE AT 5300.....	106
FIGURE 4.4 OIL RECOVERY FROM SLIMTUBE AT 3300.....	106
FIGURE 4.5: OIL RECOVERY FROM SLIMTUBE AT 5300.....	108
FIGURE 4.6: OIL RECOVERY FROM SLIMTUBE AT 3300.....	108
FIGURE 5.1: RELATIVE PERMEABILITY CURVES FOR GAS/OIL SYSTEM.....	113
FIGURE 5.2: RELATIVE PERMEABILITY CURVES FOR WATER/OIL SYSTEM.....	114
FIGURE 5.3: SLIM-TUBE 1-D MODEL	115
FIGURE 5.4:OPTIMIZING THE CELL NUMBERS.....	116
FIGURE 5.5:OIL RECOVERY AT PRESSURE OF 3300 PSIG	117
FIGURE 5.6:OIL SATURATION AT PRESSRE OF 3300 PSIG	118
FIGURE 5.7: GAS SATURTION AT PRESSURE OF 3300 PSIG.....	118
FIGURE 5.8: OIL AND GAS DENSITIES AT PRESSURE OF 3300 PSIG.....	119
FIGURE 5.9 K-VALUE OF C1 AT PRESSURE OF 3300 PSIG	120

FIGURE 5.11: OIL RECOVERY AT PRESSURE OF 4010 PSIG	121
FIGURE 5.12: OIL SATURATION AT PRESSURE OF 4010PSIG	121
FIGURE 5.13: GAS SATURATION AT PRESSURE OF 4010PSIG.....	122
FIGURE 5.14: OIL AND GAS DENSITIES AT PRESSURE OF 4010 PSIG.....	122
FIGURE 5.15: K-VALUE OF C1 AT PRESSURE OF 4010PSIG.....	123

List of Tables

TABLE 1.1: UNCRITICAL PARAMETERS FOR EACH EOR METHOD	20
TABLE 1.2: CO ₂ SCREEN RANGES FOR MISCIBLE PROJECTS	23
TABLE 1.3 TECHNICALLY RECOVERABLE SHALE OIL IN THE WORLD RESOURCES	24
TABLE 1.4 TOP 10 COUNTRIES WITH TECHNICALLY RECOVERABLE SHALE OIL RESOURCES ..	24
TABLE 2.1: THE CRITICAL TEMPERATURES AND SOLUBILITY OF SOME OF SOLVENT GASES	53
TABLE 3.1 THE COMPOSITION OF RESERVOIR FLUID AND SEPARATOR GAS	96
TABLE 3.2 FLASH CALCULATIONS FOR DETECTING THE SINGLE AND THE 2- PHASE REGION .	96
TABLE 3.3: THE FIRST MIXTURE MCM CALCULATION	97
TABLE 3.4: THE SECOND MIXTURE IN MCM CALCULATION	97
TABLE 3.5: THE THIRD MIXTURE IN MCM CALCULATION.....	98
TABLE 4.1: THE MOLAR COMPOSITION OF SEPARATOR GAS	104
TABLE 4.2 OIL WITH LIGHTER COMPOSITION	107
TABLE 5.1: RELATIVE PERMEABILITY FOR GAS/OIL SYSTEM.....	112
TABLE 5.2: RELATIVE PERMEABILITY VALUES FOR WATER /OIL SYSTEM.....	113
TABLE 5.3: THE PREDICTED MMP BY BOTH EOS(MCM) AND 1-D SLIMTUBE.....	124

Nomenclature

Abbreviations

BP	British Petroleum Company
BBL	Barrel
BOPD	Barrel of Oil per Day
Km	Kilometer
Mi	Mile
Ft	Feet
M	Meter
API	American Petroleum Institute
GOR	Gas Oil Ratio
(Ft-ss)	Feet-Subsurface
Psi	Pound per Square-Inch
FVF	Formation Volume Factor
Pb	Bubble Point Pressure
Cp	Centipoise
PPM	Part Per Million
MM	Million
BSCF	Billion Standard Cubic Feet
MMSCF/D	Million Standard Cubic Feet Per Day
SCF/STB	Standard Cubic Feet Per Stock Tank Barrel
MMSTB/D	Million Stock Tank Barrel Per Day
WO, ESP	Work over, Electrical Submersible Pump
1D	1 dimension
3PR, PR	3 Parameters Peng-Robinson equation of state
AAE	Average absolute error
AF	Acentric factor
AIM	Adaptive implicit
B, FVF	Formation volume factor
BHP, BHS	Bottomhole pressure, Bottom hole 'oil' sample
BIC	Binary interactive coefficient
b^m	Molar densities
CCE	Constant composition/mass expansion "flash liberation"
CGD	Condensing gas drive
CPU	Simulation model computational time
CVGD	Combined condensing/vaporizing gas drive
DC	Displacement condition
DLE	Deferential liberation expansion
E	Overall displacement efficiency

EA or EH	Areal (or horizontal) sweep efficiency
Ed	Microscopic displacement efficiency
EOR	Enhanced oil recovery
EOS, cEOS	Equation of state or cubic equation of state
FCM	First-contact miscibility or first-contact miscible
FCMME	First-contact minimum miscibility enrichment
FCMMP	First-contact minimum miscibility pressure
FULLIMP	Fully implicit numerical solution
HC	Hydrocarbon
IFT, ST	Interfacial tension (=same as surface tension)
IMPES	Implicit pressure explicit saturation numerical solution
IOR	Improved oil recovery
K_w	Watson factor
L	Liquid
LPG	Liquefied petroleum gas (C3 and C4)
M	Miscibility contact
MB	MCM Multi-contact miscibility or multi-contact miscible
MCMME	Multi-contact minimum miscibility enrichment
MCMMP	Multi-contact minimum miscibility pressure
MMP	Minimum miscibility pressure (FCMMP and MCMMP)
M_w	Molecular weight
N	Miscibility exponent
N_x, N_y, N_z	Number of grid cells in x, y and z directions
OOIP	Original oil in place
P	Parachors
P, Press	Pressure
P_c	Capillary pressure
PV	Pressure-volume or pore-volume
PVI	Pore volumes injected
PVT	Pressure, volume, and temperature
RBA	Rising-bubble apparatus
RF	Recovery factor
K_r	Relative Permeability
ROS	Remaining oil saturation
R_s,	GORs Solution gas oil ratio
S	Saturation
SC	Standard conditions
SEP	Separator test
SF	Swelling factor
T,	Temp Temperature

V	Volume
VGD	Vaporizing gas drive
VIFT	Vanishing interfacial tension experiment
Vsh	Volume shift
WAG	Water alternating gas
WF	Water flooding
X, Y	Liquid mole fractions, vapor mole fractions

1.1 Enhanced Oil Recovery (EOR)

1.2 Introduction

1.2.1 Definition of EOR

Oil recovery has to pass through at least two of three stages of recoveries: primary, secondary and tertiary recovery. In the primary recovery the reservoir is producing by its own natural energy. As the natural energy of reservoir started to be depleted the secondary recovery is implemented to bring the production to its normal rate or to maintain the decline in reservoir pressure resulted from production, pressure maintenance water flooding and gas injection are well known methods of secondary recovery. Tertiary recovery is the third stage of recovery after whatever secondary process was used. Methods like miscible gases, chemical and thermal are used as tertiary recovery methods.⁽¹⁾

Recently improved oil recovery has been used alternately and mutually with EOR. Even though there is no rigorous definition, IOR refers to any process or practice that improves oil recovery. IOR therefore includes EOR processes but can also include other practices such as water flooding, pressure maintenance, infill drilling, and horizontal wells.⁽²⁾

1.3 Classification of Enhanced Oil Recovery (EOR) Methods

1.3.1 Thermal

The thermal methods are processes of injection or generation thermal energy. The example of thermal processes is steam flooding. In heavy oils reservoir, the main mechanism in thermal method is to reduce the oil viscosity and making the oil capable to flow easily toward the production well. The most effective way of steam flooding is the cyclic steam injection or (huff and puff) in which the steam is injected at high rates for a period of time, basically for weeks; and allowing the formation to soak this slug for a few days by closing the well and then put it back into production. In situ combustion or air injection is often referred to as fire flooding. This is done by injecting air or oxygen to burn a portion of the oil in place. Depending on the oil, two basic modes occur: low-temperature oxidation (LTO) and high temperature oxidation (HTO).⁽³⁾

1.3.2 Chemical

Conventionally, the reason behind this method was to increase the capillary. Micellar-polymer is the most well-known method. After many trial tests in the fields, the process gave way to new alternatives, such as alkaline-surfactant-polymer (ASP) flooding, and a renewed interest in surfactant-polymer (SP) flooding. In ASP, the polymer controls the mobility, while the alkali and surfactant act interactively to widen the range of ultra-low interfacial tension (10-3mN/m). In SP, which is a combination of two surfactant (a surfactant and a co-surfactant) co-solvents, no caustic agent is used.⁽¹⁻³⁾

1.3.3 Miscible or Solvent Injection

This method relies on the miscibility of the injected fluid with the oil phase. The solvent is injected by using one of the following fluids:

Hydrocarbon Miscible Injection: The main mechanisms in this method include generating miscibility, increasing the oil volume, or swelling and decreasing the oil viscosity.

Carbon Dioxide Injection: The CO₂ flood develops miscibility by extraction of oil fractions. Lower pressure is needed in this method. The mechanisms are the same of those developed by other miscible flooding more specifically (e.g. Vaporizing gas drive) processes.

Nitrogen and Flue Gas Injection: Because they require very high miscibility pressure in order to achieve miscibility and also for economic reasons, these processes are rare used. Vaporizing light oil fractions creates miscibility.^(1,3)

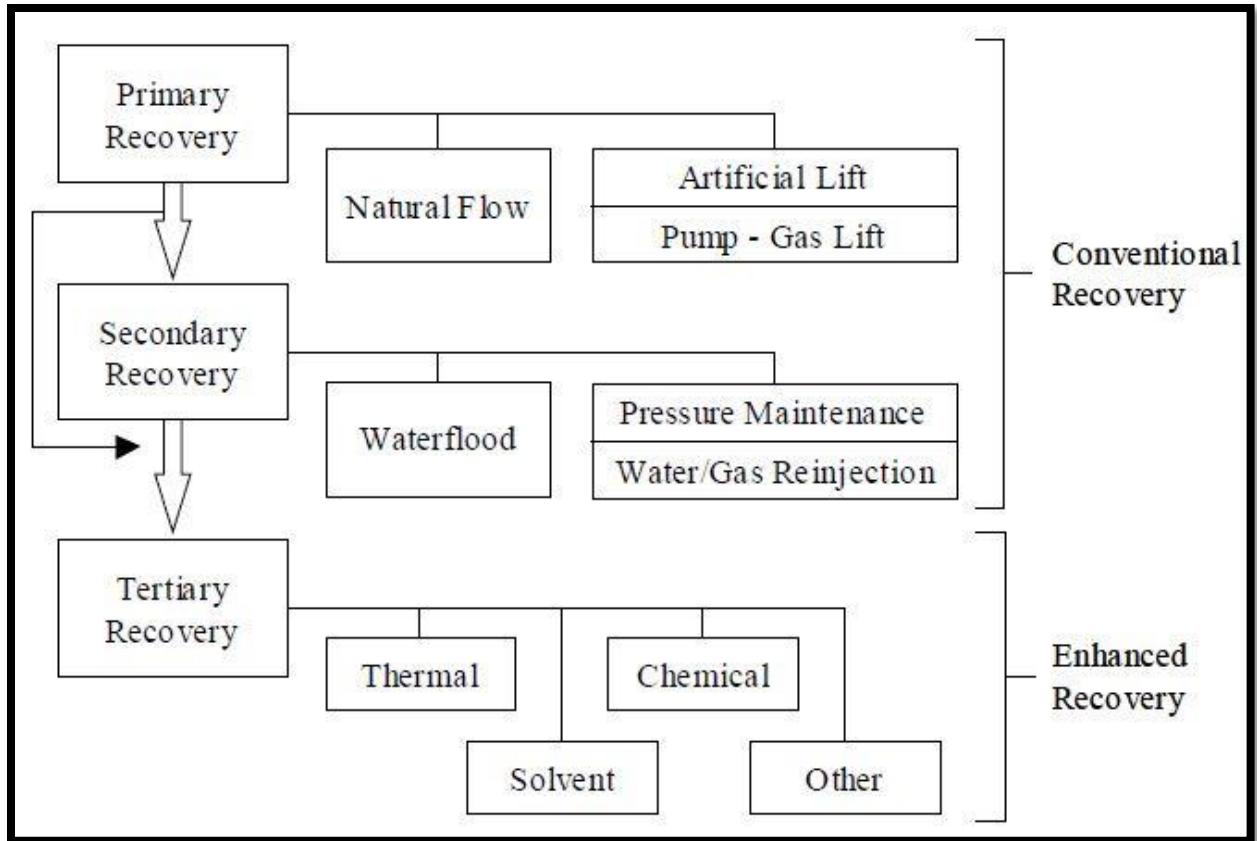


Figure 0.1: Oil recovery classifications (adapted from the Oil and Gas Journal Biennial surveys).

1.4 General EOR Screening Criteria

After reviewing and validating the main EOR methods dependency with maintain the consistency with the published literature range. The most important parameters that have been identified to apply the suitable EOR method are:-

- Oil gravity, API
- Oil viscosity, CP
- Reservoir depth, ft
- Reservoir temperature, F
- Porosity, %
- Permeability, md
- Formation type

The parameters that are not critical for each EOR methods are listed in the table below .⁽⁴⁾

Table 0.1: Uncritical Parameters for Each EOR Method

	Thermal	Chemical	Immiscible	Miscible
Gravity	X	X	X	X
Viscosity	X	X	X	X
Depth	X	X	X	X
Permeability	X	X		
Porosity	X	X		
Temperature		X		

1.5 Miscible Displacement Processes

1.5.1 Introduction

Miscible displacement processes are the process where the displacement is generated primarily from miscibility between the oil in place and the injected fluid. Injected fluid can be one of these fluids: Hydrocarbon solvent, CO₂, Flue gas, and Nitrogen.⁽¹⁾

The displacement processes maybe categorized into first-contact miscible (FCM) or multiple-contact miscible (MCM) depending on the development of miscibility. When the injected fluid and crude oil are miscible in all proportions they will form only a single phase upon the first contact this miscibility known as (FCM) but if the miscibility developed in situ with the changing in the composition of crude oil or injected gas or both then this miscibility will be (MCM).⁽¹⁾ Regardless of whether the displacement is developed or first-contact miscible, the solvent must displace any mobile water present with the resident fluids immiscibly.⁽²⁾

1.5.2 History

Miscible flooding methods have been investigated and field tested since the early 1950's. Early center of attention was on hydrocarbon solvents, and three types of hydrocarbon-miscible processes were developed: the First-contact miscible process; the vaporizing-gas drive process; and the Condensing-gas drive process, sometimes called enriched-gas drive or vaporizing/condensing drive. Hydrocarbon miscible processes have been subjected to a comprehensive field testing since the 1950's, primarily in the U.S .and Canada. More than

100 projects were implemented during that period of time. Most of them were small-scale pilot tests involving one or a few injection wells; However, a large number of projects of several thousand acres or more ($> 4 \times 10^6 \text{ m}^2$) were promising.⁽⁵⁾

An old article" listed the field applications of vaporizing gas drive, condensing gas drives and miscible slug injection operations. There were about, 41 miscible slug floods known project from 1950- 1959 in the United States, Canada, Venezuela and Peru. Figure (1.2) shows the yearly number of miscible slug injection projects from 1950 to 1960. Many of the field miscible slug operations were conducted in reservoirs which were completely unsuited for this recovery method. Others have been various forms of LPG storage operations. Only 10 of the 41 field applications of solvent injection was considered as a valid tests of miscible flooding.⁽⁶⁾

As early as 1952, Whorton and Brownscombe received a patent for an oil-recovery method with CO₂. Laboratory research was published through the 1950's and 1960's and research continues today (Huang and Dyer, 1992; Srivastava, 1994; Buckley, 1995; Mangalsingh and Jagai, 1996; Obi and Blunt, 2006).⁽⁷⁾

Several pilot tests of CO₂ EOR injection were conducted in the offshore Gulf of Mexico during the 1980s (Hsie and Moore 1988, Nute 1983). None of these projects attributed to economical projects but were generally regarded as technically successful. The most significant current activity related to offshore CO₂ EOR is the CO₂ EOR pilot test being conducted by Petrobras at Lula field offshore of the cost of Brazil (Pizarro and Branco 2012).⁽⁸⁾

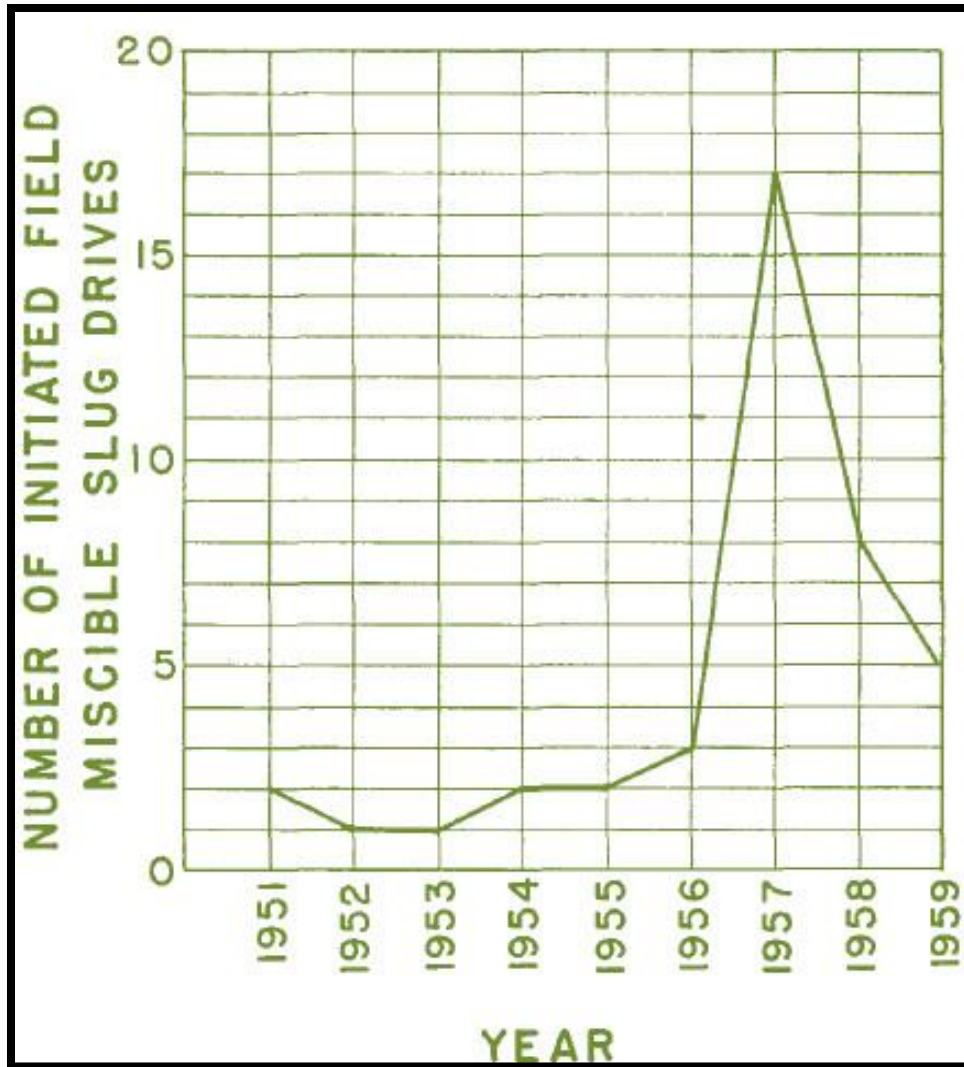


Figure 0.2: Number of Field Miscible Slug Drives Initiated Between a Period of (1950-1960)

1.6 Screening Criteria Ranges for CO₂ Miscible Projects

According to the experience of the industry, the criteria for developing a successful miscible flood includes the following:-

- 1- Oil reservoir with a good response to water flood are the best candidates for CO₂ flooding.
- 2- The water flood recovery should be between (20%-50%) of the OOIP before implementing CO₂ flooding.
- 3- Formation porosity should be greater than 12% with effective permeability greater than 10md.⁽⁷⁾

The three critical parameters for miscible projects which have high contribution for recovery gravity and oil viscosity and also the depth at which the displacement can be achieved effectively are listed in the table below.

Table 1.2 shows the CO₂ Screen ranges for Miscible Projects the last row is a comparison between literature ranges and ranges derived from database.⁽⁴⁾

Table 0.2: CO₂ Screen Ranges for Miscible Projects

CO₂ Screen ranges for Miscible Projects						
Gravity (Deg API)		Viscosity (Cp)		Depth(ft)		
Sandstone	Carbonate	Sandstone	Carbonate	Sandstone	Carbonate	Source
>27	>27			>2300	>2300	Clancy (1985) (NPC(1976))
>22	>22	<10	<10	>2500	>2500	Taber(1997)
>25				>3000		shrichard (2007)
28-45	28-45	0-35	0-35	1500-13365	1500-13365	Aladasani(2010)
>25	>25	>15	>15	>2000	>1800	Previous Inhouse Analysis
16-46	12--46	0.3-5000	0.3-592	1150-15600	4000-11100	Project Database

1.7 The Potential of Unconventional Oil Reservoir in Libya (Shale Oil)

According to the report published recently by EIA shale oil in and in 137 shale formations in 41 other countries represent 10% of the world's crude oil technically recoverable resources. EIA released the study in the 10th of June 2013 the table below shows the recoverable oil and gas shale worldwide.⁽⁴⁶⁾

Table1.0.3 Technically Recoverable Shale Oil and Shale Gas Resources in the Context of Total World Resources

	Crude Oil (Billion Barrels)	Wet natural gas (Trillion Cubic Ft)
Outside The United State		
Shale Oil and Shale Gas	278	6634
Non-Shale	2847	13817
Total	3134	20451
Increase in total resources due to inclusion of shale oil and shale gas	10%	48%
shale as a percent of Total	9%	32%
United States		
Shale/tight oil and shale gas	58	665
Non-Shale	164	1766
Total	223	2431
Increase in total resources due to inclusion of shale oil and shale gas	35%	38%
Shale as a percent of Total	26%	27%
Total World		
Shale/tight oil and shale gas	345	7299
Non-Shale	3012	15583
Total	3357	22882
Increase in total resources due to inclusion of shale oil and shale gas	11%	47%
shale as a percent of Total	10%	32%

More than half of the identified shale oil resources outside the United States are concentrated in four countries—Russia, China, Argentina, and Libya. ⁽⁴⁶⁾

Table 0.4 Top 10 Countries with Technically Recoverable Shale Oil Resources

Shale Oil (Billion Barrels)		
Rank	Country	
1	Russia	75
2	U.s	58
3	China	32
4	Argentina	27
5	Libya	26
6	Australia	18
7	Venezuela	13
8	Mexico	13
9	Pakistan	9
10	Canada	9
	World Total	345
		355

Libya is also ranked fifth-highest in the world for recoverable shale oil reserves, estimated at 26 billion barrels.

This report's methodology for estimating the shale resources outside the United States is based on the geology and resource recovery rates of similar shale formations in the United States (referred to as analogs) that have produced shale oil and shale gas from thousands of producing wells.⁽⁴⁶⁾

1.8 The CO2 is the future candidate for Shale Oil

A recent study shows a promising result of the miscible gas injection to recover oil from shale reservoir. The strongest evidence that the method does work is EOG's growing testing program. At the time of the first announcement last May, the company said its 15 initial wells performed consistently, adding from 30 to 70% to reserves. It added 32 wells to the program last year, which produced an average of 80 B/D per well for an average finding cost of \$6/bbl. It has not yet reported on this year's 100wellprogram. There are still challenges and high risk it still there when dealing with reservoirs with such a high complexity.⁽⁴⁵⁾

Results from lab experiments indicated that the process was technically feasible, but the economics and operational execution were going to be challenged without some creative problem solving.⁽⁴⁵⁾

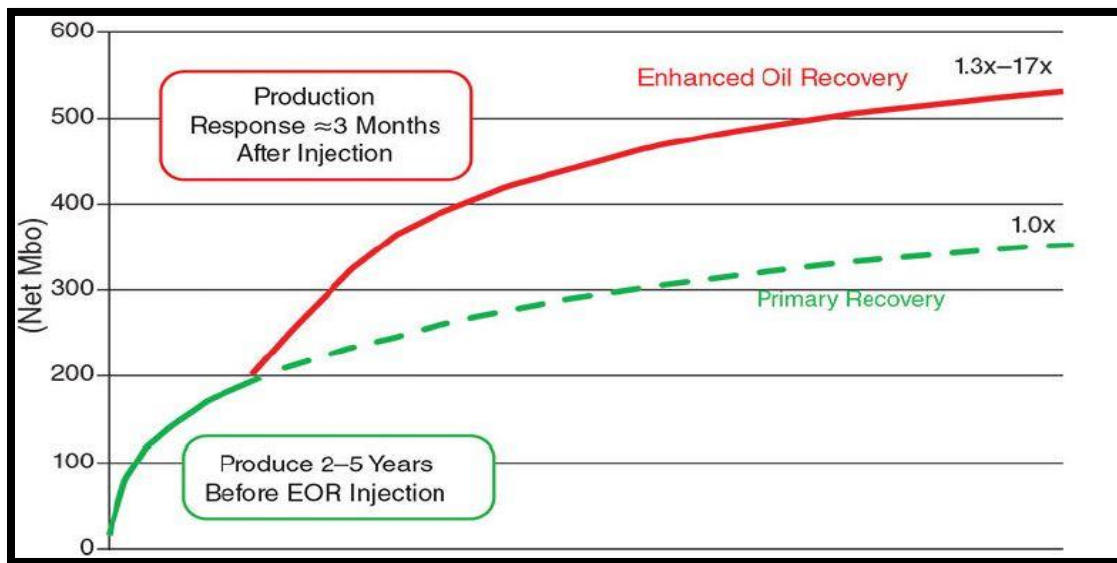


Figure 0.3: EOG's prediction for how gas injection EOR will increase output. The company did not provide a time scale. Source: EOG Resources.

1.8.1 Some considerations of using the CO₂ in unconventional Reservoirs

- In order to the injected gas to be effective the formation needs to be pressurized, and the injected gas has to stay long enough to have a decent effect on recovery.
- Based on lab results, natural gas injection should be able to extract more oil from rock. Small samples from various parts of the Middle Bakken were tested by the University of North Dakota's Energy and Environmental Research Center (EERC). When exposed to natural gas or CO₂, the chips produced more than 90% of the oil in the rock samples within 24 hours.⁽⁴⁵⁾

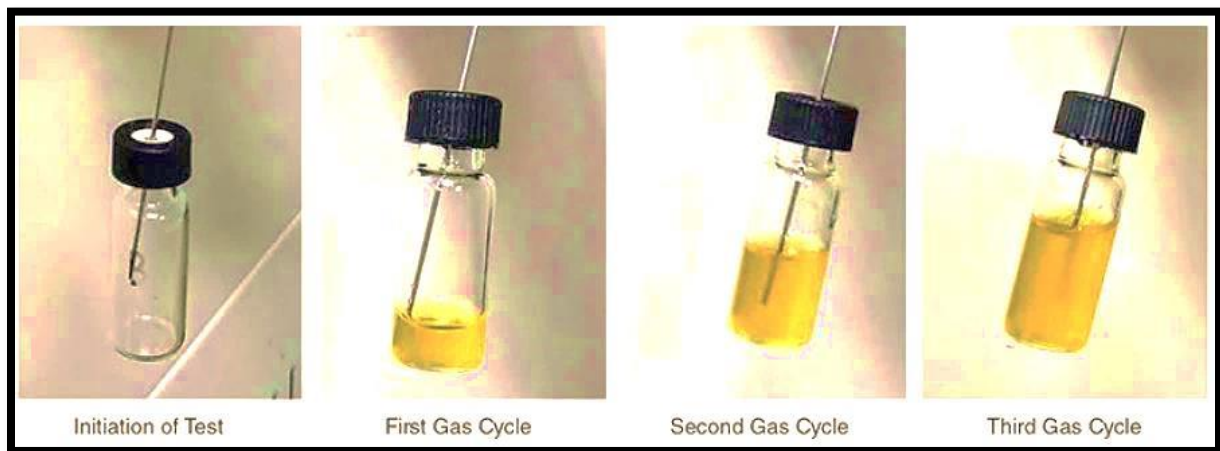


Figure 0.4: Repeated gas injection cycles increased the hydrocarbon output from this core sample. Source: Core Lab.

- In field tests, the “CO₂ moves so quickly through fractures that it did not have enough time, or became too dispersed, to interact with stranded oil in the matrix” rock in the reservoir.⁽⁴⁵⁾
- By injecting CO₂ in the Bakken using an old vertical well that had pierced an unfractured spot in the Middle Bakken. After three periods of injection, lasting a total of 80 hours, and two shut-in Periods giving the gas time to diffuse in the tight rock, there was a spurt of oil production, with 9 bbl produced over 45 minutes before it stopped.⁽⁴⁵⁾

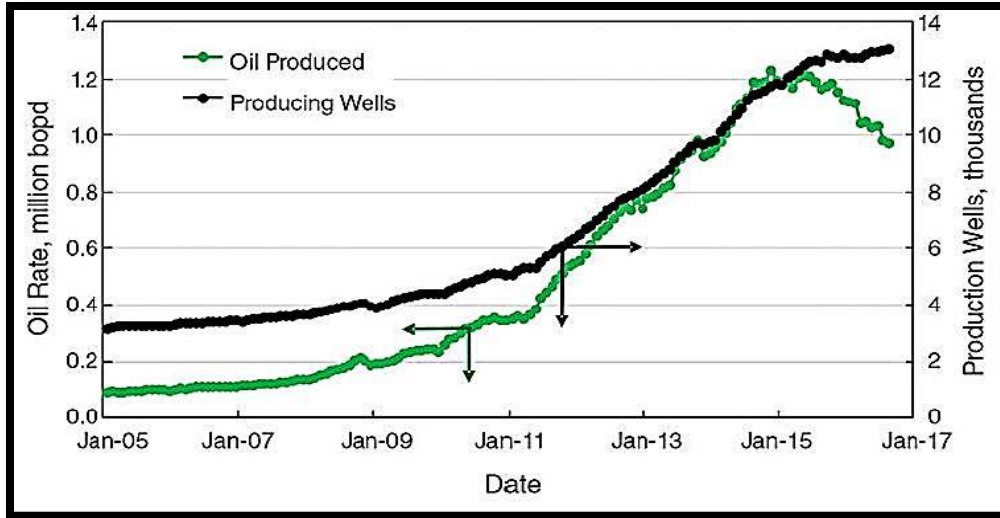


Figure 0.5: an old vertical well was used to inject CO₂ into an un-fractured part of the Bakken as part of a Program to reverse production decline from older wells. Source: Energy and Environmental Research Center, University of North Dakota (SPE 184414)

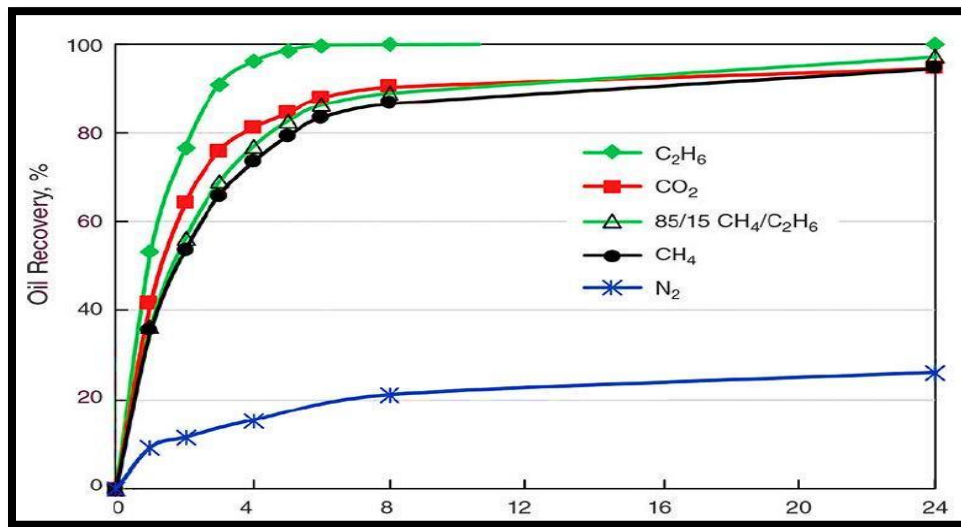


Figure 0.6: Natural gas and CO recovered most of the oil in a rock sample from the Middle Bakken, but not Nitrogen. Source: SPE 184414.

- Using (huff and puff method) where the gas is injected into the well the (huff) and it is shut in for several weeks to diffuse into the tight rock around the fractures—and then it is opened up for production—the puff.
- While huff ‘n’ puff has been around a long time, it is not widely used because no one wants to interrupt production. But at this point, soak time appears necessary in ultra-tight rock .The ups and downs of a huff ‘n’ puff well, with production starting low, a period with no production, and then a significant gain.

1.9 Some Selective Successful Miscible Gas and CO₂ Injection Projects

1.9.1 Miscible Gas Injection in Rhourde El Krouf Field, Algeria

The Rhourde El Krouf field (RKF) in the Berkine basin, southeast of Hassi Messaoud, has been producing injection from the TAGI since 1996 under partial pressure maintenance by miscible-gas. The makeup gas for the project was provided from deeper volatile-oil and retrograde gas-condensate reservoirs. After 9 years of surrounding RKF with downdip, high-pressure gas injection, the field has recovered more than 50 million bbl of oil with 90 Bcf of gas injection. Primary recovery was predicted to be less than 40 million bbl of oil. The field is still producing at the 20,000 BOPD designed plateau rate.⁽⁹⁾

1.9.2 Miscible Gas Injection in a Mature U.K. North Sea Field

The South Brae Field is located in Blocks 16/7a and 16/7b of the UK North Sea, 160 miles northeast of Aberdeen. It has been developed and produced from Brae Alpha, which is a fixed leg platform in 350 ft. of water. Production began in July 1983, with the support of natural water drive (aquifer) and produced gas re-injection. Water injection was introduced since 1984 onwards and eventually replaced gas injection. Oil production stabilized at rate of 100,000 BOPD at the end of 1984 and declined sharply after water breakthrough at the main producers in 1989. The full field gas injection project started in November 1998, and by the end of 1999 three gas injectors were capable of injecting a total of up to 90 MMscf/D. after three years of gas injection for the pilot project, The oil rate increased ten times from 400 to 4,000 BOPD, the water-cut decreased from 90% to 15%, and the GOR increased from 2,000 to 7,000 scf/STB.⁽¹⁰⁾

1.9.3 Miscible Gas Injection in Harweel Field Oman.

The Harweel field is a carbonate cluster and consists of eight fields and 11 high-pressure/high-temperature reservoirs. The cluster is in the south of Oman and produces light 38°API crude oil. Because of the high reservoir pressure and light-oil conditions, miscible-gas injection was selected, with the potential to increase the recovery factor from 10 to 50%. The availability of large quantities of sour gas was capitalized by re-injecting the produced sour gas into the reservoir. The project was fully commissioned in late 2010. Harweel oil production is expected to increase by 40,000 B/D.⁽¹¹⁾

1.9.4 CO₂ Injection in Rumaitha Field, UAE

Abu Dhabi Company for Onshore Oil Operations recently piloted CO₂ injection in the Rumaitha field. This field is a carbonate reservoir with thickness between 130 and 150 ft. The porosity and permeability values are 14 to 17% and 1 to 3 md, respectively. The project had only three wells—one injector and one producer spaced approximately 70 m apart and one observation well in between. The objective of the project was not to assess recovery, but aimed at understanding operational challenges associated with CO₂ injection in the oil field.⁽¹¹⁾

1.9.5 Immiscible-CO₂ Injection in Bati Raman Field, Turkey

The Bati Raman field is the largest oil field in Turkey. This field is a limestone reservoir on an elongated east/west anticline, approximately 17 km long by 4 km wide. The reservoir rock is a fractured vuggy limestone in the western and central parts of the field, but is chalky and tighter to the east. Porosity and permeability values range from 14 to 20% and 10 to 100 md, respectively. The reservoir contains 12°API heavy oil at an average depth of 4,300 ft. The reservoir temperature is 150°F, and the original reservoir pressure was 1,800 psi.

A cyclic CO₂ injection or (huff and puff) application was considered to increase the bottom hole pressure of the wells before putting the wells back on production. The project was started in 1986 by injecting roughly 50 MMscf/D of CO₂ gas. Positive results of the pilot project were observed in 1988, at which time CO₂ injection was expanded to the whole field. The reservoir pressure increased from 400 psi to a 1,300- to 1,800-psi level. The total oil production increased from 300 B/D to approximately 4,000 B/D. The per-well oil-production rate also jumped from 25 STB/D to 100 STB/D by mid-1991, increasing the recovery factor by 5%.⁽¹¹⁾

2. Literature Review

2.1 General Description of Miscible Displacement

Miscible phase displacement processes that use a specific amount of gases as injectants have been developed as a useful means for increasing oil recovery from many reservoirs. In order to understand these processes it is very important to make a good distinguish between “miscibility” and “solubility”. *Solubility* is defined as the ability of a specific amount of substance to mix with another substance to form a homogenous phase in the other hand the miscibility is physical condition between two or more fluids to allow them mix in all proportions without the existence of the interface. If there another phase developed after adding some amount of fluid to another fluid then the fluids are considered as immiscible. The so called interfacial tension (IFT) will developed between these two fluids .When a remarkable IFT (>0.1 dynes/cm) exists between phases in a porous medium, capillary forces prevent the complete displacement of one of those phases by the other. Substantial residual oil saturation preserved in a porous medium after an injected immiscible fluid is used to displace oil from the medium, as in water flooding. Figs. 2.1 and 2.2 illustrate the differences between immiscible and miscible conditions for certain fluids.^(1,12,13)

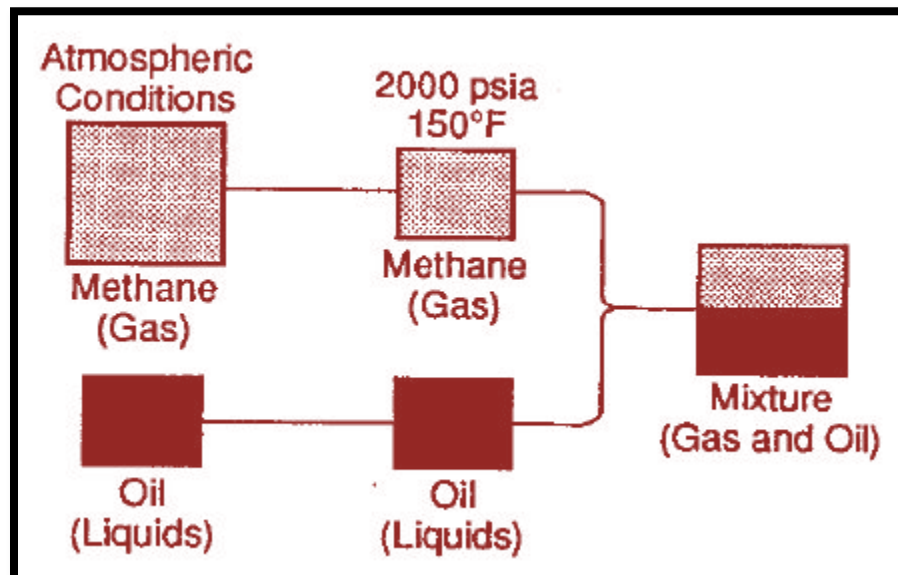


Figure 2.1: Immiscibility of methane (gas) and oil (liquid) at reservoir condition of temperature and pressure (from Clark et al¹³).

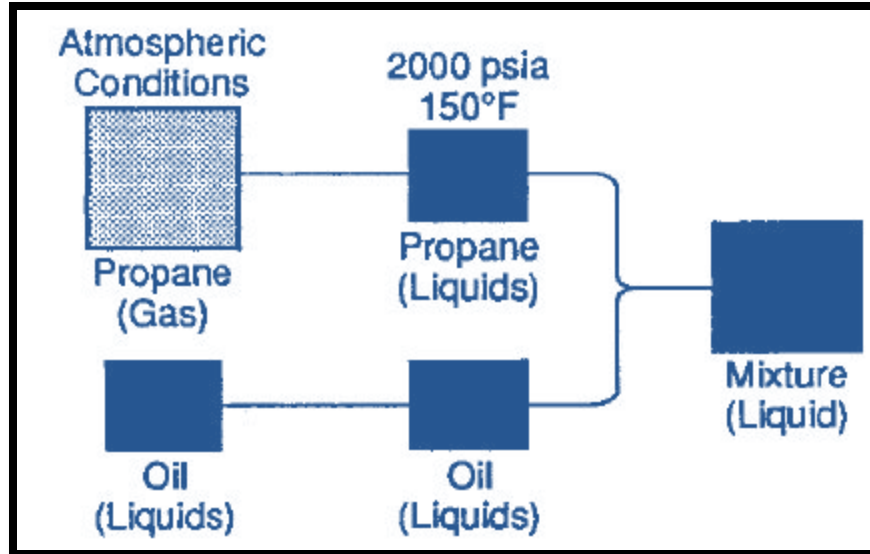


Figure 2.2: Miscibility of methane (gas) and propane (or LPG) liquid at reservoir conditions of temperature and pressure, here the propane or (LPG) is a gas in the presence of a gas (from Clark et al ¹³).

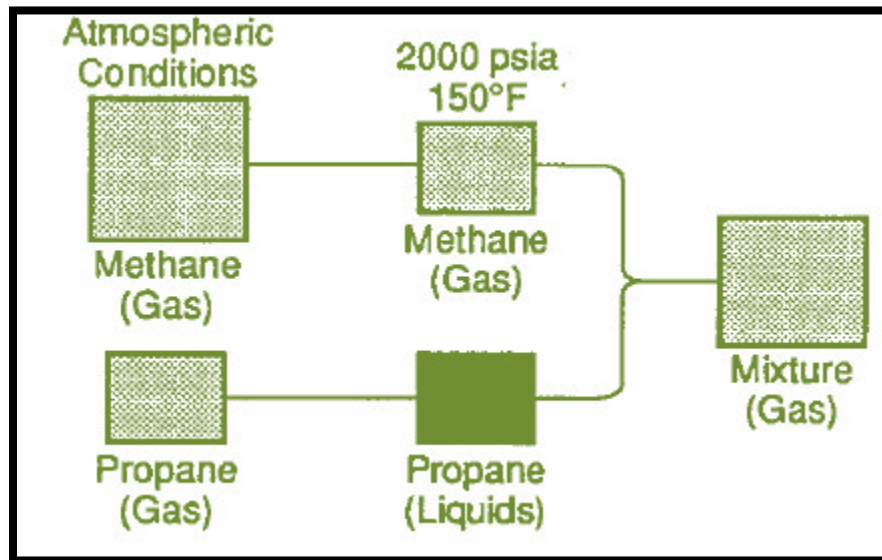


Figure 2.3: Miscibility of methane (gas) and propane (or LPG) liquid at reservoir conditions of temperature and pressure, here the propane or (LPG) is a liquid in the presence of a liquid (from Clark et al ¹³).

2.2 Miscible Displacement

In the Miscible displacement processes the interfacial tension (IFT) and residual oil saturation are approximately reduced to zero. figure2-3 shows schematically an idealized First contact miscibility displacement at which the injected fluid is a mixture of low molecular weight hydrocarbon (LPG's) because the injected fluid that's FCM with crude oil is more expensive than water and gas so it has to be relatively small for economic reasons as a result of that the primary slug maybe flowed by larger volume of secondary slug such as water or a lean gas .ideally the secondary slug should be miscible with primary slug this will increase the displacement efficiency of the primary slug .Under certain condition of temperature and pressure methane CH4 can be miscible with primary slug but if the water is used as chasing(secondary slug) fluid the residual saturation of injected fluid (primary slug) will be retained in the rock and primary slug will be broken down.⁽¹²⁾

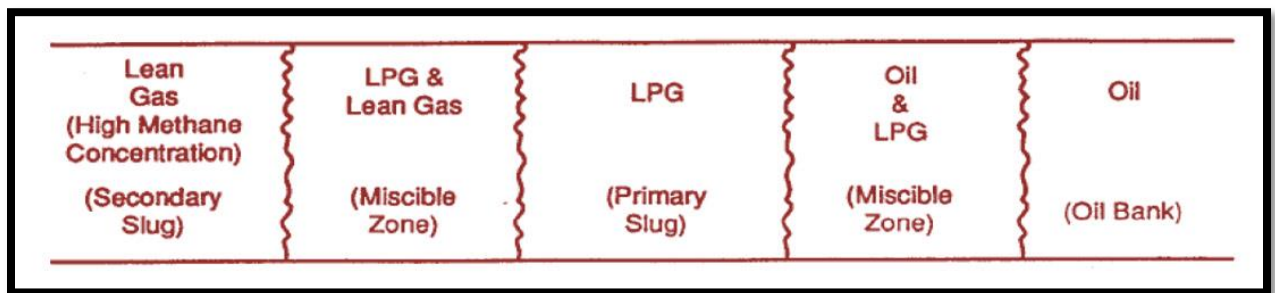


Figure 2.4: Miscible Displacement ⁽¹⁾

in multiple contact miscibility (MCM) processes the injected fluid and oil are not miscible upon the first contact.in this case the miscibility does not exist initially but it develop as the process continuous such a process is called dynamic miscible process because of the modification that occur to the oil or injected as the injected fluid moves through the reservoir. Various gases and liquids are suitable to be used as injectants in either FCM or MCM^(1,12,13). These gases are

- Low molecular weight hydrocarbon
- Mixture of hydrocarbon (LPG's)
- CO2 and Nitrogen or mixture if these gases

The particular application depends on some factors like the reservoir temperature, pressure, the composition of crude oil and injected fluid .also the development of miscibility depends on the phase behavior of the system which is in turn depends on the previous factors.⁽¹⁾

2.3 Principles of Phase Behavior Related to Miscibility

There are a lot of methods available to represent vapor-liquid phase behavior of multicomponent system .theses method include the following:-

- Pressure/temperature diagram
- Pressure/composition diagram
- Ternary diagram

2.3.1 Phase Rule

It is appropriate at this stage to introduce and define the concept of the phase rule. Gibbs (1948 [1876]) derived a simple relationship between the number of phases “P” in equilibrium, the number of components ”C” and the number of independent variables “F” that must be specified to describe the state of the system completely. Gibbs proposed the following fundamental statement of the phase rule:

$$F=C-P+2 \quad \text{Eq. 1}$$

Where

- F = number of variables required to determine the state of the system at equilibrium or number of degrees of freedom (such as pressure, temperature, density)
- C = number of independent components
- P = number of phases A phase was defined as a homogeneous system of uniform physical and Chemical compositions.

The degrees of freedom, F, for a system include the intensive properties such as temperature, pressure, density, and composition (concentration) of phases. These independent variables have to be specified to define the system completely. In a single component (C=1), two-

phase system ($P=2$), there is only one degree of freedom ($F=1-2+2=1$) to be specified to determine the thermodynamic state of the system either (temperature or pressure).⁽¹⁴⁾

A problem in dealing with crude oils is they are complex fluid made up of numerous chemical components also a precise chemical composition is unknown. Because of the technical difficulty and expenses involved in obtaining such an information.

According to phase rule, F degrees of freedom (temperature, pressure composition, density) have to be specified before the phase behavior can be described completely. For a typical crude oil F is a large number and thus a strict specification of phase behavior is impossible. For a practical purpose an approximation method such as pseudo-ternary diagram is used for simplicity.⁽¹⁾

2.3.2 Pressure/Temperature Diagram for Two-Component System

The phase behavior of multicomponent system is the same as the binary mixture but it is much more complex than the binary system because it contain a large number of components also the pressure and temperature ranges in which the two phases lie increases significantly.⁽¹⁴⁾

This diagram is used to understand principles of phase behavior that relate to understanding of miscibility.

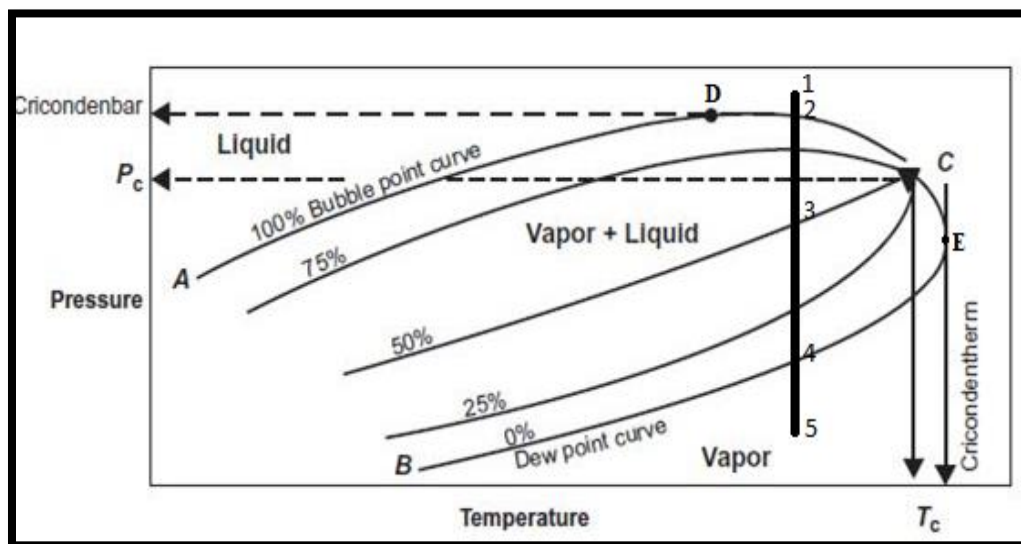


Figure 2.5: Typical P-T diagram for 2-components system⁽¹⁾

In order to understand the full picture of P-T diagram it is necessary to identify the key points in the diagram

- Cricondenterm (T_{ct}): The cricondenterm is the maximum temperature at which no liquid can be found (point E). The pressure at this point is the cricondenterm pressure, P_{ct} .
- Cricondenbar (P_{cb}): The cricondenbar is the maximum pressure at which no gas can be found (Point D). The temperature at this point is called the cricondenbar temperature, T_{cb} .
- Critical point: is the point at which all intensive properties of the gas and liquid phases are equal (point C). At the critical point, the corresponding pressure and temperature are called the critical pressure, p_c , and critical temperature, T_c .
- Phase envelope (two-phase region): The region surrounded by the bubble point curve and the dew point curve (line BCA), where gas and liquid coexist in equilibrium, is identified as the phase envelope of the hydrocarbon system.
- Quality lines: The lines within the phase diagram are called quality lines. They describe the pressure and temperature conditions for equal liquid percentage by volumes (% of liquid). Note that the quality lines converge at the critical point (point C).^(1,14)

If the system exist at point 1 and has been subjected to isothermal pressure reduction .the change in the phase behavior will be as the following:-

- At point 1 the system exists as single phase liquid this system is called under-saturated liquid.
- At point 2 the system changes to saturated liquid the bubble point curve is reached at this point first bubble of vapor is formed however this bubble is negligible and the system is still identified by liquid composition.
- At point 3 and as the pressure reduced further more vapor is formed until 50/50 vol% is of liquid and gas.
- At point 4 the last droplet of liquid at dew point pressure is reached however the amount of liquid at this point is negligible.

- At point 5 any pressure below this dew point pressure will cause the system to be in a single phase “vapor” with no liquid at all. Thus we can summarize that as the following:

At fixed temperature all mixture is miscible above bubble point pressure in a “liquid” phase and below the dew point pressure in a “vapor” phase. It should be noted that figure 2-4 shows the system with fixed composition of multicomponent if the composition changed then the position of two phase envelop on P-T diagram will change.^(1,14)

The effect of composition change on the two-phase envelope for binary mixture on P-T diagram is shown in the figure below

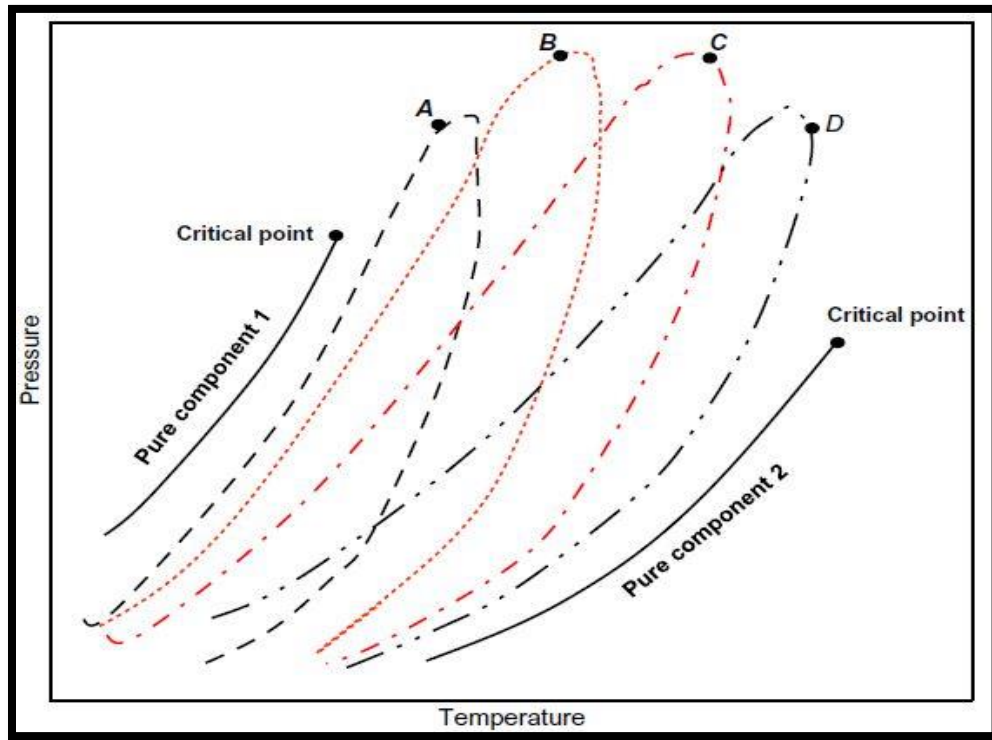


Figure 2.6: The effect of composition change on the two-phase envelope for binary mixture on P-T diagram⁽¹⁴⁾

This figure illustrates how the changing in the composition of the binary system will affect the shape and location of the phase envelope. The first vapor pressure curves for the pure lighter component is represented by line 1, and the second vapor curve for other component is represented by line 2. also there are four phase boundary curves (phase envelopes) labeled A through D, represent various mixtures of the two components with increasing The

concentration component 2. The points labeled A through D represent the critical points of the mixtures. It should be noted by examining figure2-5 that, when one of the components becomes predominant, the binary mixture will exhibit a relatively narrow phase envelope and displays critical properties close to the predominant component. The size of the phase envelope enlarges noticeably as the composition of the mixture becomes evenly distributed between the two components.⁽¹⁴⁾

2.3.3 Pressure/Composition Diagram “P-X” for Binary Systems

In the p-x diagram shown in figure 2-6, the composition is expressed in terms of the mole fraction of the more volatile component.

Let say that the overall composition of z exists in the vapor phase state as represented by point A. If the pressure on the system is increased, no phase change occurs until the dew point, B, is reached at pressure p_1 . At this dew point pressure, an negligible amount of liquid forms whose composition is given by x_1 . At this point the overall composition of the vapor still equal to the original composition z. As the pressure is increased, more liquid forms and the compositions of the coexisting liquid and vapor are given by drawing the straight, horizontal line through the two-phase region of the composition axis picking the ends of that line. For example, at p_2 , both liquid and vapor are present and the compositions are given by x_2 and y_2 . At pressure p_3 , the bubble point, C, is reached. The composition of the liquid is equal to the original composition z with a very small amount of vapor still present at the bubble point with a composition given by y_3 .⁽¹⁴⁾

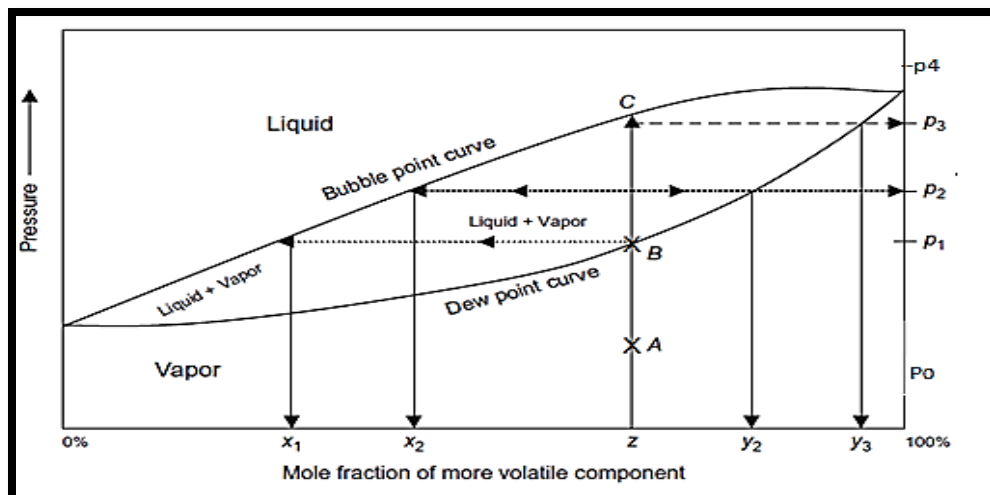


Figure 2.7 P-X diagram ⁽¹⁾

The composition within the two phase envelope should not be difficult to describe for instance only a negligible amount of vapor exists at bubble point.

As indicated already, the sides of a horizontal line through the two-phase region represent the compositions of coexisting phases. These points are of the practical interest for reservoir engineering calculations as pointed by Burcik (1957).⁽¹⁴⁾

Before going deep in the derivation of the equation for the relative amount of liquid and vapor in the two phase envelope it is necessary to identify some terminologies related to this manner.

Terminologies:

n =total number of moles in the binary system

n_L =number of moles of liquid

n_V =number of moles of vapor

z =mole fraction of the more volatile component in the system

x =mole fraction of the more volatile component in the liquid phase

y =mole fraction of the more volatile component in the vapor phase

An equation for the relative amounts of liquid and vapor in a two-phase system may be derived on one of the two components (the more volatile or less volatile). Selecting and developing molar material balance on the more volatile Component, let

$$n = n_L + n_V \quad \text{Eq. 2}$$

nz = moles of the more volatile component in the system

$n_L x$ = moles of the more volatile component in the liquid

$n_V y$ = moles of the more volatile component in the vapor

A material balance on the more volatile component gives

$$nz = n_L x + n_V y \quad \text{Eq. 3}$$

And

$$n_L = n - n_V \quad \text{Eq. 4}$$

Combining these two expressions gives

$$nz = (n-n_v) x + n_v y \quad \text{Eq. 5}$$

Rearranging the above expression, gives

$$n_v/n = (z-x)/(y-x) \quad \text{Eq. 6}$$

Similarly, if n_v is eliminated in Eq. (2.2) instead of n_L , it gives

$$n_L/n = (z-y)/(x-y) \quad \text{Eq. 7}$$

The geometrical interpretation of Eqs 5&7 is shown in Fig 2.8 which indicates that these equations can be written in terms of the two segments of the horizontal line AC. Because $z-x$ =the length of segment AB, and $y-x$ =the total length of horizontal line AC, Eq. 7 becomes

$$n_v/n = (z-x)/(y-x) = (AB/AC) \quad \text{Eq. 8}$$

Similarly, Eq8 becomes

$$n_L/n = (BC/AC) \quad \text{Eq. 9}$$

Eq.8 suggests that the ratio of the number of moles of vapor to the total number of moles in the system is equivalent to the length of the line segment

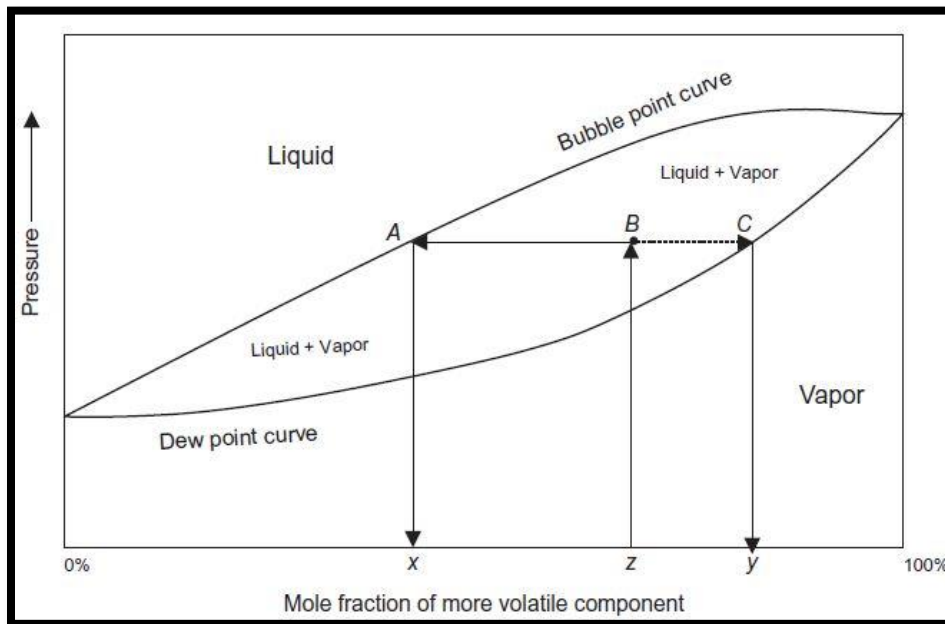


Figure 2.8: P-X diagram ⁽²⁾

AB that connects the overall composition to the liquid composition divided by the total length (P_{sia}). This rule is known as the inverse lever rule. Similarly, the ratio of the number of moles of liquid to the total number of moles in the system is proportional to the distance

from the overall composition to the vapor composition BC divided by the total length AC. It should be pointed out that the straight line that connects the liquid composition with the vapor composition, that is, line AC, is called the tie line. Note that results would have been the same if the mole fraction of the less volatile component had been plotted on the phase diagram instead of the mole fraction of the more volatile component.⁽¹⁴⁾

For this system the binary would be miscible overall concentrations at pressure greater than P_4 (liquid) or less than P_0 (vapor) between these pressures the system would be single phase only over limited concentration ranges.

2.4 Principle of Using Ternary Diagram

2.4.1 Hypothetical System with Three Components

Ternary diagram can be used to plot the phase behavior if systems contain 3-components .in some cases when there is a system of more than three components certain components can be grouped to form pseudo components .a common example is the partition of the crude into CH_4 , C2-C6 components, and C7+ components the phase behavior of ternary diagram is plotted at fixed temperature and pressure.

Ternary diagram for hypothetical components A, B, and C is shown in the figure2-8. if the three components were miscible no multiphase region would appear on the diagram. The vertex represents the pure components, and the sides of the triangle are scaled to represent the binary composition of the three possible pairs.

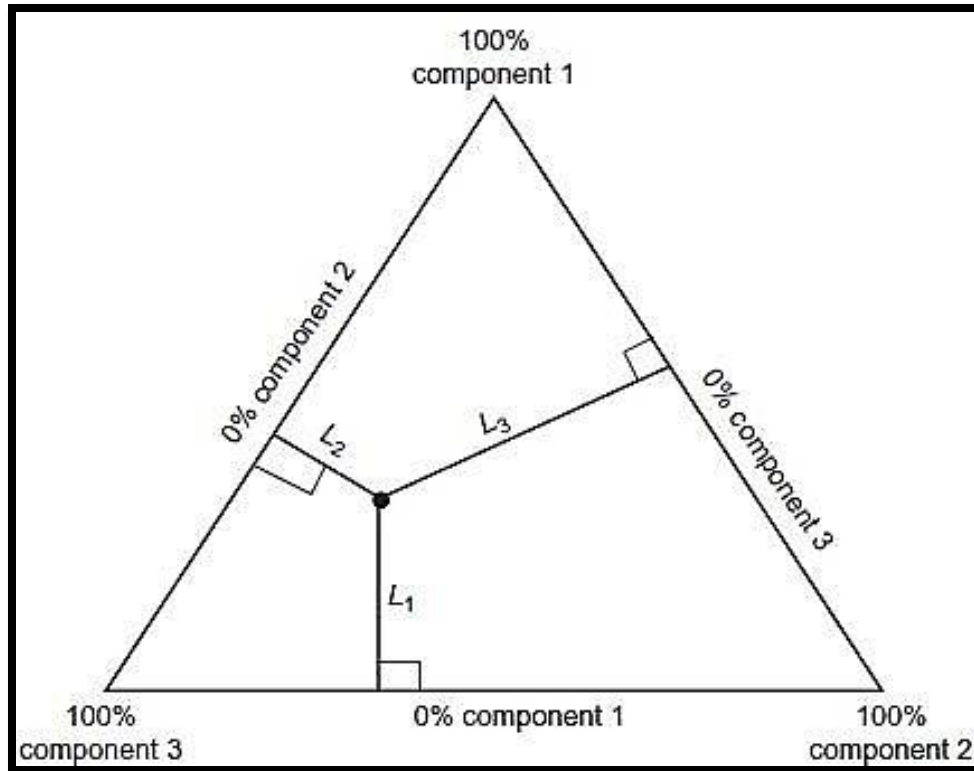


Figure 2.9: Ternary diagram ⁽²⁾

Such diagrams are based on the property of equilateral triangles that the sum of the perpendicular distances from any point to each side of the diagram is a constant and equal to the length on any of the sides. Thus, the composition x_i of the ternary system as represented by point A in the interior of the triangle of figure 2.9 is:

- Component 1 $x_1 = L_1/LT$
- Component 2 $x_2 = L_2/LT$
- Component 3 $x_3 = L_3/LT$

Where

$$LT = L_1 + L_2 + L_3 \quad \text{Eq. 10}$$

Typical features of a ternary phase diagram for a system that exists in the two-phase region at fixed pressure and temperature are shown in figure 2-9. Any mixture with an overall composition that lies inside the bimodal curve (phase envelope) will split into liquid and vapor phases. The line that connects the composition of liquid and vapor phases that are in equilibrium is called the tie line. Any other mixture with an overall composition that lies on

that tie line will split into the same liquid and vapor compositions. Only the amounts of liquid and gas change as the overall mixture composition changes from the liquid side (bubble point curve) on the bimodal curve to the vapor side (dew point curve). If the mole fractions of component in the liquid, vapor, and overall mixture are x_i , y_i , and z_i , the fraction of the total number of moles in the liquid phase n_l is given by

$$n_l = (y_i - z_i) / (y_i - x_i) \quad \text{Eq. 11}$$

This expression is another lever rule, similar to that described for binary diagrams. The liquid and vapor portions of the binodal curve (phase envelope) meet at the plait point (critical point), where the liquid and vapor phases are identical.⁽¹⁴⁾

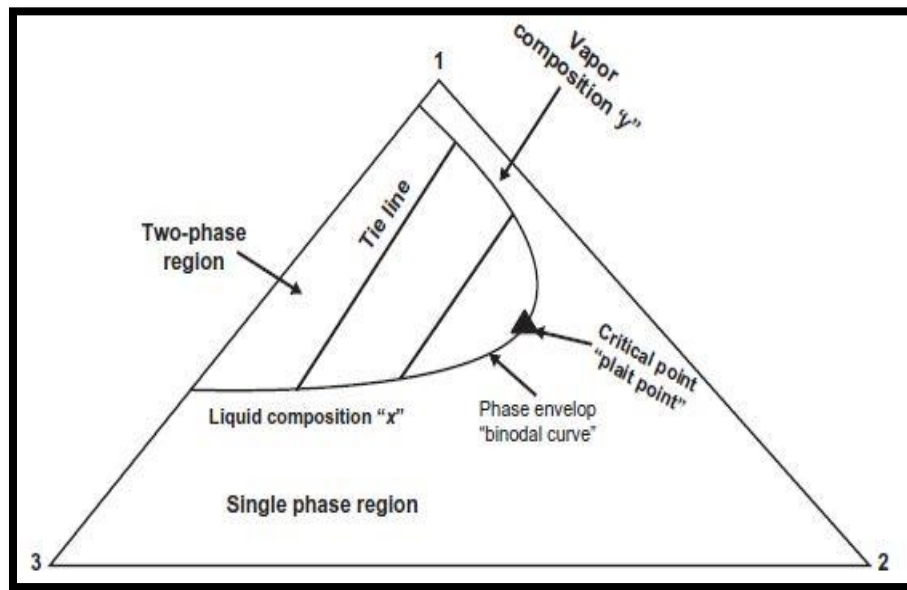


Figure 2.10 : Properties of the Ternary diagram ⁽²⁾

2.4.2 Multi components system (Pseudo-ternary Diagram)

Reservoir fluids are complex mixture of hydrocarbons with components ranging from methane to C40+. In miscible displacement processes the fluid that has to be come miscible with crude oil is injected into reservoir. The injection of the fluid alters the chemical composition of the total system and thus the thermodynamic properties. Strict thermodynamic analysis of such a process is impossible because all chemical constituents need to identified and the compositions are known and also the availability of thermodynamic properties. These conditions are never met in practice. As mentioned before

the experience has shown that complex hydrocarbon system can be represented with groups of hydrocarbons that preserve many of important properties of the system. A typical representation of the system is a Pseudo-ternary diagram with C1, C2-C6, and C7+ as pseudo components as shown in Figure 2.11

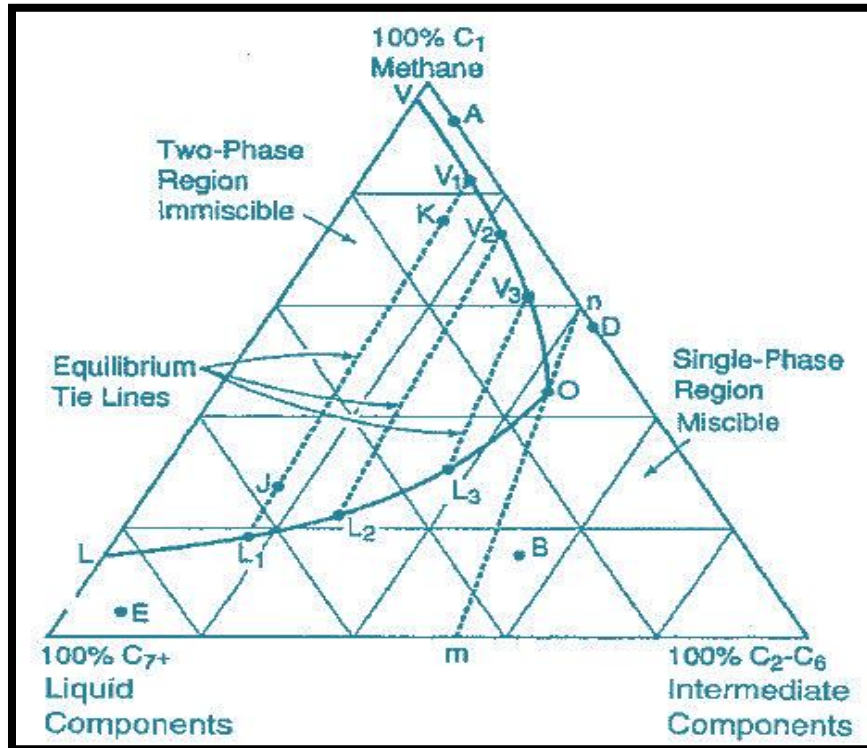


Figure 2.11: Pseudo-Ternary Diagram ⁽¹⁾

The pressure and temperature are remained constant, thus the concentration of two components are sufficient to define any point on the diagram. Phase boundary VO is saturated vapor curve and boundary LO is saturated liquid curve. It should be noted that the important assumption in using pseudo-components and pseudo ternary diagram is that the composition of pseudo-components does not change in the different phases .for instance the relative composition of components that make up the C7+ pseudo-components must be approximately the same in the liquid phase as in the equilibrium vapor phase .if this does not hold then the use of pseudo ternary diagram could lead to a serious errors in the calculation of phase compositions and amounts .

However this assumption for the lighter components C2 through C6 (C2-C6) Pseudo-component is not valid. C2-C6 pseudo components tended to go to the vapor phase while the heavier components moved to the liquid phase. This movement can be seen for example by noticing the ratio of C2/C6 in vapor and liquid phases. The ratio is significantly larger in the vapor phase than in the liquid phase. Nonetheless, a pseudo-ternary diagram is often a useful approximation, especially in describing how miscibility is achieved in the displacement processes.^(1,15)

2.5 Miscible Gas Injection Mechanisms

2.5.1 First Contact Miscibility (FCM) Process

An FCM process typically consists of injecting a small amount of primary slug such as low molecular-weight hydrocarbons (LPG or propane) that are completely soluble with oil at most reservoir condition followed by a less expensive slug secondary slug such as methane (CH₄). It is economically important to determine the size of the slug .in the best possible way the secondary slug has to be miscible with primary slug, and thus the phase behavior has to be considered at both trailing and leading edges of the primary slug (in front and the back of the primary slug. if the slugs are immiscible then a residual saturation of primary slug will be trapped in the rock.⁽¹⁾

The displacement of crude by a primary slug (solvent) can be shown on the schematic ternary diagram in Figure 2-11. The crude is in the interior of the ternary, indicating some of the light component is present initially in the crude. If a straight line dilution path between the primary slug (solvent) and the crude do not intersect the two-phase region, the displacement will consist of a single hydrocarbon phase that changes in composition from crude to undiluted primary slug (solvent) through the solvent oil mixing zone. The dilution path is linear since the only mechanism for mixing is dispersion, there being no water or fractional flow effects associated with the single hydrocarbon phase. A displacement that occurs entirely within one hydrocarbon Phase is first-contact miscible.⁽²⁾

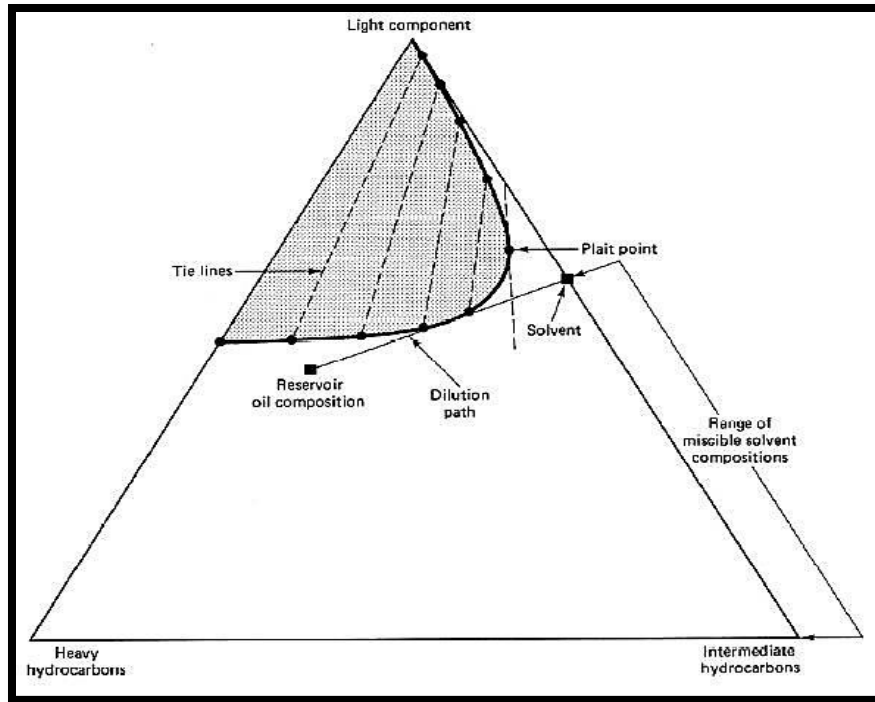


Figure 2.12: Schematic of the first-contact miscible process ⁽²⁾

The primary slug that is a liquid such as propane and butane (solvent) sometimes is not completely miscible with reservoir oil. Because it may form a precipitation of asphalts when they contact with certain type of crude oils .if a significant amount of crude oil displaced miscibly in a reservoir that it deasphalted by slug material (propane is used as deasphalting agent in the refineries). Asphalt could plug some pores and reduce the effective permeability .however when oil is displaced by primary slug a transition zone form between the primary slug and undeasphalted reservoir oil. This zone is miscible behind with primary slug and from front with oil this will allow the miscible displacement process to proceed. Asphaltene deposition could cause a serious problems near to the production and injection wells .another consideration that is related to phase behavior should be mentioned is the possibility that mixing will occur between the three fluid included in the displacement . “a significant mixing or dispersion does occur in the reservoir the effect of dispersion is to dilute the primary slug by both reservoir oil and secondary slug.”^(1,2)

2.5.2 Minimum Miscibility pressure (MMP)

is one of the important parameters that has to be considered when designing a miscible gas flooding project .MMP defined as minimum pressure at which the injected gas become miscible with crude oil. It is necessary to operate the miscible gas flooding projects close to this pressure for getting the maximum benefit from these projects.

There are several techniques for measurements and prediction of the Minimum Miscibility Pressure

a- Experimental measurements of MMP

- 1- The slim-tube test
- 2- A rising Bubble apparatus (RBA)
- 3- Vanishing interfacial tension (VIT)

b- Prediction of MMP

- 1- Empirical correlation based on experimental results
- 2- Phase-behavior calculation based on an EOS and computer modeling

2.6 MCM processes (Vaporizing Gas Drive, Condensing Gas Drive, and Combined Drive (VGD+CGD) :

Some solvents are not directly miscible with reservoir oils, but under appropriate conditions of pressure and solvent composition these solvents can achieve miscibility in-situ by mass transfer of oil and solvent components through repeated contact with the reservoir oil. Miscibility achieved in this manner is called "multiple-contact" or "dynamic" miscibility. The vaporizing-gas drive process achieves dynamic miscibility by in situ vaporization of the intermediate molecular-weight hydrocarbons from the reservoir oil into the injected gas. Dynamic miscibility is achieved in the condensing-gas drive process by in-situ transfer of intermediate-molecular-weight hydrocarbons from the injected gas into the reservoir oil. The natural gas at high pressure and natural gas with appreciable concentrations of intermediate-molecular-weight hydrocarbons are injectants in vaporizing-gas drive and condensing-gas drive floods. Flue gas and nitrogen also have been found to achieve dynamic miscibility at high pressures with some oils by the vaporizing-gas drive mechanism. CO₂ has several advantages compared with hydrocarbon solvents or flue gas. It often achieves dynamic miscibility at a significantly lower pressure than Natural gas or flue gas, so more reservoirs

can be miscibly flooded with CO₂ than with these other gases. CO₂ can be developed and transported to favorably located oil fields by pipeline at acceptable costs.⁽⁵⁾

2.6.1 Vaporizing Gas (Lean Gas) Displacement

In Vaporizing-Gas Drive Process High-Pressure Gas Injection displacement the mechanism for achieving dynamic miscibility relies on in-situ-vaporization of low-MW hydrocarbons (C₂ to C₆) from the reservoir oil into the injected gas to create a miscible transition zone. This method for attaining miscibility has been called both the “high-pressure” and the “vaporizing” gas process. Miscibility can be achieved by this mechanism with methane, natural gas, flue gas, CO₂; nitrogen as injection gases, provided that the miscibility pressure required is physically possible in the reservoir.

The concept was introduced in 1950; the process requires a higher pressure than normally used in conventional, immiscible gas drives. This increase in oil recovery at higher pressures is believed to result from : (1).absorption of injected gas by the oil to cause volume increase in oil phase in the reservoir : (2) enrichment of gas resulting from vaporization of low –boiling- ranges hydrocarbons from oil to injected gas phase; and (3) reduction in the viscosity and the interfacial tension(IFT) between the displacing and displaced phase as a result of mixing .the mechanism of miscible displacement by high pressure gas injection has been described in details by several investigators. Figure2.13 a pseudo ternary diagram illustrates the phase relationship of the mechanism. Initially a relatively lean gas of composition C is injected into reservoir oil A.

a line connecting A and C cross the two phase region EBO indicating that the displacement between these two phase will not be upon a first contact miscibility however as gas C moves through reservoir it will become enriched because of the effect of vaporization ,until ultimately reaches a critical composition B. this fluid now is miscible in all proportion with reservoir fluid A or any reservoir fluid lying at the right of I-M boundary .

Miscibility by the vaporizing- gas drive mechanism also can be achieved by using another gases such as nitrogen and flue gas(about 88% nitrogen and 12% CO₂) even though these gases have low solubility in oil .because the cricondenbar pressure for nitrogen and for low-intermediate-MW hydrocarbons is high ,the pressures required for dynamic miscibility

depends on the methane content of the in-situ oil also the concentration of other hydrocarbons in the oil .if the reservoir contains high methane concentration then the pressure required to attain vaporizing gas drive miscibility with the nitrogen will be minimized .also a high reservoir temperatures promote miscibility. (16, 18, 19, 20, 21)

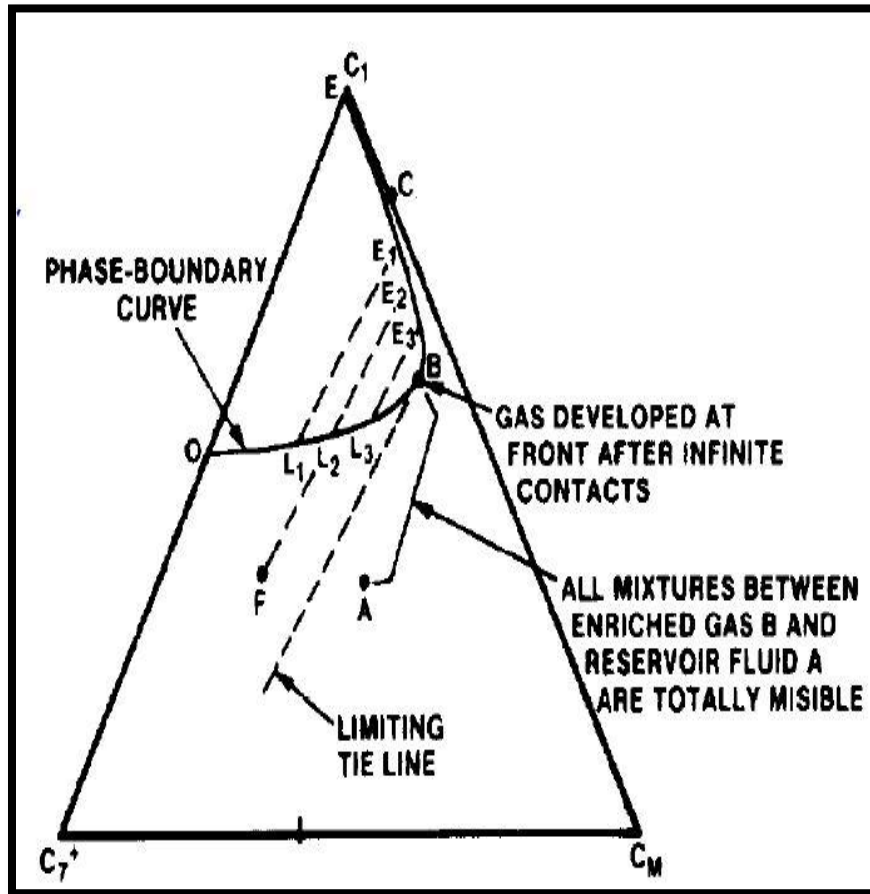


Figure 2.13: illustration of miscible displacement (high-pressure gas injection) ⁽⁶⁾

the vaporizing gas drive process can be described on pseudo-ternary diagram assuming that thermodynamic equilibrium exists between different phases .this assumption taught to be valid at reservoir displacement conditions where the advance rates are very low (except near to wellbore vicinity). The process operates conceptually as follows see figure2.14.

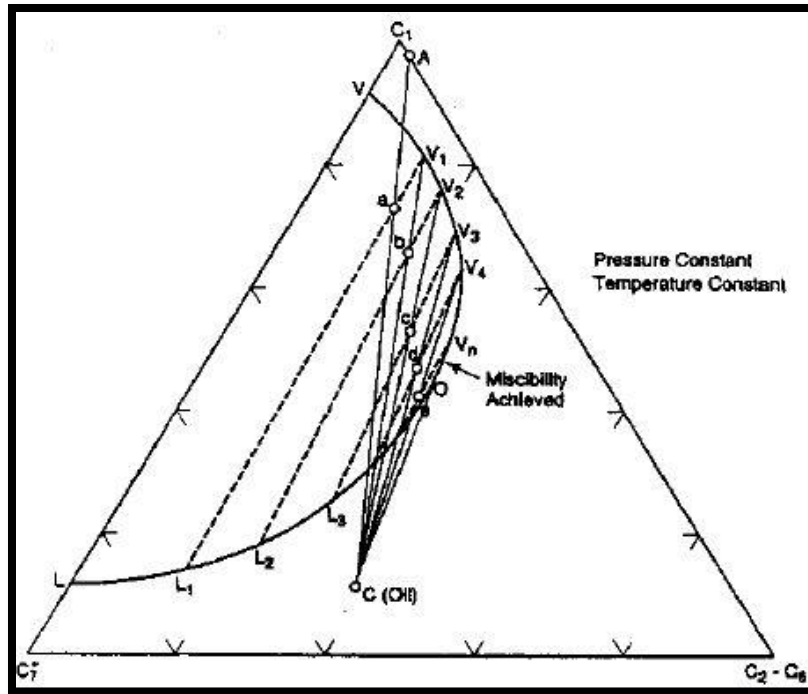


Figure 2.14: vaporizing gas drive process ⁽²⁾

- 1- At the leading edge of the front the gas A mixes with the oil C the resulting composition is along AC. Say at point a
- 2- The mixture in the two-phase region will split into a vapor V1 and a liquid L2.
- 3- The vapor V1 moves in front of the liquid L1 and contacts a new oil of composition C. the resulting mixture is along line V1 C, let say b.
- 4- Mixture b will split into vapor V2 and Liquid L2.
- 5- The process continues with changing in vapor phase composition along the saturated vapor curve, V3, V4...etc.
- 6- Finally at point e the vapor becomes miscible with oil C in all proportions as the mixing line lies entirely in the single phase region.

The minimum pressure at which the limiting tie-line just passes through the oil reservoir composition is called MMP. That is the minimum miscibility pressure at which in-situ miscibility can be achieved in MCM process for a specified fluid system. In the vaporizing MCM process the injected gas composition must lie to the left and the reservoir fluid must lie to the right of the limiting tie-line.

2.6.2 Condensing gas drive (or enriched gas drive)

A condensing-gas drive is that process of oil displacement by gas that makes use of an injected gas containing low-MW hydrocarbon (C₂ to C₄) components, which condense in the oil being displaced. To affect conditions of miscible displacement, sufficient quantities of low- MW components must be condensed into the oil to generate a critical mixture at the displacing front. An aid helpful for understanding the process is a pseudo-ternary phase diagram Figure 2-14a. This phase diagram represents the hydrocarbon system, composed of the lean gas, the NGL, and the reservoir crude, as three pseudo-components at varying compositions and constant temperature and pressure. The three components are methane (CH₄) an ethane-propane butane fraction (C₂-C₄), and a pentanes and heavier fraction (C₅+). In the case of Fig 2.15 the lean gas is 100% methane and the NGL is 100% C₂ -C₄. The reservoir crude is a more complex mixture. The fourth fluid on the Figure is an enriched gas that is 60 mole % methane and 40 mole % ethane-propane-butane. The diagram includes the phase envelope, tie lines, the plait point (Hereafter called the critical point), and the four fluid compositions.

Figure 2.15 will be used to illustrate how Multiple-contact miscibility is developed in the reservoir. As the enriched gas is injected into the reservoir and contacts the crude, the reservoir crude and enriched gas will mix and the resulting composition may be represented by the Point A. This mixture will flash into a liquid (AL) and a vapor (AV). As more enriched gas is added, it will mix with the liquid (AL) and form a composition represented by Point B. This mixture will flash into a liquid (BL) and a vapor (BV). Again, more enriched gas is injected which mixes with the liquid (BL) and forms a new system with a composition of point C. The process repeats in this fashion until a liquid is formed that will not flash into two phases when mixed with the enriched gas. This is represented graphically when a line is drawn between two points, such as between the enriched gas and E, and it does not cross a phase boundary. At this time, a miscible displacement will begin. The enriched gas will miscibly displace liquid EL, which will miscibly displace liquid DL, and so on. The vapors are also miscibly displaced.

In the diagram, it can be seen that any enriched fluid to the right of the tie line which passes through the critical point (the limiting tie line), is capable of producing a miscible

displacement by "**stair-stepping**" the crude around the phase envelope until it reaches a liquid composition which is miscible with the enriched gas. In the minimum enrichment case, this liquid is at the critical point. The miscibility was achieved through the transfer of intermediate weight hydrocarbons from the enriched gas to the crude. 40%.^(17,16)

The MMP in condensing gas process is the minimum pressure at which the limiting tie –line just passes through the composition of the injected fluid .the injected fluid composition must lie to the right of limiting-tie line while the oil composition must lie to the left. In the condensing gas drive process there is alternative to increase the pressure in that the injected gas composition can be enriched to achieve miscibility.at fixed reservoir pressure the minimum enrichment at which the limiting tie line passes through the injection gas composition is called the Minimum miscibility enrichment gas (MME).

More recent investigations of enriched gas process have shown an existence of another mechanism .this due to the fact that a combination of (condensation and vaporization) is responsible for high displacement efficiency in the this process. Zick and stalkup prove the existence of the mechanism as the following

1. When enriched gas contacts reservoir. it will make it lighter because the lighter components in the injected gas will condense in the oil .the gas moves faster than oil so that depleted gas moves ahead .additional fresh injected gas contacts fresh oil and continuous decreasing its density, if this continued until the oil became miscible with the injected gas then it would not be a condensing gas process as previously described. However there is a counter effect that as oil the oil strips the lighter components from enriched injected gas the gas strips the heavier components from the oil. If this what actually happens then the development of miscibility ceases. well actually the downstream injection point is a positive mechanism because period of time the oil will be enriched with lighter components therefore the components do not condense out of the gas into the oil but the gas strips oil intermediate components).^(1,23,24,25)
2. Due to the limitation of applying the pseudo-ternary diagram representation for a system having more than three components therefore it is not easy to represent combined gas drive condensing /vaporizing process straight away but it is still

applicable in case of illustrating one problem at a time either condensing or vaporizing gas drive .

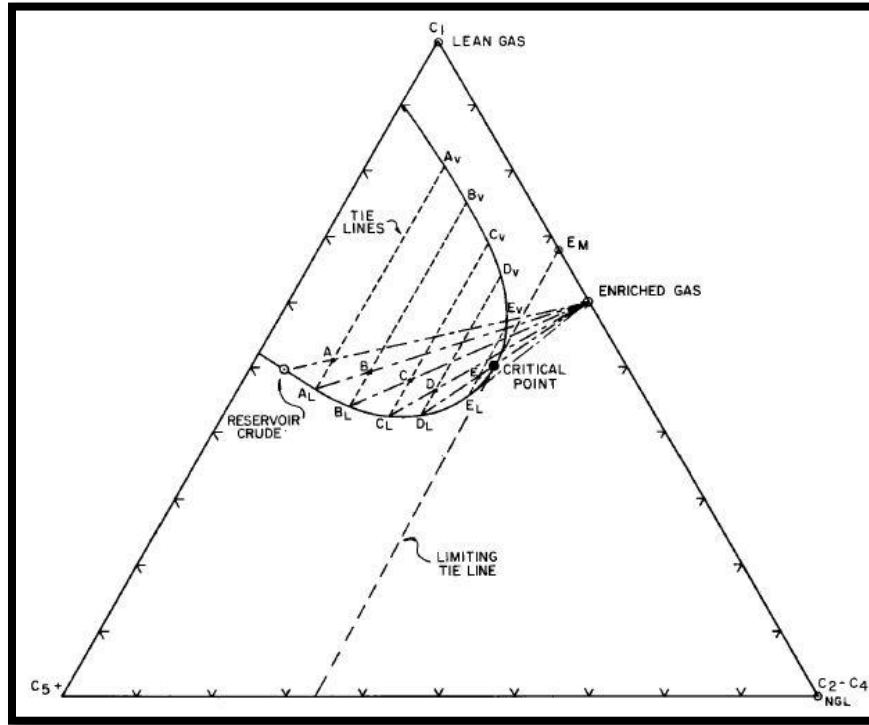


Figure 2.15: condensing gas drive process ⁽¹⁷⁾

2.6.3 Critical Displacement (stair-stepping)

The displacement at the critical point or a critical mixture occurs when the two phases flash into one and the composition changes in the reservoir from displacing Gas D to a critical mixture at the front to Oil 3, Oil 2, Oil 1, and displaced Oil D without a change in phase present as is normally represented by gas-oil interfacial surfaces ⁽¹³⁾

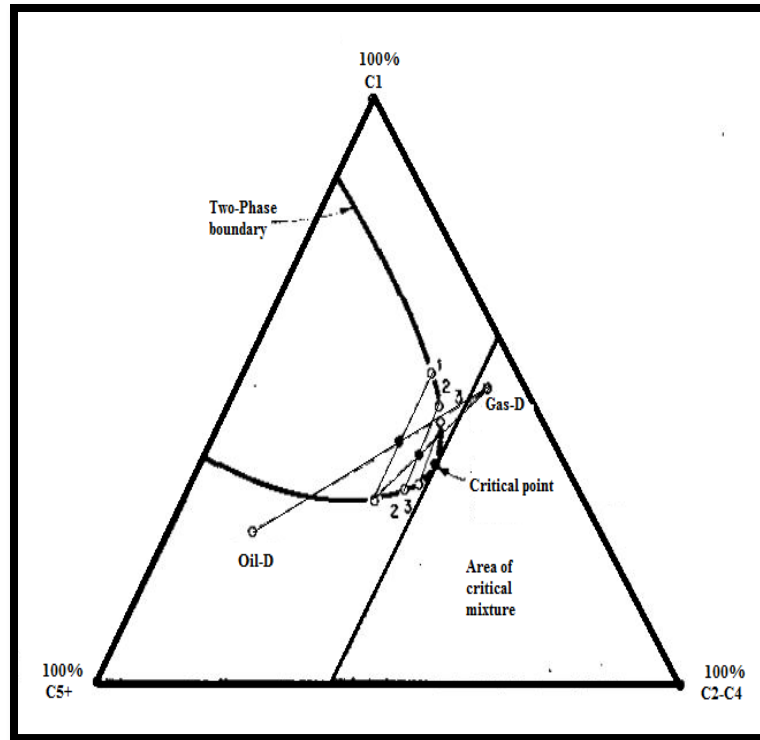


Figure 2.16: Condensing gas-drive critical displacement on triangular graph ⁽²⁾

2.6.4 CO₂ Miscible displacement processes

CO₂ Miscible Process is the fourth mechanism for achieving dynamic or multiple-contact miscibility involves the injection of a solvent gas (such as CO₂, ethane, N₂O, or H₂S), which is not first-contact miscible with reservoir oils but is highly soluble in them. Table 2.1 shows the critical temperatures and solubility of some of these solvent gases for comparison with methane.

Table 2.1: the critical temperatures and solubility of some of these solvent gases for comparison with methane.

Critical Temperature and Solubility of Solvent Gases			
Gases	Critical Temperature		solubility of gases in a crude oil at 1000psi and 135F (scf/bbl)
	F	C	
<u>Carbon dioxide</u>	88	31	634
<u>Ethane</u>	99	32	640
<u>Hydrogen sulfide</u>	213	100	522
<u>Methane</u>	-117	-82	209

The critical temperatures of these gases are close to reservoir temperatures and the gases are very compressible at these conditions Figure 2.17

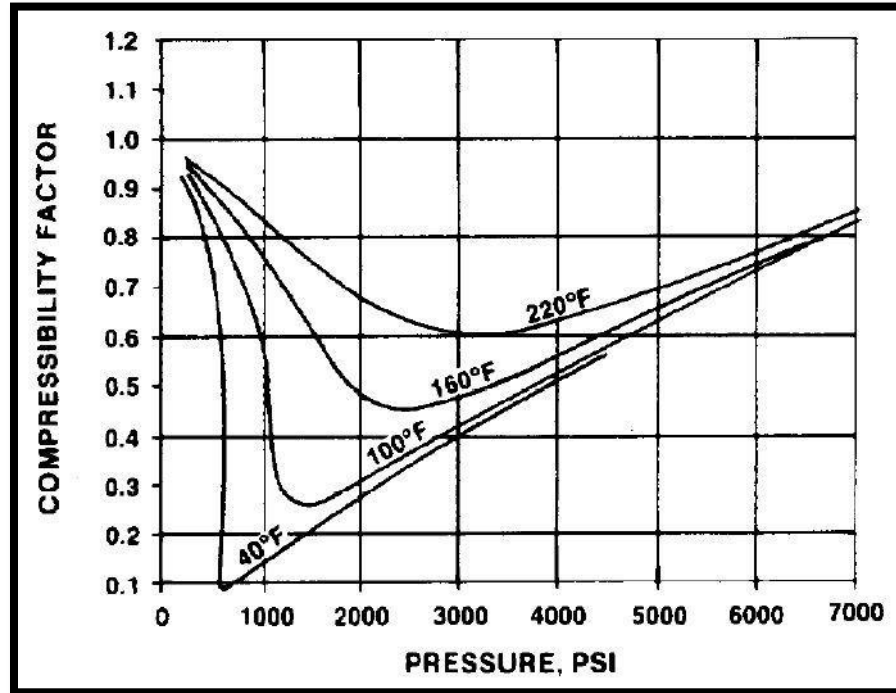


Figure 2.17: Compressibility factor for CO2

CO₂, from the standpoint of availability, cost, and operational handling, is the most practical of these fluids. As a liquid, or as a dense, critical fluid solvent, CO₂ extracts from the oil hydrocarbons of higher MW than the predominantly C₂ to C₄ hydrocarbons that methane vaporizes. In addition to the C₂ to C₄ hydrocarbons, these fluids include C₅ to C₁₂ hydrocarbons from the gasoline fraction of the crude and even C₁₃ to C₃₀ gas-oil fractions of the crude. In fact, the C₂ to C₄ hydrocarbons are not needed to achieve miscibility, so reservoir oils, which are depleted in methane and the low-MW hydrocarbons (dead oils), are still candidates for CO₂ miscible flooding. This greatly increases the application potential for miscible Displacement. After multiple contacts with the reservoir oil, the hydrocarbon-enriched-CO₂ phase miscibly displaces reservoir oil. ^(26, 27, 28, 29, 30)

An ideal description of the CO₂ miscible displacement on pseudo-ternary diagram is the same as the vaporizing process. At temperature of approximately 120F the phase behavior of the CO₂/ (C₂-C₆)/C₇+ system has the same appearance as C₁/ (C₂-C₆)/C₇+ system. But at

the same temperature and pressure the 2 phase envelope for CO₂ system is much smaller than for CH₄ system .see figure 2.18

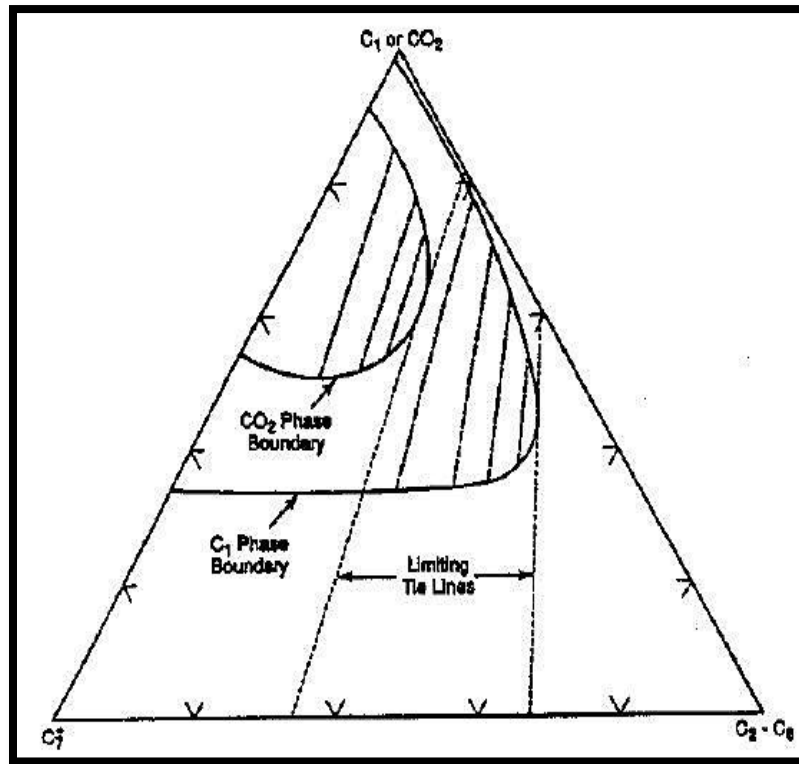


Figure 2.18: CO₂ Process

As shown in Figure 2.18 the limiting tie line is shifted to the left comparing with CH₄ system and also tends to have slope that is more parallel CO₂/C₇₊ side of pseudo-ternary diagram.as a result of that the miscibility between CO₂ and oil reservoir can be achieved at lower pressure than between oil and methane .This characteristic of CO₂ makes it much more favorable than methane.

At lower temperature (above 120 F or less), CO₂ phase envelope is often consists of either two liquid phases or two liquid phases and vapor phase. This makes the description of the process on pseudo ternary diagram much more complex. It has been revealed that there are two typical type of phase behavior in CO₂/Hydrocarbon systems. ⁽³¹⁻³²⁾

Figure 2.19 shows the simplest type of the phase behavior the x-axis is the concentration of CO₂ in the CO₂/hydrocarbon mixture.in this type the two phase region in the phase envelope consists of liquid and vapor in equilibrium .bubble point (100% liquid) and Dew point

(100 % vapor) connects at the so called critical point .at constant temperature and pressure the phase boundary on pseudo-ternary diagram would be of the form in Figure 2.19

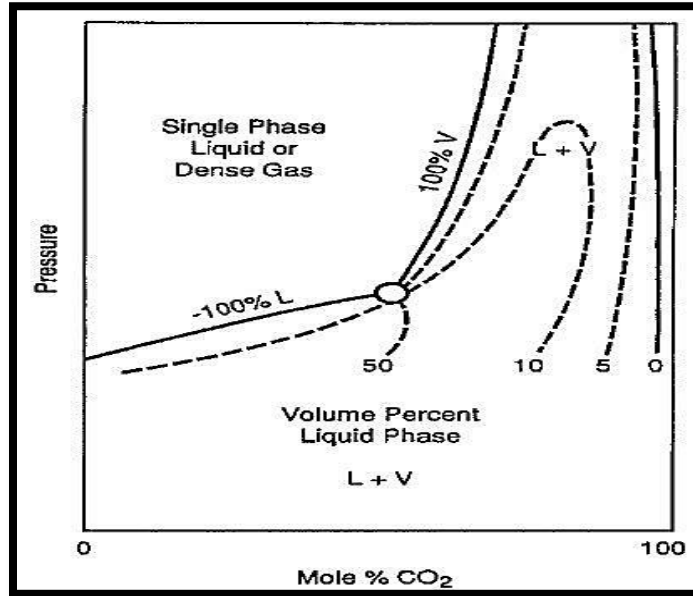


Figure 2.19: CO2/Hydrocarbon system at temperature above 120F

Figure 2.20 shows the phase behavior of CO2 at temperature below 120 F. the change that occur in the two-phase phase region in the phase envelope can be described as the following:

- 1- At lower pressures the two-phase region will only contain liquid and vapor at equilibrium
- 2- at higher pressure a liquid/liquid two-phase region exists see pseudo ternary diagram for case2
- 3- at intermediate pressure there is a relatively small composition region in which the three phases exist in equilibrium

Pseudo-ternary diagram representations for each case are shown below:-

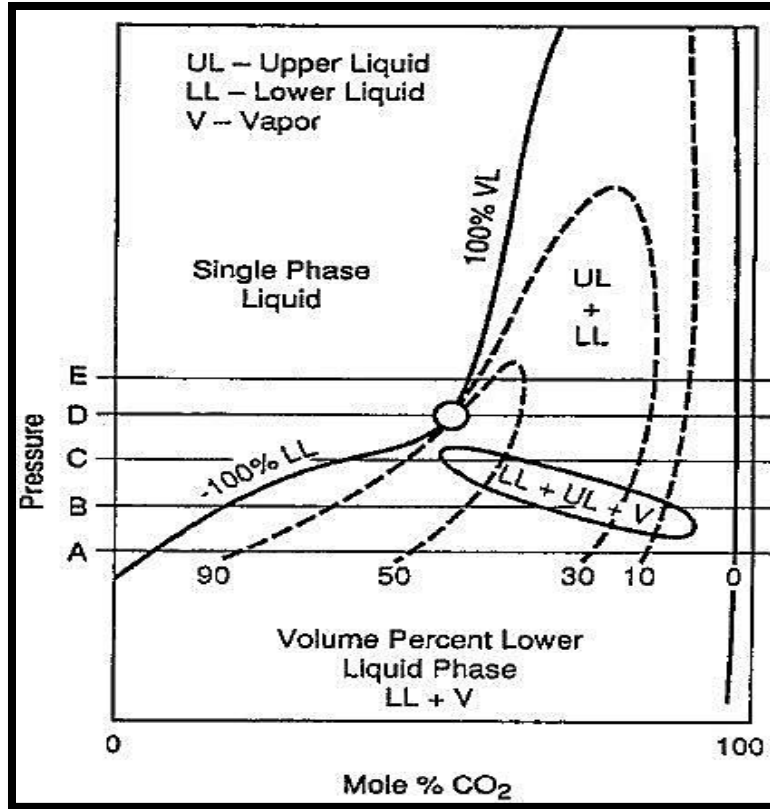


Figure 2.20: CO₂/Hydrocarbon system at temperature below 120F

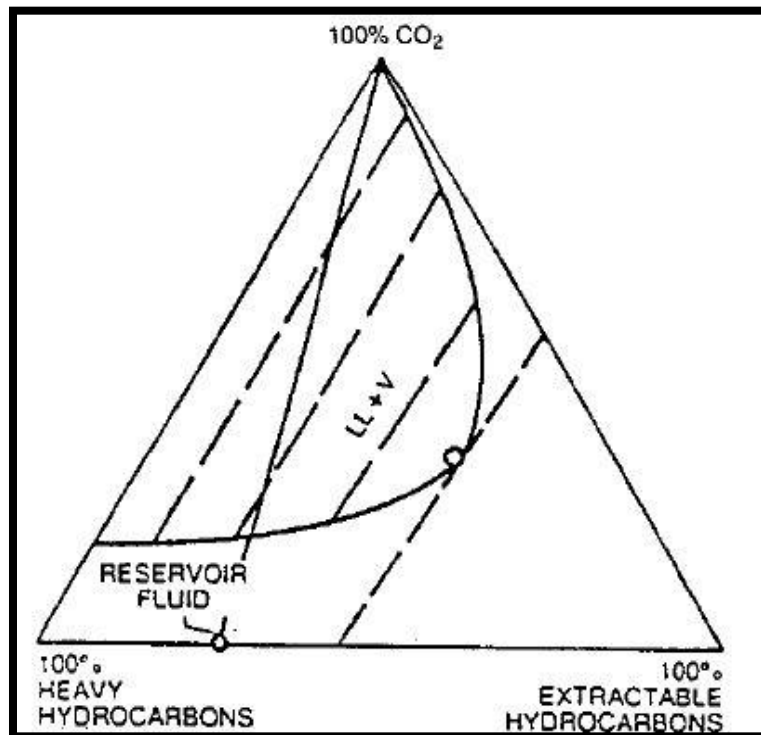


Figure 2.21: case 1

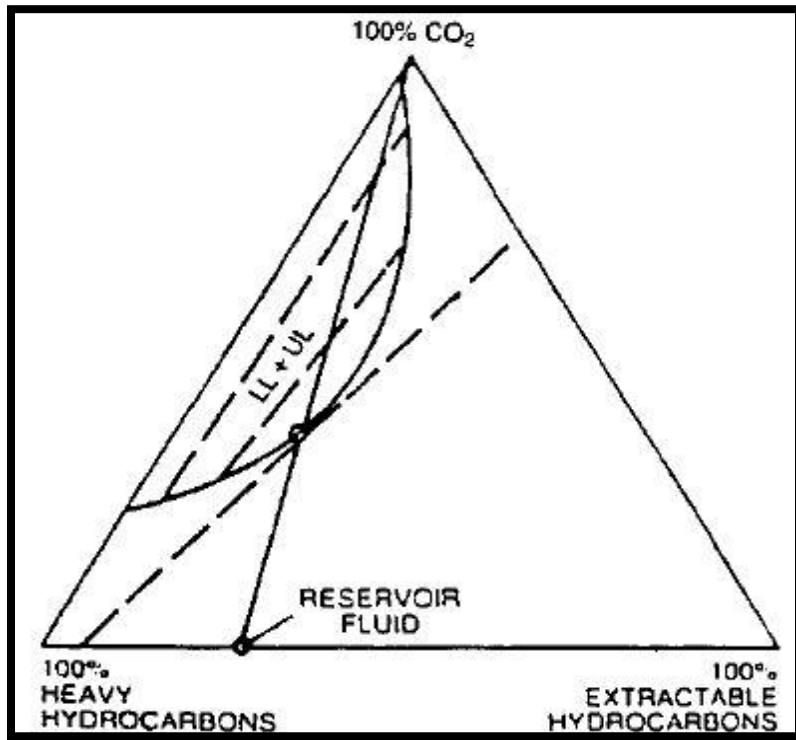


Figure 2.22: Case 2

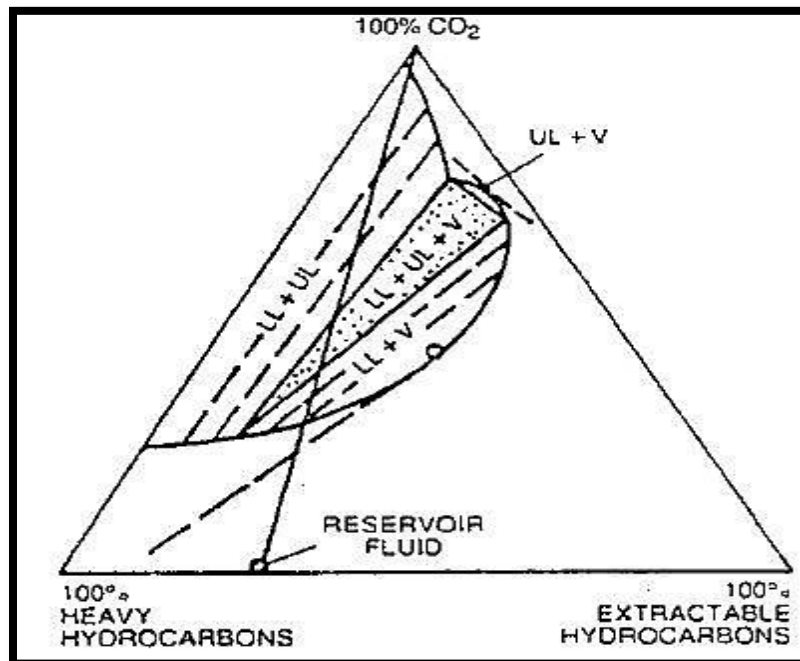


Figure 2.23: Case 3

2.7 Summary of the Classification of Solvent Displacement

Figure 2.24 summarizes the classification of solvent displacements. A dilution path (I_2 - J_3) that does not pass through the two-phase region is a first-contact miscible displacement. A dilution path entirely on the two-phase side of the critical tie line constitutes immiscible displacement (I_1 - J_1). When initial and injected compositions are on opposite sides of the critical tie line, the displacement is either vaporizing gas drive (I_2 - J_1) or a condensing gas drive (I_1 - J_2). The last two cases are developed or multiple-contact miscible displacement. ⁽²⁾

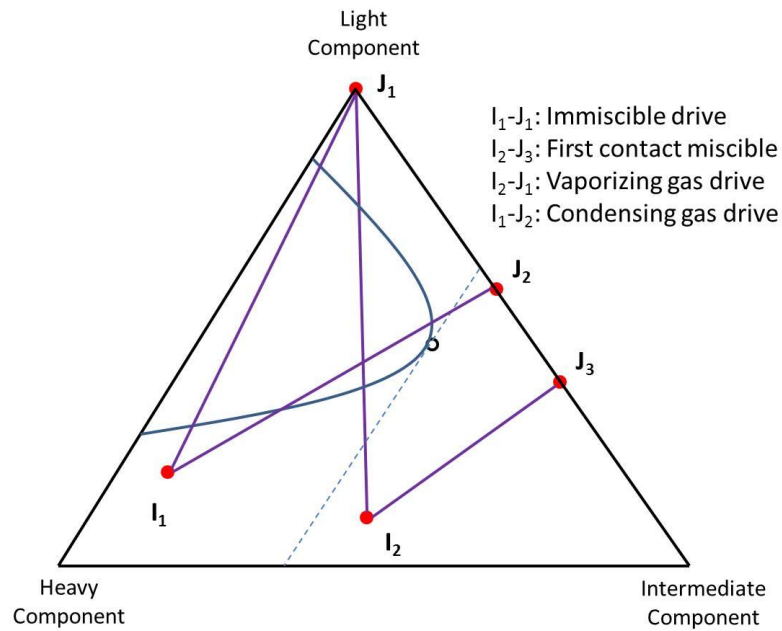


Figure 2.24: classification of solvent displacement

The other mechanisms in miscible displacement that lead to increasing in the oil recovery are:

1- Mobility control

The mobility is a key factor to develop a successful flood .injecting CO₂ into the crude oil will change the properties of crude oil more specifically its viscosity and by the reduction of the crude oil viscosity the flow-ability of the oil would be increased significantly. ⁽⁷⁾

2- Swelling

The oil volume increases as a result of CO₂ dissolution in the oil phase. Also the density of the oil will be decreased .therefore the swelling increases the recovery factor as the residual

oil saturation is decreased .the mass of the oil remaining in reservoir is lower than if the residual oil was CO₂ free. ⁽⁷⁾

2.8 Methods of Assessing and Evaluating Miscible Gas Injection Projects

2.9 Solvent Phase Behavior Experiments

Solvent phase behavior determines the character of a solvent flood, so that it is important to dedicate a section to some of the common experiments used to measure phase behavior.

2.9.1 Single Contact

In a single-contact experiment, a known amount of solvent is charged into a transparent pressure cell containing a known amount of crude oil. After equilibrium is established at the desired temperature and pressure, a small amount of each phase is withdrawn. The phase compositions represent the ends of an equilibrium tie line. Only the composition of one phase need be measured since the composition of the other phase can be calculated from material balance. Single-contact experiments are useful for measuring P-z diagrams since the pressure can be changed, at fixed overall composition, by changing the cell volume. If the experiment is repeated for various amounts of solvent, the single-contact experiment traces a dilution path on a ternary diagram between the solvent and crude.

2.9.2 Multiple Contact Experiment

In this experiment known amounts of solvent and crude are charged to a transparent pressure cell as in the single-contact experiment, but after equilibration, the upper phase is decanted and mixed in a second cell with fresh crude. The lower phase in the cell is similarly mixed with fresh solvent. The upper phase is repeatedly decanted in this manner to simulate, discretely, the mixing that would take place at the forward contacts of the solvent–crude mixing zone. The successive mixings with the lower phase are the reverse contacts. All contacts are at a fixed temperature and pressure. The solvent enrichment in the forward contacts or the crude enrichment in the reverse contacts can cause one of the phases to disappear. This is exactly what is predicted by the arguments used in the process classification section: A single phase cell in the forward contacts indicates a vaporizing gas drive; in the reverse contacts, a condensing gas drive; and two or more phases in all contacts, an immiscible

process. If the original cell is single phase for all combinations of solvent and crude oil, the process is first-contact miscible. The experiment depends somewhat on the initial charges to the first cell, so the results are no more than indications of process classification. If phase compositions are measured at every step, the binodal curve and tie lines on a ternary diagram are established. This experiment is a convenient way to determine complete ternary equilibrium data figure 2.25 shows a schematic diagram for multiple contact experiment. ⁽²⁹⁾

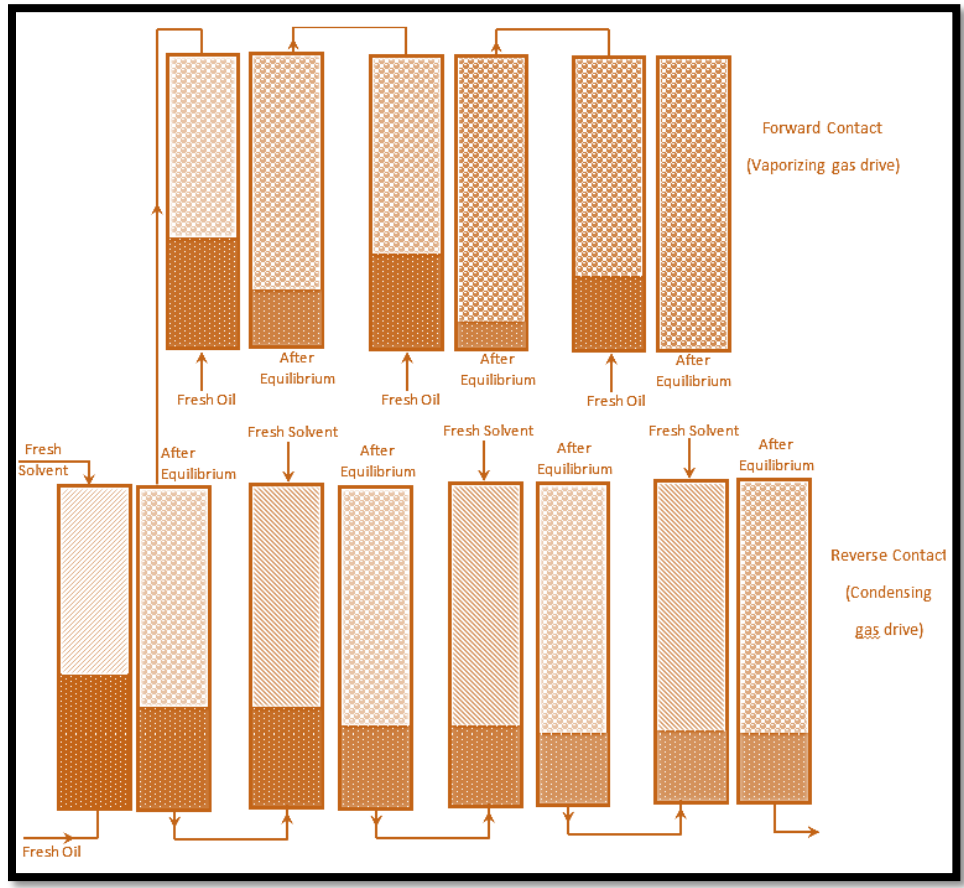


Figure 2.25: a schematic diagram of multiple contact experiment

a- Multiple Contacts Miscibility (Forward and Backward):

This test it normally done to simulate multiple contact process when the solvent (CO₂) is injected and contact the reservoir fluid .there are some factors that make the CO₂ very useful as a displacing fluid. These factors are:

- 1- the solubility of CO₂ in the oil improves the mass transfer rates
- 2- the operation can be adjusted by changing temperature and pressure

- 3- Its physical properties (low viscosity and interfacial tension IFT), and high diffusivity give at the advantage for being widely used in extraction process (vaporizing or extracting hydrocarbons from crude oil).

The forward and backward methods in multiple contact miscibility are different in terms of experimental method and the reason behind them. The forward multiple contact tests simulate the conditions at injection front or transition see figure (2.26). At which the oil and gas are contacted at reservoir pressure and temperature. The equilibrated gas in each contact is used as the injected gas to contact the fresh oil reservoir .this procedure is continued until the injected gas either becomes miscible or achieves equilibrium with it. In other word the forward method is following the injected gas front that continuously being enriched with hydrocarbons and this front is always in contact with fresh oil.

The backward multiple contact miscibility as shown in figure 1 simulates the immiscible oil displacement or swept zone flooding process which what takes place at the injection point in this test equilibrated oil after each contact was next mixed with fresh CO₂ at reservoir pressure and temperature. In other word backward is the method when the oil reservoir is continuously depleted from its intermediate hydrocarbons by injected gas which makes the oil heavier and heavier. ⁽³³⁾

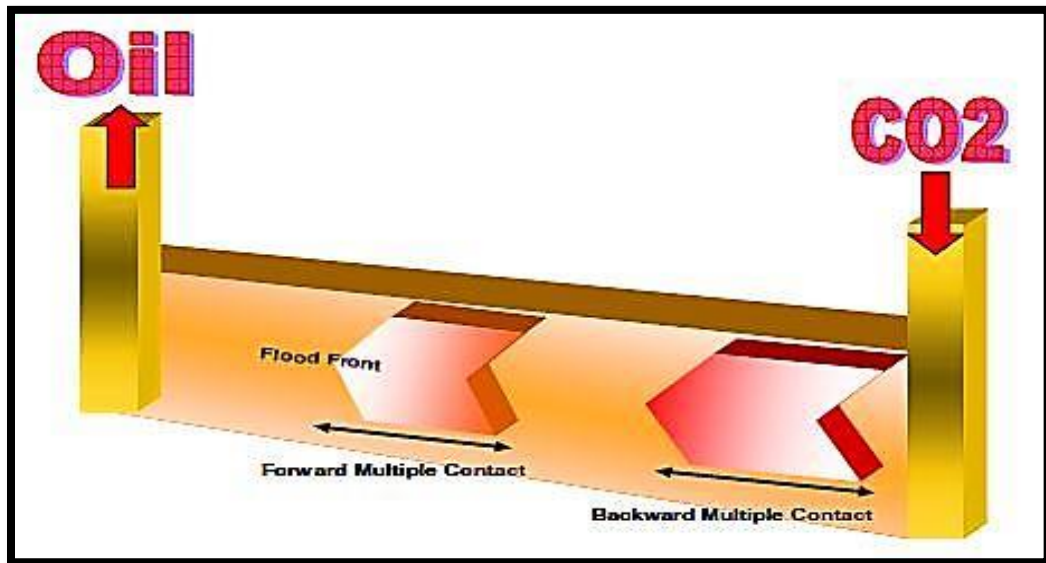


Figure 2.26: Picture diagram for forward and backward multiple contacts ⁽³³⁾

2.9.3 Swelling Test

Is the most common multi-contact PVT test .during a swelling test, gas with a known composition is added to original reservoir oil at varying proportions in a series of steps. After each addition of specific volume of gas, the overall mixture is quantified in terms of the molar percentage of injection gas .then the PVT cell is pressured to saturation pressure of new mixture (only one phase is present).the gas addition starts at saturation pressure of reservoir fluid (bubble point pressure for oil, dew point pressure for gas) and addition of gas continuous to approximately 80 mole% injected gas in the fluid sample.

Data obtained from such a test is:

- The relationship between saturation pressure to volume of gas injected
- The saturation pressure may change from bubble point to dew point after a significant gas injection
- The volume of the saturated fluid mixture in relation to volume of original saturated reservoir oil

The data derived from this test discovers the ability of injected gas to dissolve in the reservoir oil and associated swelling of the resulting mixture .these data can also be used to characterize the mixing of each separate hydrocarbon component and the effect of mixing on the volume increase of saturated fluid and testing the ability of the hydrocarbon mixture to dissolve injection gas.⁽³⁷⁾

2.9.4 CO₂ Core Floods

CO₂ core floods are very useful experiments while the interpretation of these experiments seems to be a very hard task .this is due to the fact that the core flood results are often affected by many phenomena that may not be recurring equally in the reservoir such as viscous fingering, gravity segregation, channeling or bypassing of the oil due to core heterogeneities. The purpose of core floods has always been targeting the understanding of displacement mechanisms rather than on measurement designed for use in scale-up calculation for particular reservoir however the core floods can give answers for at least three questions directly.⁽⁴¹⁾

- 1- Can CO₂ remove/mobilize tertiary oil under field displacement condition than those occur in slim-tube displacement [?]
- 2- What will be the residual oil saturation in the swept zone of CO₂ displacement [?]
- 3- Does CO₂ injection alter core permeability [?]

Experimental Setup

(Figure 2.27) shows an experimental facility for two-phase core flooding experiments. The facility allows for continuous injection of CO₂ and brine into rock cores at reservoir pressures and temperatures, while obtaining high resolution 3-dimensional maps of CO₂ and brine saturations. The core sample is wrapped in a heat-shrinkable Teflon sleeve and placed in an aluminum core holder. A pump (Pump D) injects water around the sleeve to create the overburden pressure (reservoir pressure). Two electric heaters warm the water inside the core holder to maintain the core at the reservoir temperature (T_{res}). Two dual-pump systems are used to inject brine and CO₂ in the core sample (Pumps A1 & A2 for CO₂ and B1 & B2 for brine). Both of them are composed of two pumps connected with a set of electric valves.

The dual pump configurations provide continuous fluid delivery by synchronizing the pump and refill strokes so that at least one pump is always delivering fluid. Electric valves support automated functions and are ideal for CO₂ Application. The pumps can inject CO₂ and brine either at a constant volumetric flow rate or a constant pressure gauge. The liquid level gage is equipped with a transparent ½ inch thick glass which allows measuring and following the height of the interface between brine and liquid CO₂ during the experiments. After the separator, the CO₂ returns back to the CO₂ pump system and the brine is conducted back to the brine pump system. Between the separator and the CO₂ pump system, another pump (Pump C) is used to maintain the back pressure in the system. The back pressure, also called pore pressure, is always at least 200 psi below the overburden pressure value in order to avoid any leakage through the Teflon sleeve surrounding the core. The dual-pump configuration allows for continuous experiments over week to months. In addition, the two fluids are in constant contact each other, ensuring that the CO₂ and brine are in thermodynamic equilibrium, thus avoiding inter-phase mass transport. These precautions meant to avoid drying the core, which often happens when dry CO₂ is injected into a core. During the experiments, the pressure drop across the core is measured with two high resolution pressure transducers (~100 Pa). The temperature inside the core holder, the

pressure drop, the injection flow rate, the injection pressure and the volume of each pump is measured and recorded by a data acquisition system. The entire setup, despite its size, is easily movable and can be transported to a room where X-ray CT scanning is used to measure CO₂ and brine saturations, in real time, inside the core sample.⁽⁴²⁾

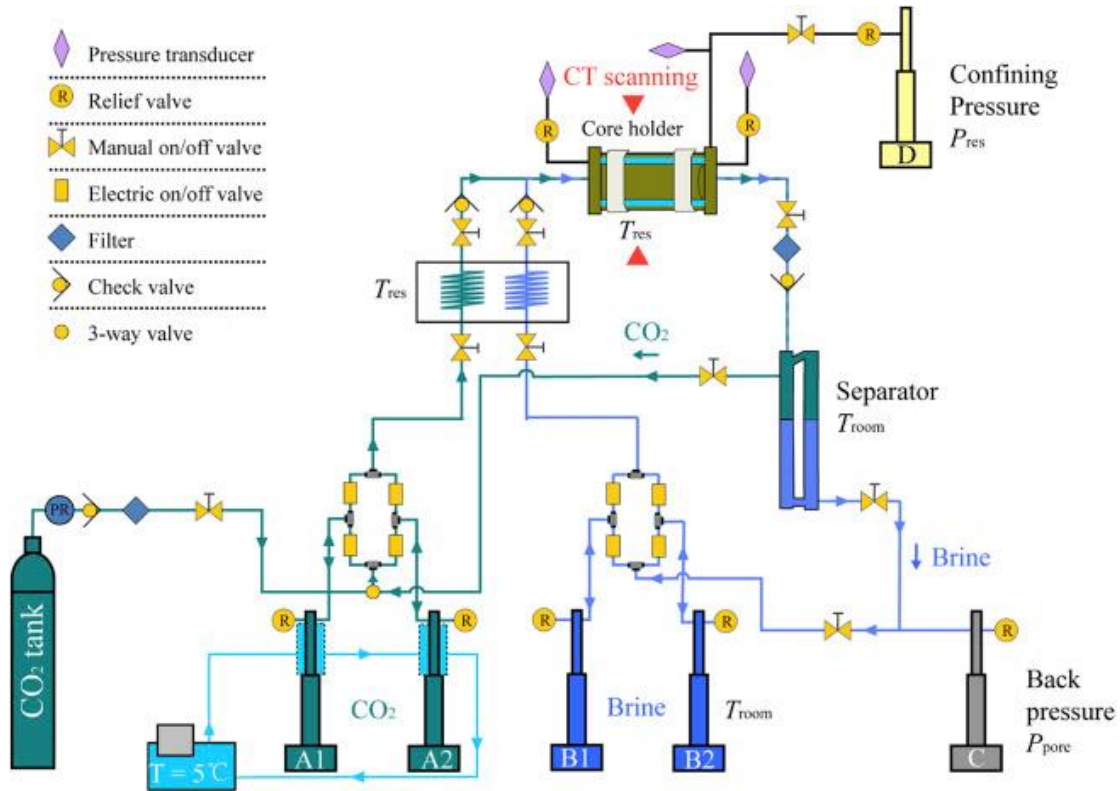


Figure 2.27: schematic of a typical core flooding experimental setup (Perrin and Benson (2010))

2.9.5 Slim-tube Experiment

Filling the gap between the above static measurements and core floods are the *slim-tube* experiments. Figure (2.28) is a schematic of typical slim-tube test equipment. The slim tube typically consists of stainless-steel tube about ^{3/16} in.ID and about 40ft long. The tube is packed uniformly with fine grade sand or glass beads of size on the order of 100 meshes. the ratio of particle size to tubing diameter is sufficiently small wall effects are negligible .the tube is coiled in a manner so that flow is basically horizontal and gravity effect are insignificant .a pump system is provided to force fluids through the porous medium pack ,and pressure is controlled by a backpressure regulator. The coiled tube and specific auxiliary equipment are place inside a constant temperature bath, usually an air bath. At the effluent end of the tube a fluid collection and measurement system are provided. The equipment may

range from a simple graduated cylinder and wet-test meter to a more complicated system involving a gas chromatograph. A small visual cell also is included at the effluent end so that the fluid product can be observed. ⁽³⁸⁾

Procedure of the experiment:

1. The porous medium in the tubing is filled with hydrocarbon to be displaced
2. The system is brought to test temperature
3. Backpressure regulator is set to the desired displacement pressure
4. The displaced fluid is injected at constant rate (linear rate of advancement considerably higher than what might be expected in an actual reservoir usually is used to complete an experiment in a reasonable amount of time).
5. The pressure drop across the system is generally a small fraction of the average absolute pressure level in the tube.
6. The hydrocarbon recovery at displacing-fluid breakthrough, recovery at the time of injection of a specific number of PV's ,and /or ultimate hydrocarbon recovery are recorded
7. The entire experiment is repeated at different pressures, but with all other variables held constant.
8. Recovery is plotted as a function of displacement pressure.

Assumptions behind slim-tube experiment:

- Displaced and displacing fluid in local thermodynamic equilibrium
- Tube length/diameter ratio of slim tube is set so that nonidealities ,such as
 - Fingering caused by porous medium heterogeneities
 - Unfavorable viscosity ratio
 - Gravity effects

Are negligible thus the efficiency of displacement is taken to be the result of thermodynamic phase behavior of the system solely. The assumption stated above are not always valid “it is recommended the slim-tube conditions be checked by use of FCM displacement as a control.

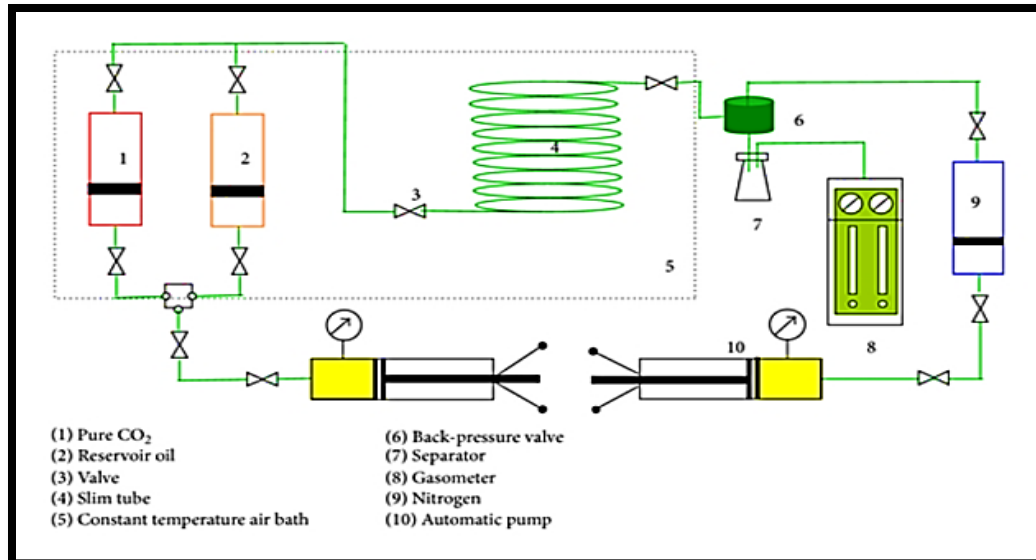


Figure 2.28: a schematic diagram of Slim-Tube experiment ⁽⁴⁷⁾

Figure (2.29) shows the actual setup of the experiment with the air bath used to achieve the required temperature.



Figure 2.29: Slim-tube experiment setup

2.9.6 Rising Bubble Apparatus (RBA)

RBA consists of a flat glass tube constructed vertically in high pressure sight gauge in a temperature controlled bath. ⁽³⁹⁾ Black light is used on sight gauge so that behavior can be observed.

1. The tube and gauge are first filled with distilled water then; the water is displaced with the oil to be tested except the short part of the column at the bottom of the tube.
2. The temperature is fixed at the desired value “reservoir temperature “and also the pressure is held at specific test value.
3. A small gas bubble is injected into the bottom of the tube (the composition of the gas is the same as the composition gas that has to be tested in MCM process).
4. The gas bubble rises first through the water column and then through the oil .the behavior of the gas bubble can be easily observed through the region of sight glass.
5. The behavior of the bubble is quite distinctive at or slightly above MMP.

As the bubble rises, it changes shape and spread into the oil. Far below MMP, the bubble preserved its near-spherical shape as it rises but it decreases in size as a result of mass transfer between gas and oil .Far above the MMP, the bubble disperses into the oil rapidly. See figure (2.30)

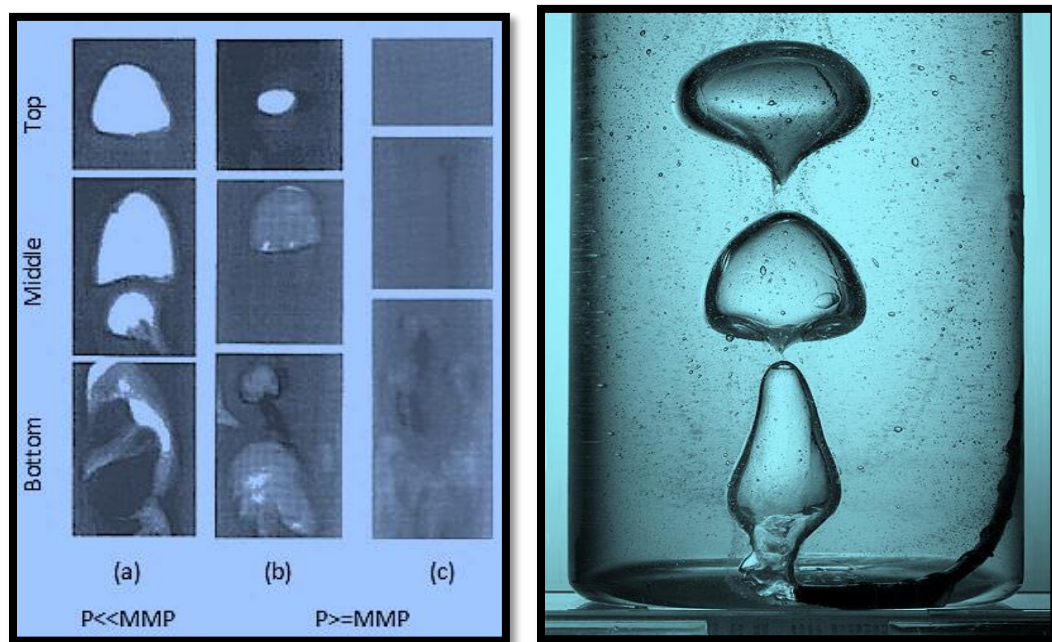


Figure 2.30: Gas bubble visualizing in the RBA experiment

It has been concluded by a researcher that MMP determined With RBA agreed within acceptable accuracy with values obtained with slim-tube apparatus⁽³⁹⁾

Also it has been proved by another researcher that the RBA method is significantly faster than slim-tube one. ⁽⁴⁰⁾

Figure (2.31) and figure (2-32) shows a schematic and actual diagram for RBA system

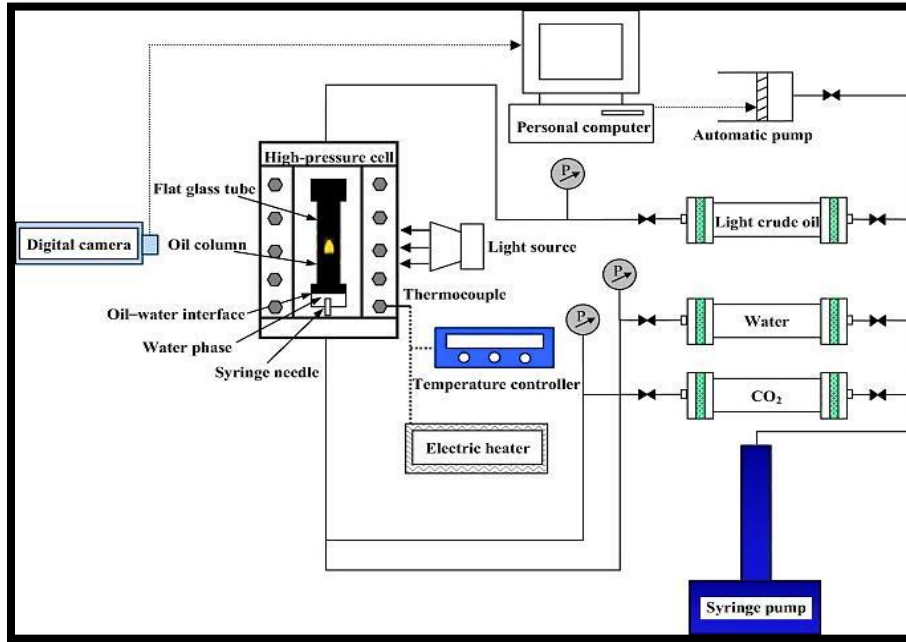


Figure 2.31: a schematic diagram for RBA system



Figure 2.32: an actual experiment setup of RBA system

2.10 Simulation (Mathematical Modeling)

The simulation of a miscible displacement process can be done with different types of models ranging from simple to very complex ones. The most comprehensive models are

numerical finite-difference simulators based on numerical solutions of partial differential equations that describe the fluid system. In numerical finite-differences simulator, the reservoir is subdivided into gridblocks. The partial differential equations are approximated by algebraic finite-difference equations, by assigning the dependent variables (pressure, composition, saturation, etc...) for each gridblock. The reservoir can be approximated in 2-D or 3-D. 3-D requires a decent number of gridblock and thus a higher computation time.

In addition to the finite-differential Equations, certain auxiliary equations are required. These include an EOS that allows computation of equilibrium phases and composition and relative permeability functions.

The two types of models that have been widely used are modified black oil simulators and compositional simulators. The different between these two models are in the treatment of phase behavior and composition of each phase. Compositional simulators are more complex and thus generally more expensive and time-consuming to apply. ⁽¹⁾

2.11 The Equation of State (EOS)

An equation of state (EOS) is an analytical expression relating the pressure, p , to the temperature, T , and the volume, V to the composition. A proper description of this PVT relationship for real hydrocarbon fluids is essential in determining the volumetric and phase behavior of petroleum reservoir fluids and predicting the performance of surface separation facilities; these can be described accurately by equations of state. In general, most equations of state require only the critical properties and acentric factor of individual components.

The main advantage of using an EOS is that the same equation can be used to model the behavior of all phases, thereby assuring consistency when performing phase equilibrium calculations ⁽¹⁴⁾. A review of empirical cubic equations of state is presented as the following:

- van der Waals
- Redlich-Kwong
- Soave-Redlich-Kwong
- Peng-Robinson

The mathematical formulas of the empirical cubic EOS are listed in Figure 2.33 in the form of:

$$P = P_{\text{repulsion}} - P_{\text{attraction}} \quad \text{Eq. 12}$$

EOS	$P_{\text{repulsion}}$	$P_{\text{attraction}}$	a	b
Ideal	$\frac{RT}{V}$	0	0	0
vdW	$\frac{RT}{V-b}$	$\frac{a}{V^2}$	$\Omega_a \frac{R^2 T_c^2}{p_c}$	$\Omega_b \frac{RT_c}{p_c}$
RK	$\frac{RT}{V-b}$	$\frac{a}{V(V+b)\sqrt{T}}$	$\Omega_a \frac{R^2 T_c^{2.5}}{p_c}$	$\Omega_b \frac{RT_c}{p_c}$
SRK	$\frac{RT}{V-b}$	$\frac{a\alpha(T)}{V(V+b)}$	$\Omega_a \frac{R^2 T_c^2}{p_c}$	$\Omega_b \frac{RT_c}{p_c}$
PR	$\frac{RT}{V-b}$	$\frac{a\alpha(T)}{V(V+b) + b(V-b)}$	$\Omega_a \frac{R^2 T_c^2}{p_c}$	$\Omega_b \frac{RT_c}{p_c}$

Figure 2.33: EOS formulas

The success of the method depends on the correct prediction of the number and composition of phases preset at given temperature, pressure, and overall reservoir fluid composition. ⁽¹⁴⁾

2.12 Simulation Methods for Assessing Gas Injection Processes

There are several computational techniques for performing multiple contacts mixing cell calculation. These methods are basically used to determine the miscibility pressure (where the displacement efficiency approaches 100%).

Brief information of the most well-known techniques follows:

First technique: a direct calculation of the MMP from an analytical solution to the flow problem. Such a method will be probably, in the near future, the quickest way to determine the MMP for a combined condensing/vaporizing mechanism. Wang and Orr⁹ began to develop such a method, but at the moment, their procedure is not yet completely general since it may only apply if the injected gas contains less than two components. Very recently, Jessen and Michelsen ⁽⁴⁹⁾ obtained very interesting results in their attempt to generalize the approach initially developed by Orr. ⁽⁴³⁾

Second technique: this technique requires the construction of a one-dimensional compositional model. This method is able to compute MMP in a very sound way. It doesn't matter if the mechanism is a combined one (condensing or vaporizing); the MMP can be determined by finding the point of break-over in a plot of the recovery factor (RF_{1.2}) at 1.2 PVI (pore volume injected) versus pressure.

It is required to run the displacement for various number of gridlocks to eliminate the dispersion effect at each pressure (e.g. 50, 100, 200, and 500 grid blocks) and to smooth the oil recovery at 1.2 PVI obtained for each run in order to determine the oil recovery (at 1.2 PVI) corresponding to an infinite number of grid blocks (RF_{1.2} a slim tube simulation with correct elimination of numerical dispersion requires at least six-seven pressures, run with 50, 100, 200, and 500 grid cells each. The slim tube simulations are thus inconvenient, not completely automated, and time-consuming.⁽⁴⁴⁾

Third technique: A new method has been introduced by Jaubert (Simple Multiple Mixing Cell Calculation) has approved its efficiency of calculating the MMP.

This method is proposed to avoid the disadvantages of the previous ones. The developed algorithm is automated, from 15 to 80 times faster than the use of a 1D simulator, and very easy to compute. Such an algorithm relies on the following key point:

- a. The MMP is completely independent of the porous material through which the flow is occurring. Like any equilibrium thermodynamic property of a system
- b. The MMP is not influenced by the relative permeability, capillary pressure, and interfacial tension. Minimum miscibility pressure is only dependent on the phase behavior of the system.

All these points were verified experimentally by the French petroleum company TOTAL SA. In particular, more than 50 MMP were determined with two slim tubes: the first one full of sand and the second one full of glass beads. In all cases, the measured MMP's were exactly the same. It means it should be possible to compute the MMP with a very simplified slim tube, i.e., with a cell to cell simulation in which no porous media and very simple flow dynamics are considered.⁽⁴⁴⁾

3. PVT Modeling

3.1 Sarir Field: A Proposed CO₂ Injection Site

A CO₂ injection feasibility simulation study has been conducted to the Sarir oil field to see the impact of CO₂ in the oil recovery. The field description is provided in the following section.

3.1.1 Description

The Sarir C–Main Reservoir is a large, basement controlled, faulted and truncated anticline structure dome (33 km long and 15 km wide). Sarir C–Main Reservoir is composed of thick lower Cretaceous age sandstone of the Sarir Group, which is subdivided into geological members designated from bottom to top as Members 1, 2, 3, 4, 5AA (5AA1 to 5AA3 as target). Oil production in Sarir C–Main field is mainly from members 3, 4 and 5 with members AA1, AA2 and AA3 above the field oil–water contact. The predominant oil recovery mechanism in the field is bottom water drive with a large regional aquifer directly underlying the hydrocarbon accumulation, providing good pressure support over most of the field. By the end of December 2012, there were 364 wells in the Sarir C–Main area. ⁽³⁴⁾

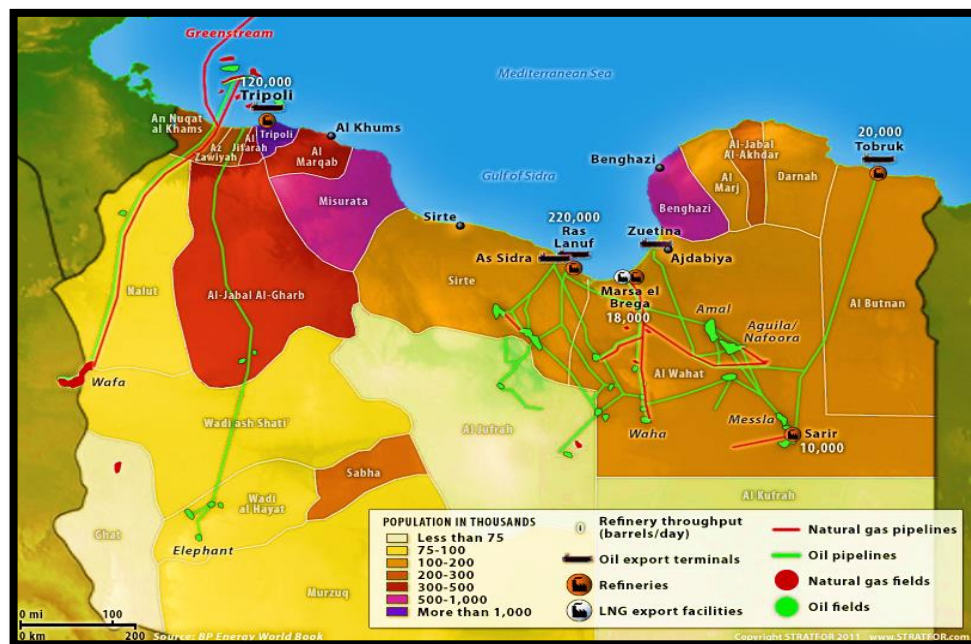


Figure 3.1: Sarir field location map

3.1.2 Location

The Sarir or, more specifically , the Sarir “C” field lies on the western edge of the Calanscio sand sea southeast Benghazi city, the second largest city in Libya after the capital Tripoli and is the largest oil field in Libya . It occurs at the southeastern margin of the upper cretaceous-Tertiary Sirte basin or embayment that contains all major oil fields of Libya and is the most prolific oil-producing basin in north Africa (Figure 3.2). Other significant fields lying in the same basin are Alamal, Gialo, Nasser(Zelten), Dafa, Augila, Hateiba, Messla, Intisar A and D, Bu Attifel, Raguba, and Bahi. The Sarir “C” field , which is a part of a complex of three fields , is 35 mile (56Km²) long and 25 mile (40Km²) wide covering approximately 146 mi² (378Km²).to its north lies the Sarir “L” accumulation ,which covers approximately 15 mi² , and situated between the a much smaller Sarir North pool (figure3.3). Estimated ultimate recovery from the “C” field is 6.5 billion bbl of oil and from the “L” field, 1.2billion bbl ranking them as the 51st and 201st largest fields in compilation of Carmalt and St.John (1986).⁽³⁵⁾

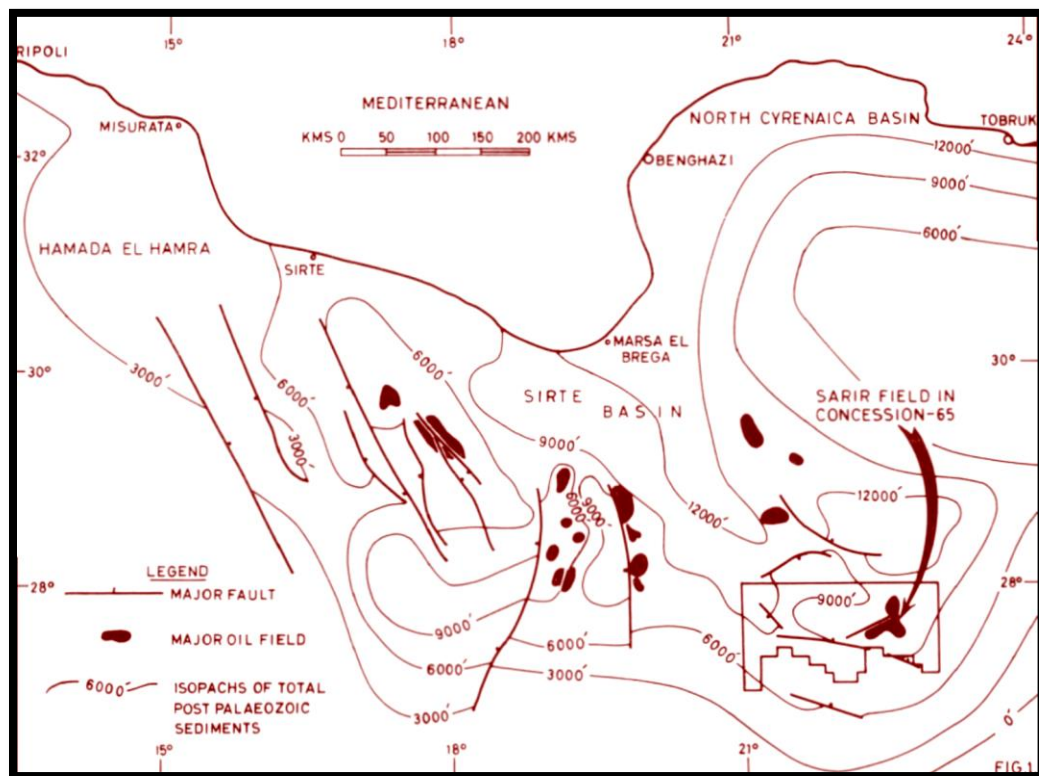


Figure 3.2: Map of Sirte Basin, Libya

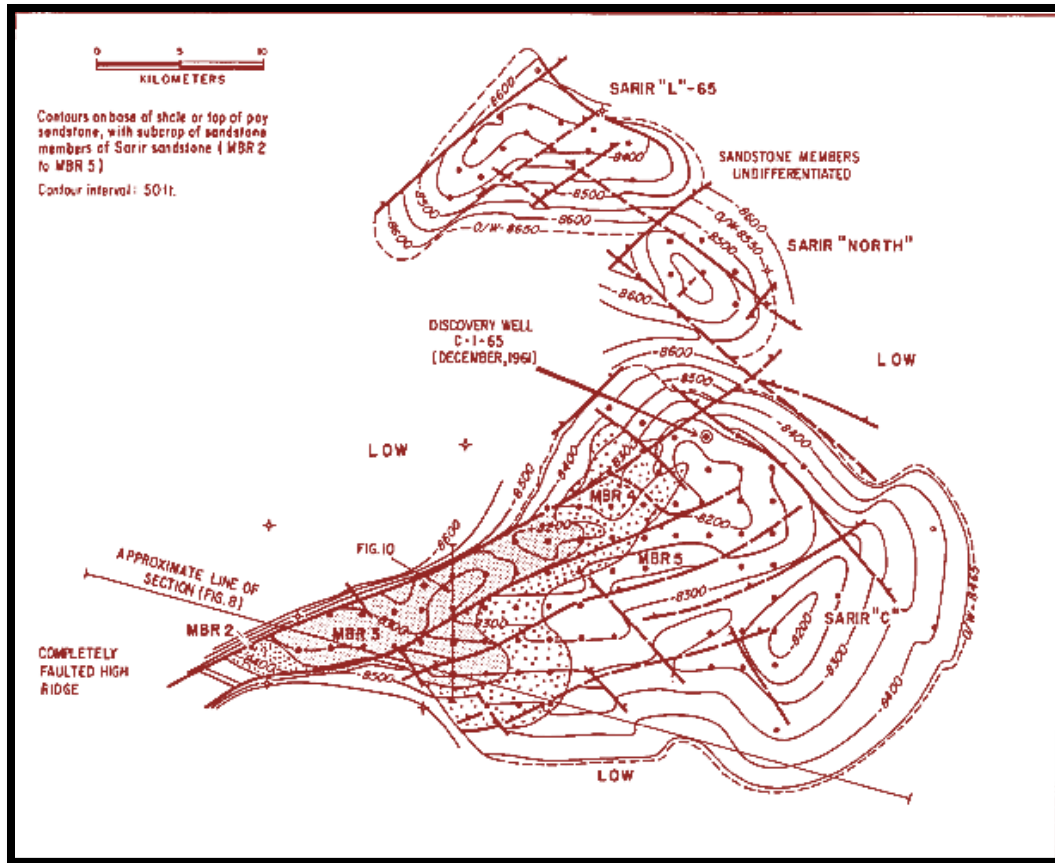


Figure 3.3: Structure map of Sarir field complex (after Sanford, 1970)

3.1.3 Reservoir and Production Data:

Arabian Gulf Oil Company (AGOCO) is an oil company based in Benghazi, Libya, engaged in crude oil and natural gas exploration, production and refining. Arabian Gulf Oil Company AGOCO has upstream operations in eight oil fields in Libya⁽³⁶⁾, one of those fields is:

- Sarir Oil Field

Reservoir and Reservoir Performance Data are listed below in Table I and Table II .These data are provided by AGOCO from a study conducted in 2012. See Appendix A

3.2 Purpose of the gas injection feasibility study

This study has been conducted to investigate potential increase of oil recovery in the Sarir Field by using Separator Gas /CO₂ gases as injection EOR method.

On July 13th, 1983 subsurface fluid samples were collected from the field and forwarded to the Aberdeen laboratory for use in routine and special PVT

The results of preliminary reservoir fluid analysis as requested by Arabian Gulf Oil Company are presented in the following:-

- hydrocarbon composition C1 through C7+
- Constant composition expansion CCE (Pressure/Volume relation & compressibility)
- Differential liberation DV(oil density ,oil gravity, gas formation volume factor)
- Viscosity
- Serious of flash separation tests (GOR,API,Bo)

Special reservoir fluid study

- Slim-tube tests.

The results of these studies are presented in the Appendix B & C

3.3 Methodology of the Present Study

In this section, the methodology followed in building the structure of this study will be discussed in details. But before starting we need to introduce the programs that have been used as tool in our study

- CMG (winprop)
- IPM suit (PVTP)
- IPM suit (Reveal)

3.3.1 CMG (winprop) program

WinProp is a commercial comprehensive Equation-of-State tool (EOS) model which, accurately identifies and models the phase behavior and properties of reservoir fluids. WinPro's robust calculation engine quickly performs complex calculations and allows the tuning of EOS against the real lab data to predict fluid behavior and to improve understanding of the reservoir exploitation process. It is an integral component in an advanced reservoir simulation

modeling package and is invaluable for multi-phase and special processes, and where compositional variations exist. Winprop has been used to perform the following calculations:

- EOS Characterization

Tuning EOS to accurately match laboratory results and predict fluid behavior.

- Miscibility Prediction (MCM Option)

Win Prop's multiple contact miscibility option performs calculations under condensing, vaporizing, or condensing-vaporizing drives.

3.3.2 Petroleum Expert (PETEX) (PVTP)

PVTP allows tuning of Equations of State (EOS) to match laboratory data. The tuned EOS can then be used to simulate a range of reservoir and production processes.

The slim tube calculation option in (PVTP) provides an easy way to input the data and conduct simulation study without the need of building 1-D model

3.3.3 Reveal

Reveal is part of an integrated production modeling IPM suit. It enables performing numerical simulation studies and special reservoir studies. Reveal has been used in the course of this study to build an 1-D model and simulate the actual slim tube experiment numerically.

The following steps has to be done in order to obtain a representative EOS

Equation of State Generation

- a- Matching the laboratory results accurately
 - Bubble point pressure
 - Constant Composition Expansion Test
 - Differential liberation test
 - Separator test

3.4 Equation of State Generation

As the purpose of this work is to model a miscible displacement tuning needs to done firstly.

Three EOS models have been generated. These models are:

- EOS C7+ base model as reported in PVT report
- Splitted EOS C31+
- Lumped EOS C15

The generated EOSs should be capable to predict accurately the PVT studies. The procedure followed to build these models is described in the following Section.

3.4.1 Base Model C7+

The Original composition as reported in the PVT report EOS C7+

COMPONENT	MOL PERCENT
Hydrogen Sulphide	NTL
Carbon Dioxide	1.12
Nitrogen	1.05
Methane	10.82
Ethane	4.34
Propane	8.22
iso-Butane	2.22
n-Butane	6.41
iso-Pentane	2.86
n-Pentane	3.54
Hexanes	4.45
Heptanes plus	54.97

The characterization of the fraction (C7+) generally consists of the following steps:

- (a) Splitting the plus fraction into a number of pseudo components (e.g., C7 to C31+)
- (b) Lumping I order to reduce the number of Pseudo-Components

3.4.2 Splitting the EOS C7+ fraction EOS C31+

Splitting refers to the process of breaking down the plus fraction into a certain number of pseudocomponents. A satisfactory prediction of the PVT behavior by the equation of state can be obtained when a sufficiently large number of pseudo components used in characterizing the heavy fraction of a hydrocarbon mixture.

Splitting Scheme

Whitson's Method

The three-parameter gamma probability function is the most widely used distributional function. This function was proposed by Whitson (1983). It has a high flexibility to describe a wide range of distributions by adjusting its variance. This variance plays the role of an adjustable parameter.

Whitson expressed the function in the following form:

$$P(M) = \frac{(M - \eta)^{\alpha-1} \exp\left[-\frac{M-\eta}{\beta}\right]}{\beta^{\alpha} \Gamma(\alpha)} \quad \text{Eq.13}$$
$$\beta = (MC_{n+} - \eta) / \alpha$$

Where,

η : is an adjustable variable with different values, used to see which value will increase the agreement between the experimental and the calculated mole fraction.

M : is the molecular weight of the component.

Γ : is the gamma function.

α : it affects the shape of the distribution, in this study it is equal to unity, because it is believed that the distribution of the mole fractions for the hydrocarbon components heavier than C_7 is exponential.

The key parameter defines the shape of the distribution “ α ” with its value usually ranging from 0.5 to 2.5. Gamma function can take any distributional shape depending on the assigned value for α :

- For $\alpha=1$, the distribution is exponential
- For $\alpha<1$, the distribution model gives accelerated exponential distribution
- For $\alpha>1$, the distribution model gives left-skewed distributions

In the application of the gamma distribution to heavy oils, bitumen, and petroleum residues, it is indicated that the upper limit for α is 25–30, which statistically approaches a log-normal distribution. Whitson indicates that the parameter η can be physically interpreted as the minimum molecular weight found in the C_{n+} fraction. Whitson recommended $\eta = 92$ as a

good approximation if the C7+ is the plus fraction, for other plus fractions (ie, Cn+) the following approximation is used:

$$\eta \sim 14n-6 \quad \text{Eq. 14}$$

And

$$\beta = (MCn+ - \eta) / \alpha$$

The cumulative frequency of occurrence for each single carbon number with molecular weight boundaries between M_{i-1} and M_i , is calculated from the integration of the probability function.

$$f = \int_{M_{i-1}}^{M_i} P(M) dM = P(M_i) - P(M_{i-1}) \quad \text{Eq. 15}$$

In order to find the integration, the molecular weight boundaries should be found, one of the two methods can be used in order to find the value of the integration.

The Mid Point Average Method which calculates the cumulative frequency of occurrence for component "i" by integrating the distribution function. These midpoints are used as the lower and the upper limits for the integration.

$$f_{i=} -e^{\left(\frac{\eta}{\beta}\right)} \cdot \left(e^{\left(\frac{M_i+0.5}{-\beta}\right)} - e^{\left(\frac{M_{i-1}-0.5}{-\beta}\right)}\right) \quad \text{Eq.16}$$

The Normal Cut Method is the second method for calculating the cumulative frequency of occurrence by integrating the gamma distribution function.

This method uses for the integration boundaries the molecular weight of component i and the previous component (i-1).

$$f_{i=} -e^{\left(\frac{\eta}{\beta}\right)} \cdot \left(e^{\left(\frac{M_i}{-\beta}\right)} - e^{\left(\frac{M_{i-1}}{-\beta}\right)}\right) \quad \text{Eq. 17}$$

The mole fraction of each SCN is calculated using the following equation:

$$z_i = z_{\text{plus}} \cdot f_i \quad \text{Eq. 18}$$

The mole fraction of the heaviest SCN group of the extended components is calculated using the following equation:

$$z_{\text{Cn+}} = z_{\text{plus}} - \sum_{i=1}^{n_e-1} z_i \quad \text{Eq.19}$$

The molecular weight of the heaviest fraction is calculated using the following equation:

$$M_{\text{Cn+}} = \frac{z_{\text{plus}} \cdot M_{\text{plus}} - \sum_{i=1}^{n_s-1} z_i \cdot M_i}{z_{\text{Cn+}}} \quad \text{Eq. 20}$$

The Plus fraction Splitting option in winprop implements all equations from (13-20). In fact this option asks for some parameters in order to perform those calculations. The data has been introduced to this option as the following:

Data Required For Plus Fraction Splitting	
Distribution Function Type	Gamma
Number of Fluid Sample	1
First Single Carbon Number in Plus Fraction	7
Number of Pseudocomponents	No Lumping
MW+	290
SG+	0.8644
Z+	0.5497
Alpha	1
No. of SCN Fraction	Defaulted (25)

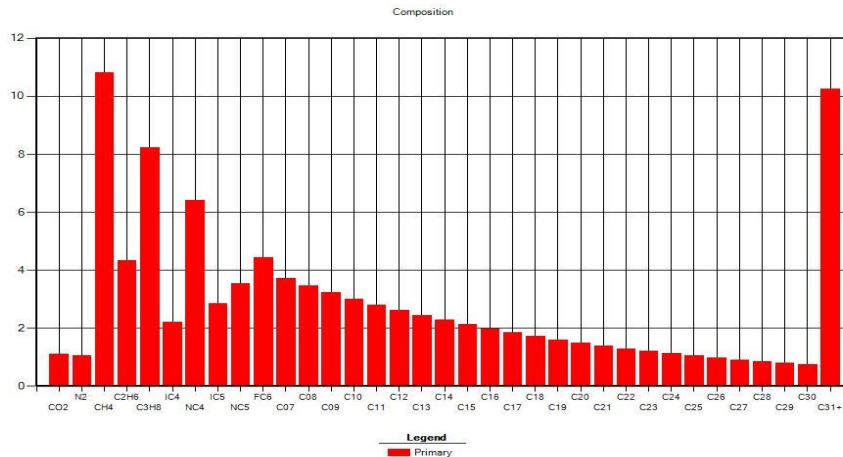


Figure 3.4: the compositional distribution of EOS C31+

The components of the model are as the following

CO2	N2	CH4	C2H6	C3H8	IC4	NC4	IC5	NC5	FC6	C07	C08	C09	C10
-----	----	-----	------	------	-----	-----	-----	-----	-----	-----	-----	-----	-----

C11	C12	C13	C14	C15	C16	C17	C18	C19	C20	C21	C22	C23	C24
-----	-----	-----	-----	-----	-----	-----	-----	-----	-----	-----	-----	-----	-----

C25	C26	C27	C28	C29	C30	C31+
-----	-----	-----	-----	-----	-----	------

3.4.3 Lumping of EOS C31+ into EOS15

In compositional models, the cost and computing time can increase significantly with the number of components in the system. Therefore, strict limitations are set on the maximum number of components that can be used in compositional models and the original components have to be lumped into a smaller number of pseudo components for equation-of-state calculations.

By taking into the account the fact that the previous EOSs have exhibited a good matching with experimental data we found that there is still a room for improvement in which the numbers of pseudo-components are reduced further.

Whitson's Lumping Scheme

As proposed by Whitson (1980) whereby the compositional distribution of the **C7+** fraction is reduced to only a few multiple carbon number (**MCN**) groups.

He suggested that the number of MCN groups necessary to describe the plus fraction is given by the following empirical rule:

$$N_g = \text{Int} [1 + 3.3 \text{Log} (N-n)] \quad \text{Eq. 21}$$

Where

N_g = number of MCN groups

Int = integer

N = number of carbon atoms of the last component in the hydrocarbon System

n = number of carbon atoms of the first component in the plus fraction; that is, $n=7$ for **C7+**

The integer function requires that the real expression evaluated inside the brackets be rounded to the nearest integer.

The molecular weights separating each MCN group are calculated from the following expression:

$$M_i = M_{C7} (M_{N+} / M_{C7})^{1/N_g} \quad \text{Eq. 22}$$

Where

(M)_{N+} = molecular weight of the last reported component in the extended analysis of the hydrocarbon system

M_{C7} = molecular weight of C7

i = 1, 2... N_g

The lumping procedure followed in our work is described below:

Step 1: Determine the molecular weight of each component in the system.

Component	Z _i	M _{wi}
C07	0.037172	96.60967
C08	0.034658	110.6357
C09	0.032315	124.6617
C10	0.03013	138.6877
C11	0.028092	152.7137
C12	0.026192	166.7397
C13	0.024421	180.7657
C14	0.02277	194.7917
C15	0.02123	208.8177
C16	0.019794	222.8437
C17	0.018456	236.8697
C18	0.017208	250.8957
C19	0.016044	264.9217
C20	0.014959	278.9477
C21	0.013948	292.9737
C22	0.013005	306.9997
C23	0.012125	321.0257
C24	0.011305	335.0517
C25	0.010541	349.0777
C26	0.009828	363.1037
C27	0.009163	377.1297
C28	0.008544	391.1557
C29	0.007966	405.1817
C30	0.007427	419.2077
C31+	0.102407	626.624

Calculate the number of Pseudo Components from Eq.

$$N_g = \text{Int} [1 + 3.3 \text{Log} (N-n)]$$

$$N_g = 5$$

Determine the molecular weights separating the hydrocarbon groups by applying Eq.

$$M_i = M_{C7} (M_N + /M_{C7})^{1/N_g}$$

m1	140.4164
m2	204.0869
m3	296.6282
m4	431.1315
m5	626.624

1st Pseudo component

$$MW_1 = 140.4164$$

2nd Pseudo component

$$MW_2 = 204.0869$$

3rd Pseudo component

$$MW_3 = 296.6282$$

4th Pseudo component

$$MW_4 = 431.1315$$

5th Pseudo component

$$MW_5 = 626.624$$

- Pseudo component 1: The first pseudo component includes all components with molecular weight in the range of 96–140. This group then includes C7-C10
- Pseudo component 2: The second pseudo component contains all components with a molecular weight higher than 138 to a molecular weight of 194. This group includes C11 to C14.
- Pseudo component 3: The third pseudo component includes components with molecular weight higher than 194 to a molecular weight of 292. Therefore, this group includes C15-C21.

- Pseudo component 4: The fourth pseudo component includes components with a molecular weight higher than 292 to a molecular weight of 432. Therefore, this group includes C22-C30
- Pseudo component 5: This pseudo component includes the entire remaining component that is C31+

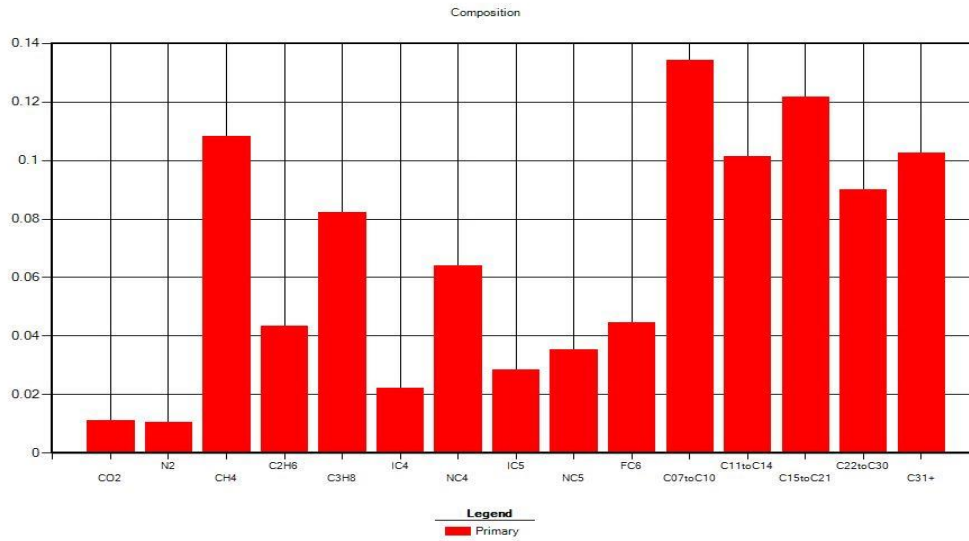


Figure 3.5: the compositional distribution the lumped EOS C15

The lumped EOS components are generated as the following

CO2
 N2
 CH4
 C2H6
 C3H8
 IC4
 NC4
 IC5
 NC5
 FC6
 C7toC10
 C11toC14
 C15toC21
 C22toC30
 C31+

Matching PVT data

We will cover in this section the tuning procedure that has been followed in order to tune the generated Eos models against the laboratory data. According to our scope of the work we give more emphasis on matching primarily the separator test data rather than the Differential liberation one.

The regression parameters that have used to tune the generated Eos models against lab data are introduced as the following:

- Interaction parameters:

They have a large effect on saturation pressure

- T_c, P_c Effects

Saturation pressure

- Volume of shift:

Oil density

- Molecular Weight both pseudocomponents and of the heavy ends C_{7+} , C_{15} and C_{31+} are Used as regression parameters:

It affects the saturation pressure, density and GOR due to SG and MW relationship.

It should be noted that the maximum allowable variation change in all regression parameters has been set to $\pm 20\%$. Also caution has been taken when we changed the critical properties of heavy ends and pseudo components to be consistent with respect to their normal distribution.

The tuned EOSs for the three models are tabulated in Appendix D.

The matched EOS models results are presented in the following section

3.5 The Results of the Tuned EOS Models

3.5.1 EOSC7+ Model

Saturation Pressure	Psat.Exp	Psat.Pred	Err%
	729.7	729.7	0
Separator Test Data			
	EXP.	PRED	Err%
GOR	132	133.26	0.95455
BO	1.162	1.133	2.4957
API	36.5	36.71	0.57534

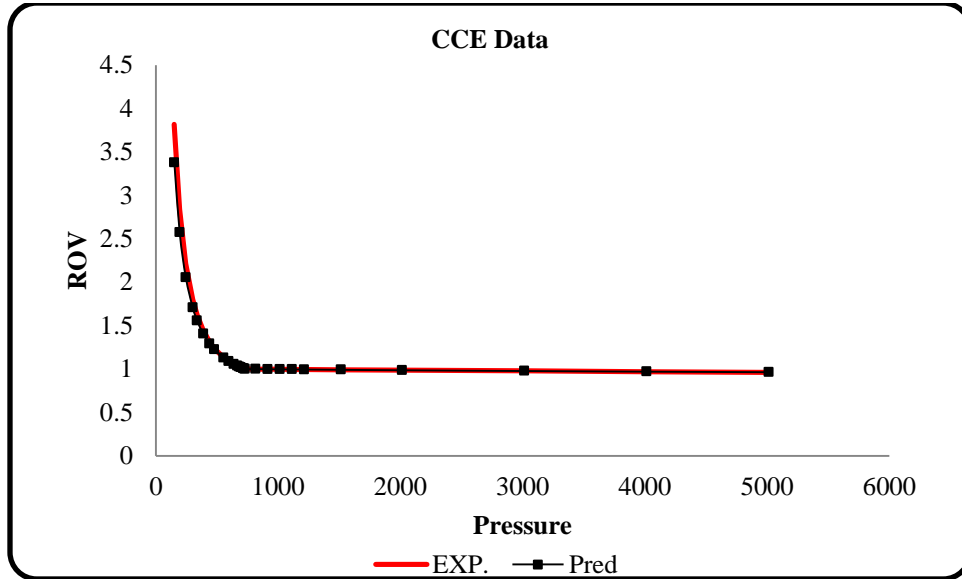


Figure 3.6: CCE data (Relative Volume versus Pressure)

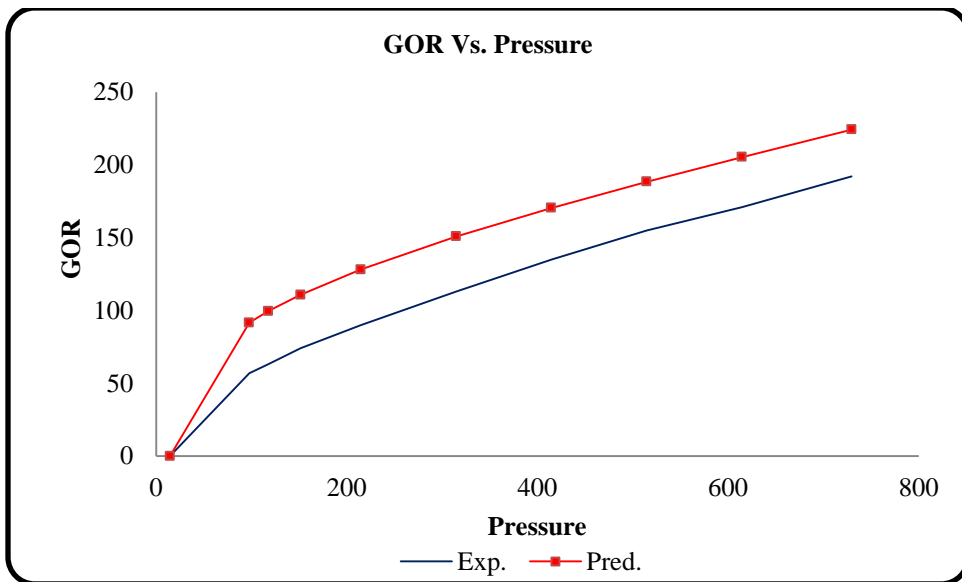


Figure 3.7: DV data (Gas Oil Ratio versus Pressure)

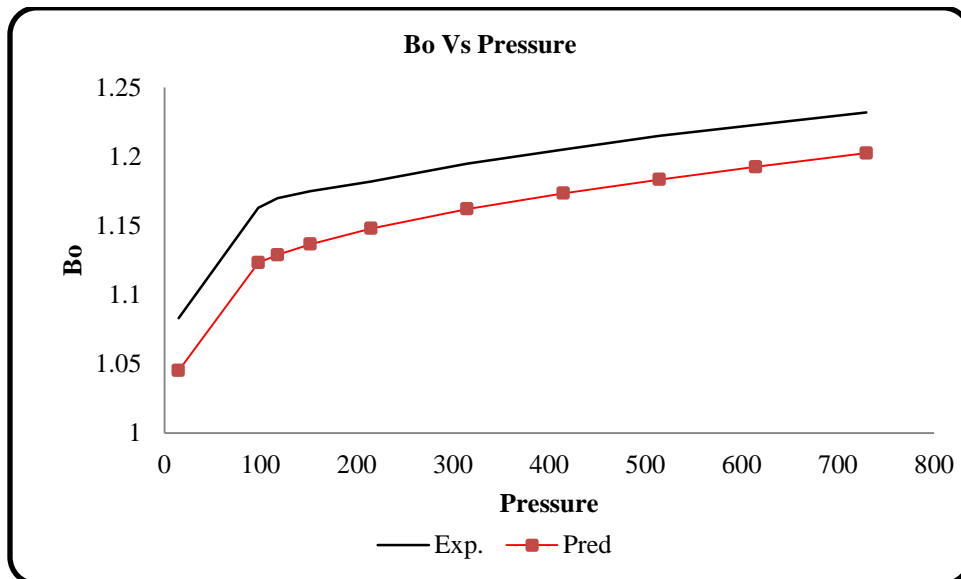


Figure 3.8: DV data (Formation volume factor versus Pressure)

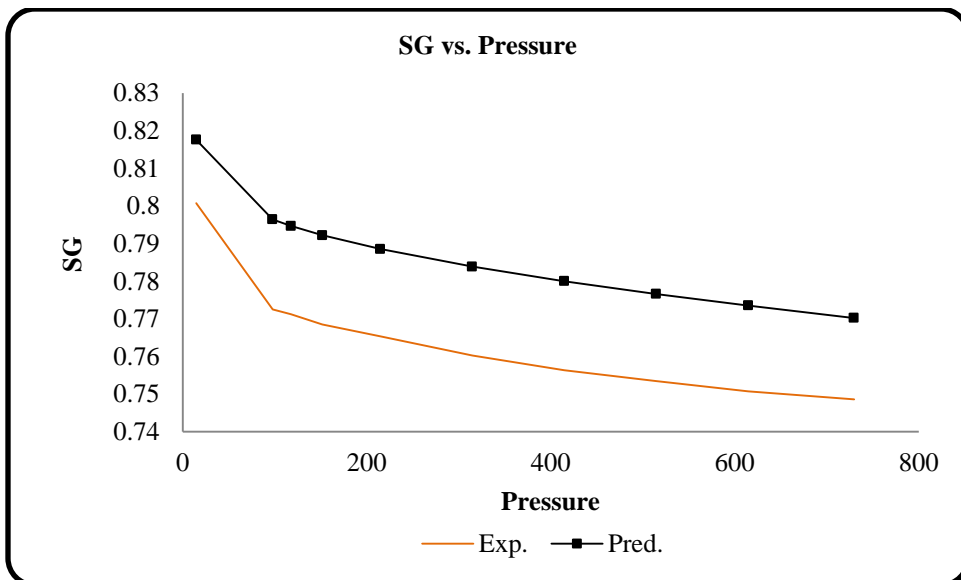


Figure 3.9: DV data (Oil Density versus Pressure)

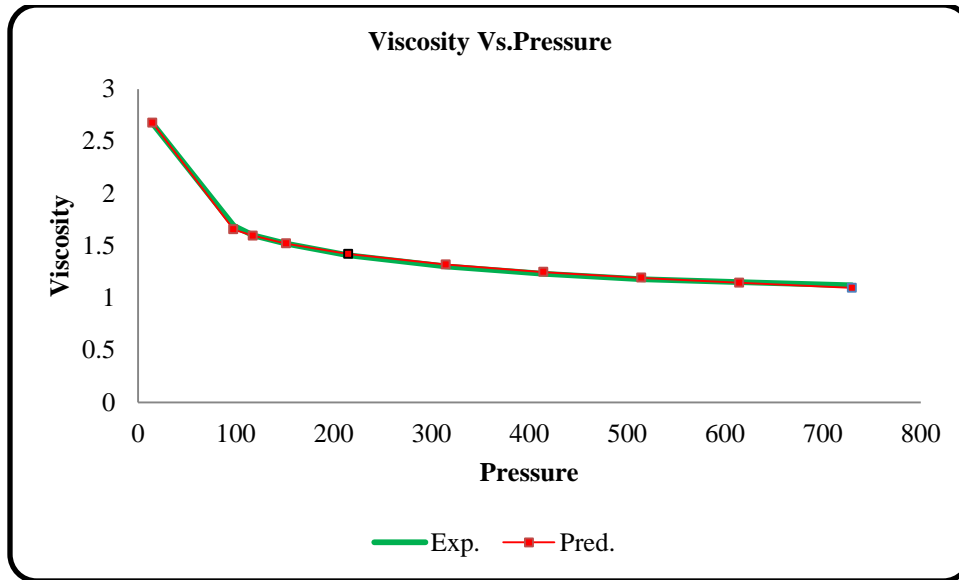


Figure 3.10: Viscosity versus Pressure

3.5.2 EOS C31+ Model

Saturation Pressure	Psat.Exp	Psat.Pred	Err%
	729.7	729.7	0
Separator Test Data			
	EXP.	PRED	Err%
GOR	132	133.35	1.02273
BO	1.162	1.128	2.92599
API	36.5	36.67	0.46575

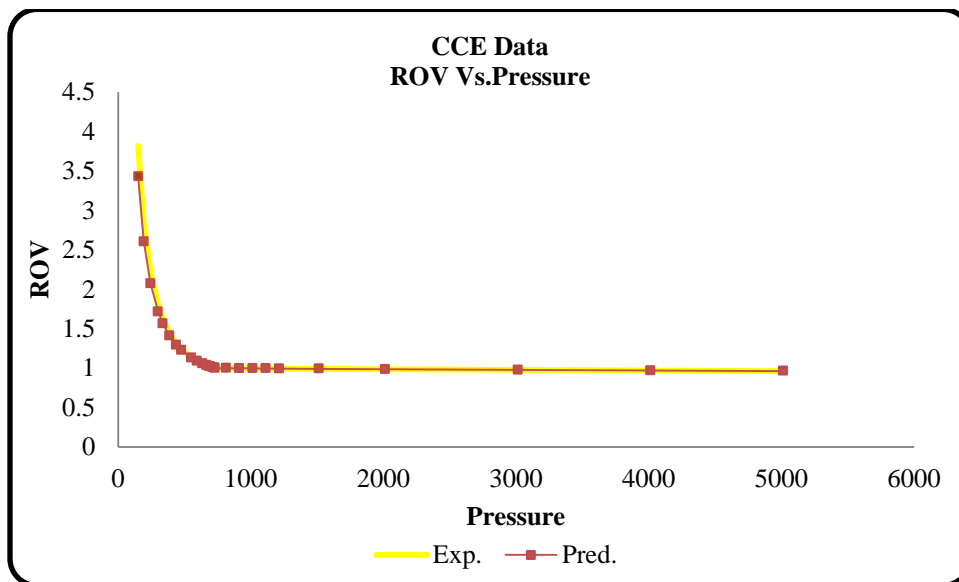


Figure 3.11: CCE data (Relative Volume versus Pressure)

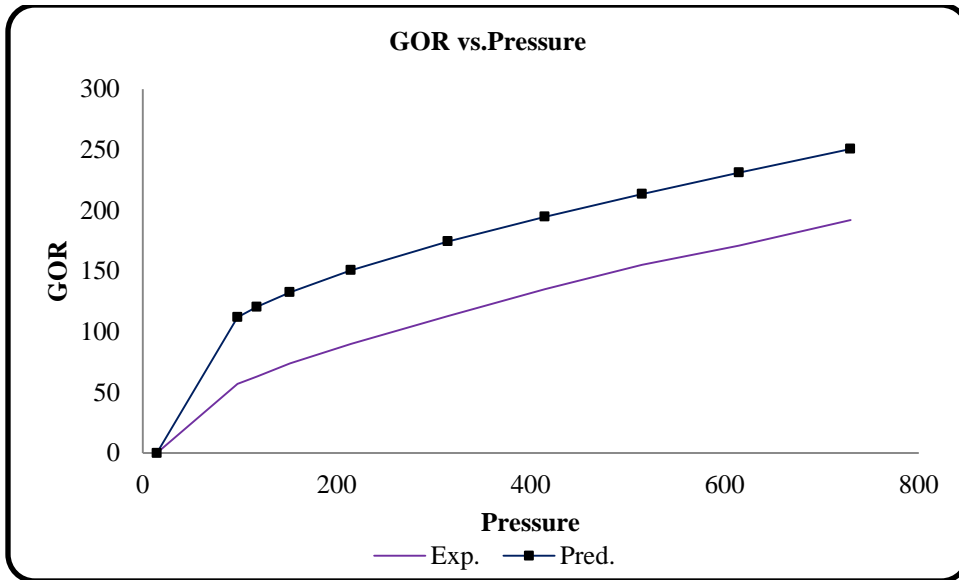


Figure 3.12: DV data (Gas Oil Ratio versus Pressure)

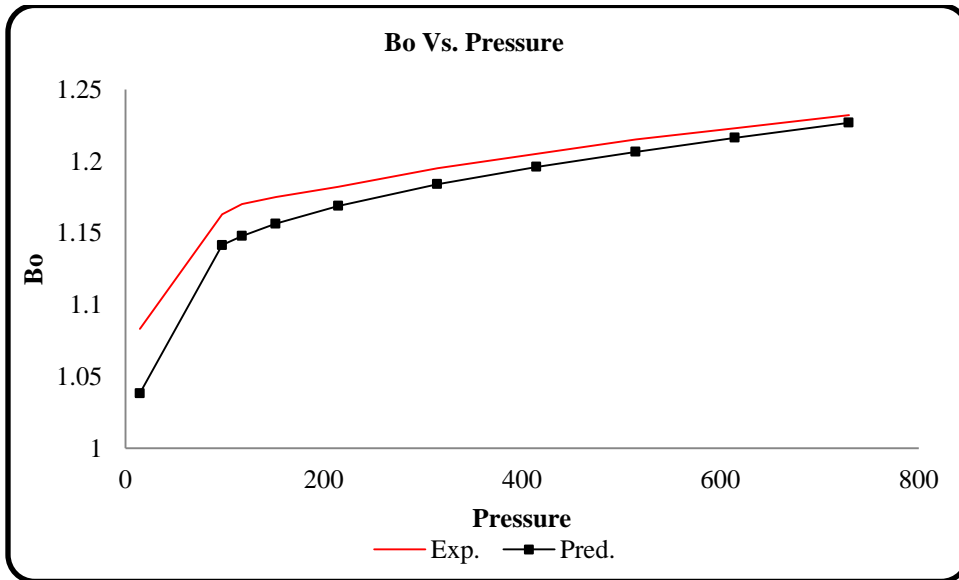


Figure 3.13: DV data (Formation volume factor versus Pressure)

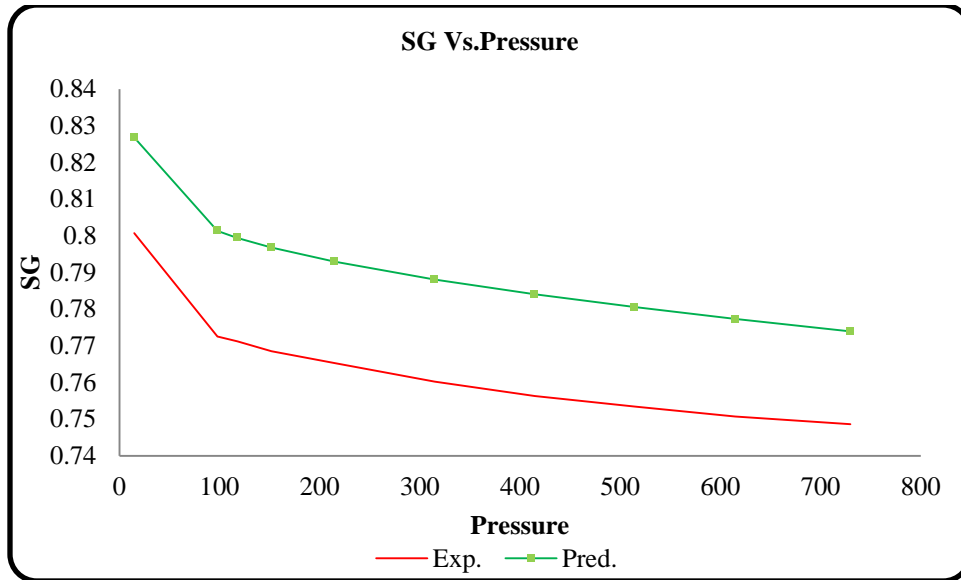


Figure 3.14: DV data (Oil Density versus Pressure)

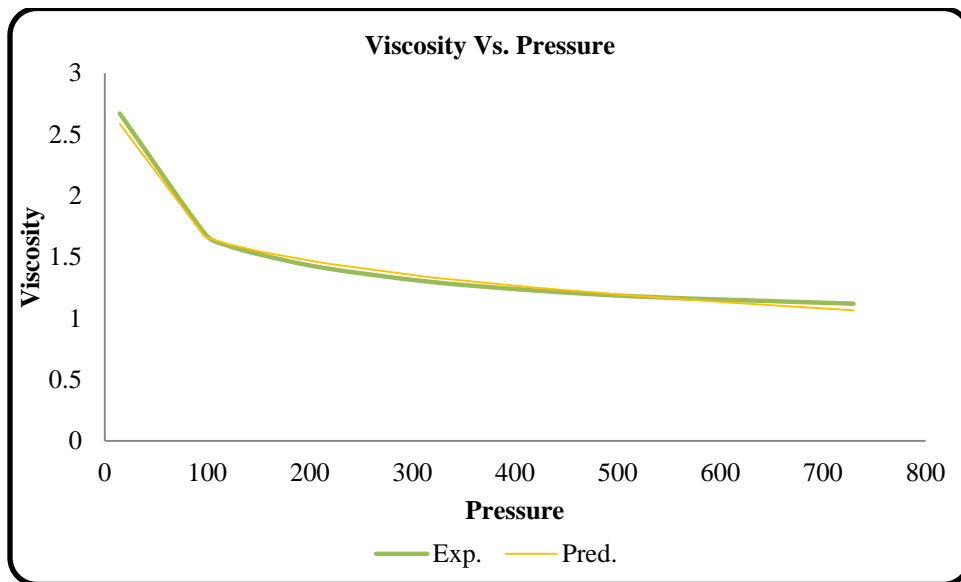


Figure 3.15: Viscosity versus Pressure

3.5.3 The lumped EOS C15

Saturation Pressure	Psat.Exp	Psat.Pred	Err%
	729.7	729.7	0
Separator Test Data			
	EXP.	PRED	Err%
GOR	132	133.35	1.02273
BO	1.162	1.128	2.92599
API	36.5	36.75	0.68493

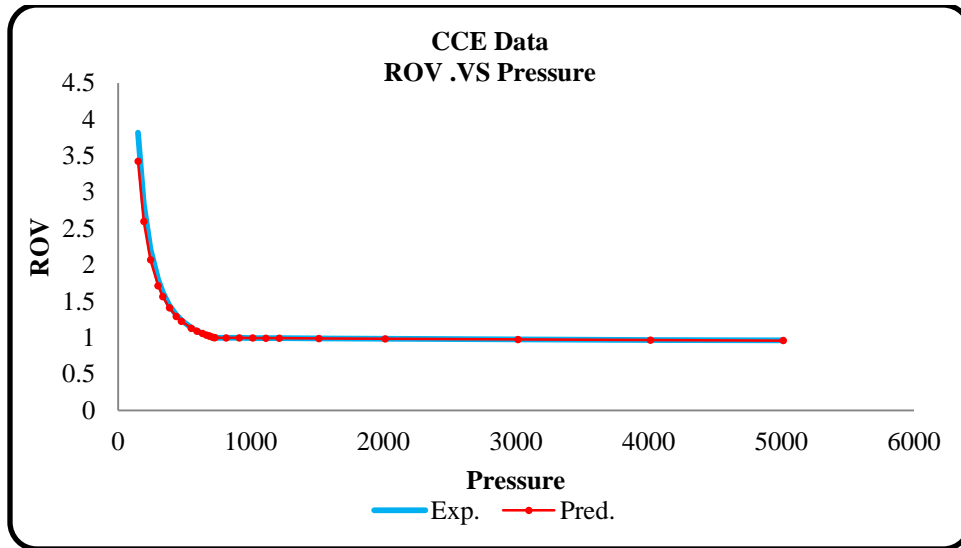


Figure 3.16: CCE data (Relative Volume versus Pressure)

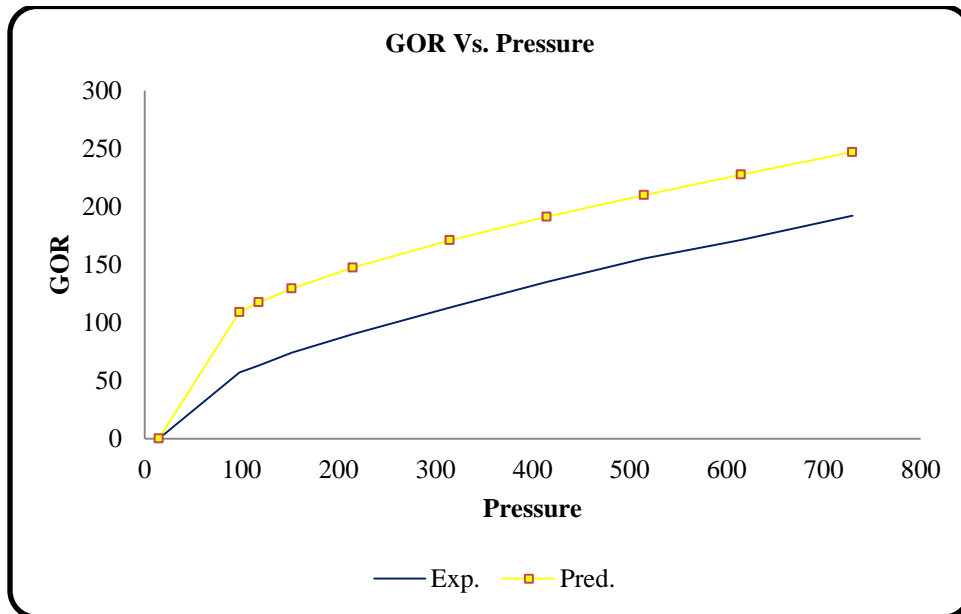


Figure 3.17:DV data(Gas Oil Ratio versus Pressure)

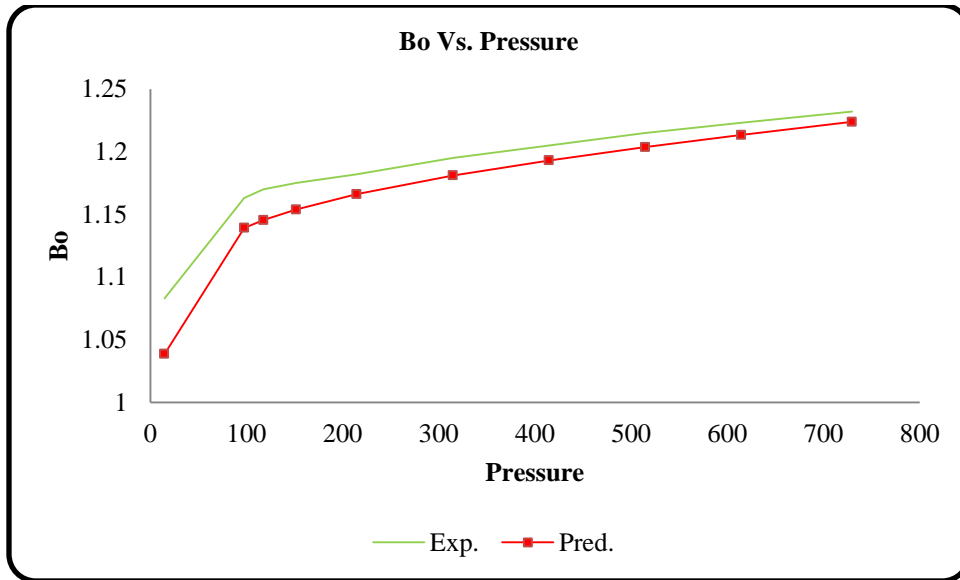


Figure 3.18: DV data (Formation volume factor versus Pressure)

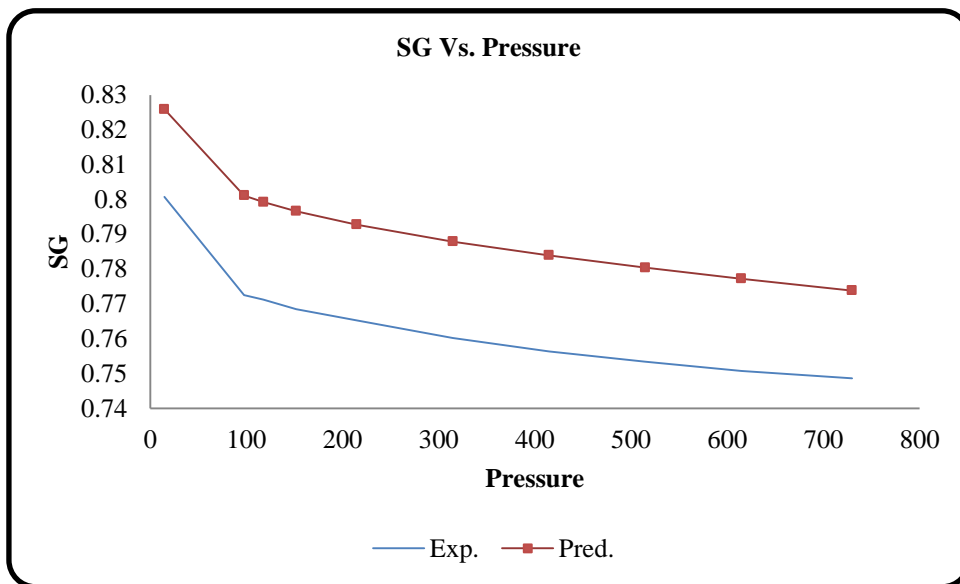


Figure 3.19: DV data (Oil Density versus Pressure)

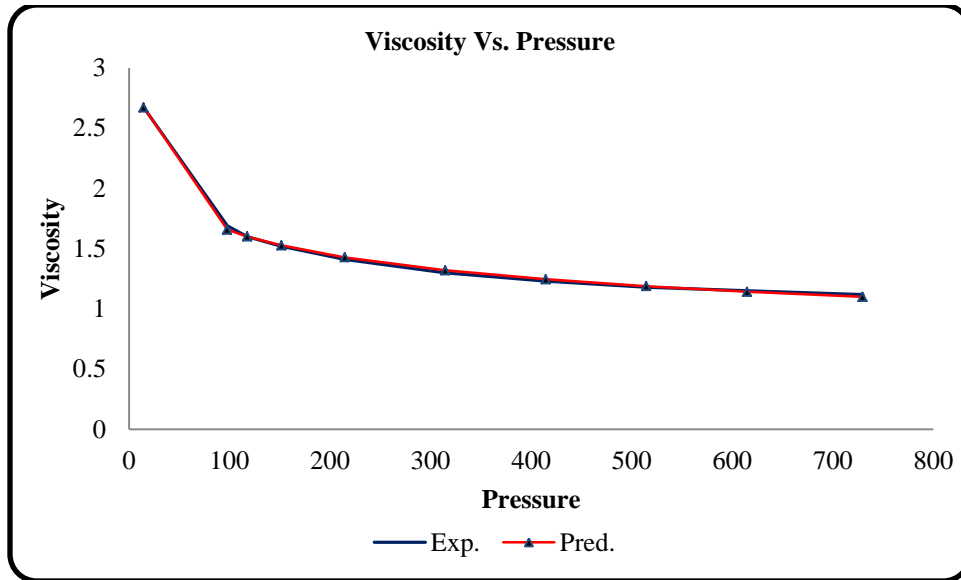


Figure 3.20: Viscosity versus Pressure

3.6 Multiple contact miscibility calculation (Cell to cell simulation)

After the EOSs have been tuned and prepared the same software CMG Winprop is used to conduct multiple contact miscibility calculation and to evaluate whether the Sarir oil can be miscible with CO₂ or not at reservoir temperature and pressure.

The MCM option in WinProp is used to calculate the minimum miscibility pressure (MMP) or the first contact miscible pressure (FCM) for a given oil and solvent at a particular temperature or the minimum miscibility enrichment level (MME) required for multiple or single contact miscibility at a given temperature, pressure, oil composition, primary and make up gas compositions.

There are three methods of calculating MMP in the MCM option (winprop)

- Cell to Cell simulation (vaporizing or condensing)
- Tie line method
- Multiple cell simulation

In our work, we only focused on the first method Cell to Cell simulation; the latter two methods determine the miscibility due to the combined vaporizing and condensing mechanisms.

This method also produces a Pseudo-Ternary diagram as an output. We should keep in mind that Cell to Cell method can only give us an estimation of MMP.

3.6.1 Methodology

A detailed description of how the MCM option (cell to cell simulation method) calculates the minimum miscibility pressure MMP (the caption of the calculation is shown in the tables and pseudo ternary diagram) is illustrated below:

Step1:

A solvent is first formed by mixing a primary gas (e.g. dry gas) with a specified mole fraction of make-up gas (e.g. LPG). There is no make-up gas in our case so the only gas that can be used is the primary gas (CO₂/or Separator Gas).

The following tables (3.1-3.5) are showing the procedure that MCM option followed to perform the calculation when the separator gas is used as a primary gas.

Step2:

Solvent is added to the oil such that the solvent to oil molar ratio increases by a specified value for each mixture. The Solvent **increment ratio has a defaulted value of. 0.01**. With this defaulted value about 100 Flash calculations are performed for a maximum of 100 mixtures of solvent and oil. If no two-phase region is detected, in the first contact, the process is judged to be first contact miscible and the calculations stop.

The numbers of flash calculations have been decreased to 10 this is done by assigning a value of 0.1 for solvent increment ratio. The reason behind this is for simplicity and to see how these calculations are done inside the software which in turns allows a better understanding of the processes.

So

$$0.01 * 100 = 1$$

And also

$$0.1 * 10=1$$

The 10 flash calculations are shown the Table 3.2

Table 3.1 the composition of Reservoir Fluid and Separator Gas

Original Oil	Separator Gas
1.12	4.16
1.05	9.94
10.82	60.68
4.34	10.98
8.22	9.2
2.22	1.29
6.41	2.64
2.86	0.5
3.54	0.46
4.45	0.09
54.97	0.06

Table 3.2 Flash Calculations for Detecting the Single Phase and the Two Phase Region

Single Phase Region (liquid)					2-Phase Region				Single Phase Region (Gas)
0.1	0.2	0.3	0.4	0.5	0.6	0.7	0.8	0.9	1
new feed	new feed	new feed	new feed	new feed	new feed	new feed	new feed	new feed	new feed
1.424	1.728	2.032	2.336	2.64	2.944	3.248	3.552	3.856	4.16
1.939	2.828	3.717	4.606	5.495	6.384	7.273	8.162	9.051	9.94
15.806	20.792	25.778	30.764	35.75	40.736	45.722	50.708	55.694	60.68
5.004	5.668	6.332	6.996	7.66	8.324	8.988	9.652	10.316	10.98
8.318	8.416	8.514	8.612	8.71	8.808	8.906	9.004	9.102	9.2
2.127	2.034	1.941	1.848	1.755	1.662	1.569	1.476	1.383	1.29
6.033	5.656	5.279	4.902	4.525	4.148	3.771	3.394	3.017	2.64
2.624	2.388	2.152	1.916	1.68	1.444	1.208	0.972	0.736	0.5
3.232	2.924	2.616	2.308	2	1.692	1.384	1.076	0.768	0.46
4.014	3.578	3.142	2.706	2.27	1.834	1.398	0.962	0.526	0.09
49.479	43.988	38.497	33.006	27.515	22.024	16.533	11.042	5.551	0.06

As shown in the Table3.2 the first mixture that had been found in the two phase region was detected at solvent increment ratio of 0.6. The mixture at 0.6 solvent increment ratio will be used as the first point of initiating multiple contacts miscibility calculation and it is represented in Pseudo-Ternary by Point A

Step3:

Using the first point (A) in the two-phase region detected in Step 2, all liquid is removed. The remaining gas is combined with the original oil in the gas oil to form B1. The mixing ratio of the equilibrated gas to the original oil is set to 0.9 which

means that the new mixture will have 90% of equilibrated gas and 10% of the original oil. A flash calculation is performed, and the liquid is removed. The procedure is repeated. This simulates a vaporizing or extraction process, and generates the portion of the phase envelope marked B. A maximum of 50 flash calculations is performed.

Table 3.3: The First Mixture MCM Calculation

		A		
		Step size		
Original Oil	Separator Gas	0.60	Eq. Oil	Eq. Gas
1.12	4.16	2.944000	2.823480	3.904740
1.05	9.94	6.384000	5.392670	14.286790
10.82	60.68	40.736000	37.983840	62.675990
4.34	10.98	8.324000	8.349380	8.121680
8.22	9.2	8.808000	9.142180	6.143930
2.22	1.29	1.662000	1.754430	0.925190
6.41	2.64	4.148000	4.409140	2.066220
2.86	0.5	1.444000	1.554180	0.565630
3.54	0.46	1.692000	1.827180	0.614400
4.45	0.09	1.834000	2.001960	0.495030
54.97	0.06	22.024000	24.761570	0.200390

Table 3.4: The Second Mixture in MCM Calculation

B1 Mixing ratio			B2 Mixing ratio		
0.9			0.9		
New feed	Eq. Oil	Eq. Gas	New feed	Eq. Oil	Eq. Gas
3.62627	2.783	3.860790	3.586711	2.741840	3.814210
12.96311	5.589	15.013720	13.617348	5.783020	15.726880
57.49039	37.918	62.933080	57.721772	37.814610	63.082140
7.74351	7.936	7.689960	7.354964	7.560240	7.299690
6.35154	8.612	5.722990	5.972691	8.177310	5.379050
1.05467	1.692	0.877580	1.011822	1.645530	0.841190
2.50060	4.329	1.992050	2.433845	4.279680	1.936820
0.79507	1.604	0.570150	0.799135	1.643250	0.571840
0.90696	1.913	0.627280	0.918552	1.976420	0.633700
0.89053	2.198	0.526960	0.919264	2.322380	0.541440
5.67735	25.427	0.185450	5.663905	26.055730	0.173020

Table 3.5: The Third Mixture in MCM calculation

B3 Mixing ratio				B4 Mixing ratio		
0.9				0.9		
New feed	Eq. Oil	Eq. Gas	New feed	Eq. Oil	Eq. Gas	
3.544789	2.578630	3.614460	3.365014	2.65954	3.71586	
14.259192	6.548880	18.460020	16.719018	6.16746	17.11461	
57.855926	37.130840	62.842070	57.639863	37.51876	63.10565	
7.003721	6.377280	6.085790	5.911211	6.90986	6.62968	
5.663145	7.107500	4.527910	4.897119	7.53275	4.8688	
0.979071	1.562360	0.762680	0.908412	1.58902	0.79197	
2.384138	4.239300	1.822360	2.281124	4.23805	1.86444	
0.800656	1.741770	0.567510	0.796759	1.70115	0.57089	
0.924330	2.119720	0.633840	0.924456	2.06335	0.6366	
0.932296	2.541780	0.543690	0.934321	2.46357	0.5477	
5.652718	28.051930	0.139660	5.622694	27.15649	0.15379	

Basically these calculation are performed until one of the following conditions is satisfied

- MCM Displacement (Vaporizing gas drive)
- MCM Displacement (Condensing gas drive)
- Immiscible displacement

The Tables (3.3-3.5) does not cover all mixtures and it just shows the calculation and the procedure, however the objective was only to understand how the MCM is conducted using MCM option in CMG winprop. It should be mentioned that the Tables 3.3-3.5 illustrate the procedure when the MCM process is a vaporizing gas.

Step4:

When the multiple contact miscibility process is a condensing gas drive the process will be performed as the following:

Again, using the first point (A) in the two-phase region detected in Step 2, all vapors are removed. The remaining liquid is combined with the original solvent in the solvent liquid ratio to form C_1 . A flash calculation is performed, and the vapor is removed. The procedure is repeated until the oil cannot be enriched further or after a maximum of 50 flash calculations are performed. This process simulates a

condensing gas drive process, and generates the portion of the phase envelope marked C.

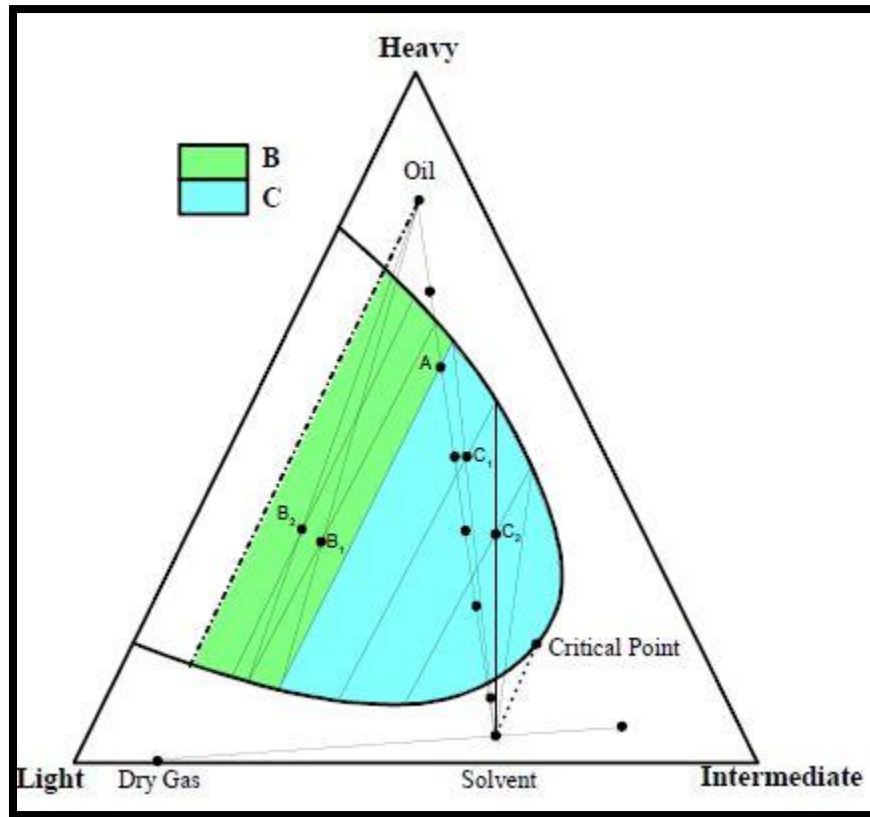


Figure 3.21:Pseudo-Ternary Diagram

3.7 Multiple Contacts Miscibility Results

3.7.1 EOS C7+

After entering the composition of Sarir oil and the solvent and specifying the reservoir temperature and pressure we run the cell to cell calculation using

- 1- CO₂
- 2- Separator gas

a- MCM calculation at 3315 **Psia** and 225 F by using Separator gas

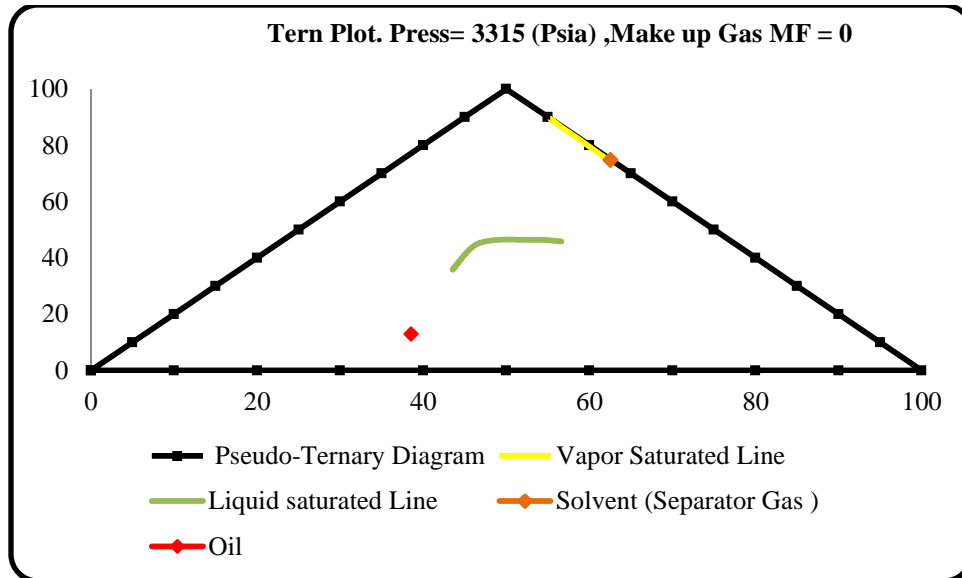


Figure 3.22: Pseudo Ternary Diagram (Separator Gas)

Summary Of Multiple Contact Miscibility	
Temperature	225 deg F
First Contact Miscibility Pressure (FCM) is Greater than	3315 Psia
Minimum Multiple Contact Miscibility Pressure (MMP) is Greater than	3315 A

b- MCM calculation at 3315 **Psia** and 225 F by using CO₂

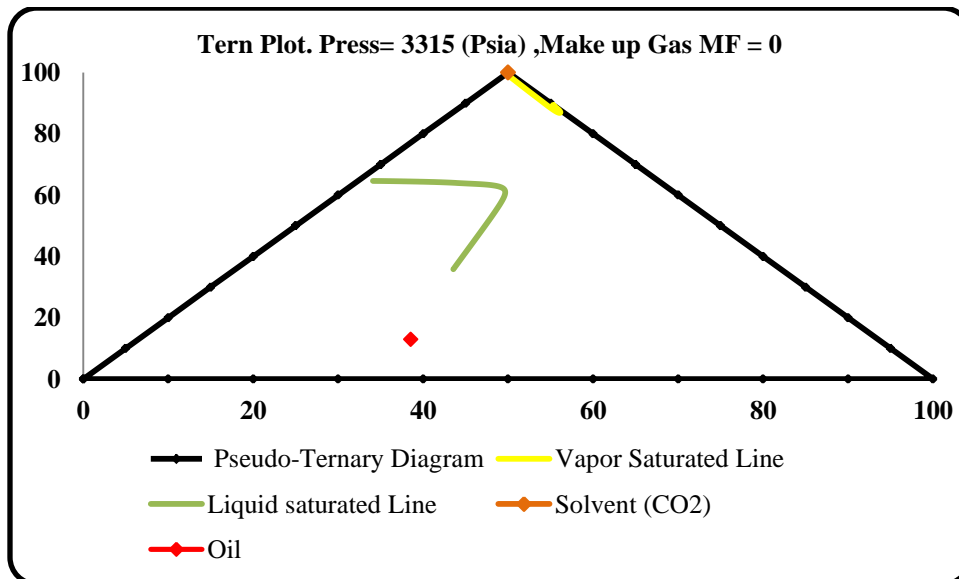


Figure 3.23: Pseudo ternary diagram CO₂

Summary Of Multiple Contact Miscibility	
Temperature	225 deg F
First Contact Miscibility Pressure (FCM) is Greater than	3315 Psia
Minimum Multiple Contact Miscibility Pressure (MMP) is Greater than	3315 Psia

c- MCM calculation at 5355 Psia and 225 F by using Separator gas

Since both solvents (Separator Gas and CO₂) are immiscible with oil at reservoir condition we increased the reservoir pressure to see at which pressure the solvent will be miscible with Sarir Oil.

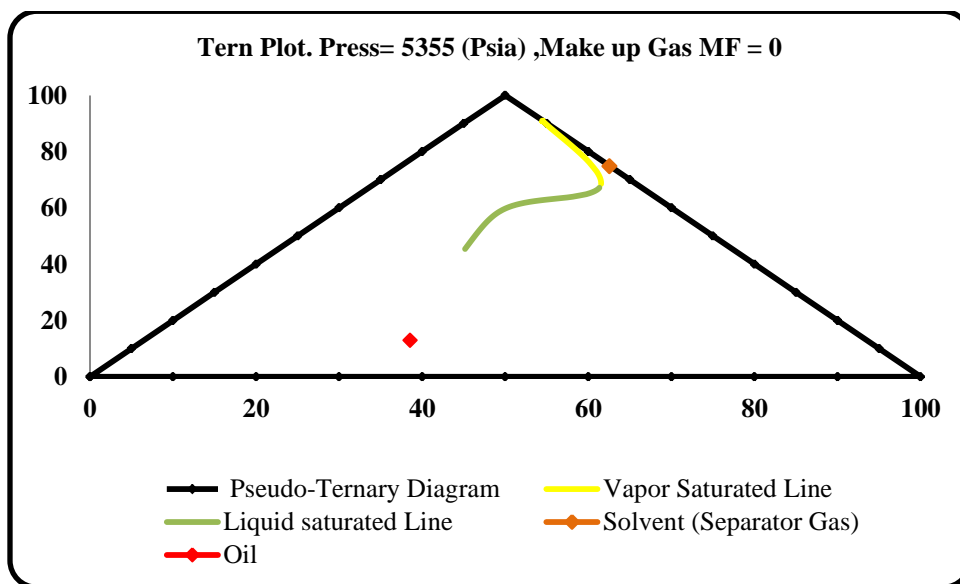


Figure 3.24: Pseudo ternary Diagram (Separator Gas)

Summary Of Multiple Contact Miscibility	
Temperature	225 deg F
First Contact Miscibility Pressure (FCM) is Greater than	5355 Psia
Minimum Multiple Contact Miscibility Pressure (MMP) is achieved by backward contacts - condensing gas drive	5355 Psia

d- MCM calculation at 5063 Psia and 225 F by using CO2

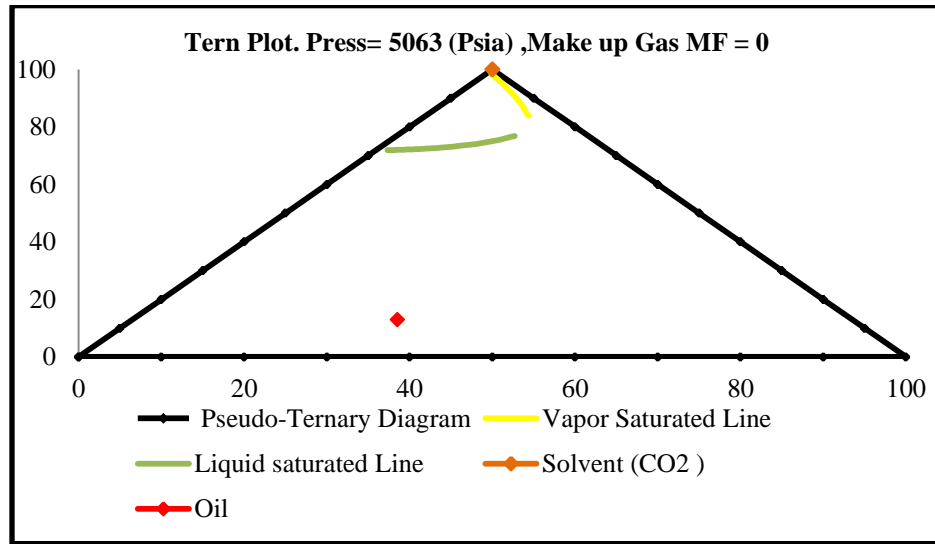


Figure 3.25: Pseudo Ternary Diagram CO2

Summary Of Multiple Contact Miscibility	
Temperature	225 deg F
First Contact Miscibility Pressure (FCM) is Greater than	5063 Psia
Minimum Multiple Contact Miscibility Pressure (MMP) is achieved by forward contacts – vaporizing gas drive	5063 Psia

It has been found that separator gas achieved miscibility at higher pressure compared with CO2. This is what it was expected.

Because Sarir oil is immiscible with the solvent at highest operation pressure (reservoir pressure) then there is no need to calculate the MMP for EOS C31+ and EOS C15

4. Slimtube Simulation

4.1 Simulating Slim-Tube Experiment Using Slimtube Calculation Option in PVTP

A good agreement has been found between Eos models generated by winprop and pvtp especially in saturation pressure, constant composition expansion CCE and Separator test data. This gives us much more confidence to proceed further as the focus of our work from the beginning was to get a good matching in these values

A slim-tube calculation can be initiated by selecting the Slim-tube simulation option from the calculation menu. This cell to cell model simulates gas injection into an oil reservoir. A series of cells is set by the program these cells are having the same size. Primary conditions of Cells are specified to be at Initial reservoir temperature and pressure. At each time step gas is added to the system. The mixed oil and gas in the first cell is flashed to find the new composition of the mixture and its properties. The material balance calculation and phase mobility criteria are used to compute how much of each phase is moved to the second cell. Once again the moved phase will mix with fresh oil in the second cell to form a new mixture. A Flash calculation is done to this mixture and the excess phase will be moved to the third cell. This process is repeated until this movable phase finally arrives at the production cell. At this point, the excess volume and composition appear as well stream products. Whether multiple contact miscibility is achieved is usually taken from the estimation of the minimum miscibility pressure (MMP). Definitions of the MMP can vary, but it is usually taken as the pressure at which the recovery is 90% when 1.2 pore volumes of gas have been injected. At pressures above MMP the gas is assumed to be miscible.

4.2 Methodology

The prepared EOS C7+ model is utilized to conduct a slim tube calculation using PVTP.

Two gases have been used as solvent in this study. These gases are:

- 1- CO₂ (100%) Gas
- 2- Separator Gas

The composition of the separator gas is shown in the Table 4.1

Table 4.1: The Molar Composition of Separator Gas

COMPONENT	MOL PERCENT
Hydrogen Sulphide	NTL
Carbon Dioxide	4.16
Nitrogen	9.94
Methane	60.68
Ethane	10.98
Propane	9.2
iso-Butane	1.29
n-Butane	2.64
iso-Pentane	0.5
n-Pentane	0.46
Hexanes	0.09
Heptanes plus	0.06

4.3 Simulation Results

4.3.1 Case 1: Conducting slim- tube simulation using 100% CO2 solvent

The composition of the injected gas has been specified in this case to be 100% of CO2. according to the slim tube experiment the CO2 is immiscible at reservoir temperature of 225F and reservoir pressure of 3300 psia. A pressure greater than the reservoir pressure was tried in order to estimate the MMP.

The recovery obtained at pressure of 5300PSIG is shown in the Figure 4.1

- RF At pressure of 5300 psig

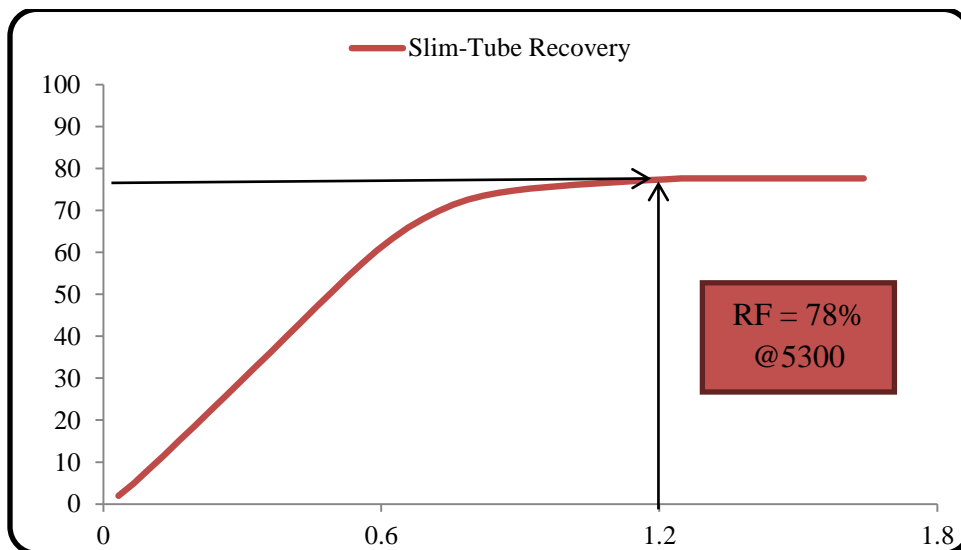


Figure 4.1: Oil Recovery From Slimtube at 5300PSIG

The recovery obtained at pressure of 3300PSIG is shown in the Figure 4.2

- RF At pressure of 3300 psig

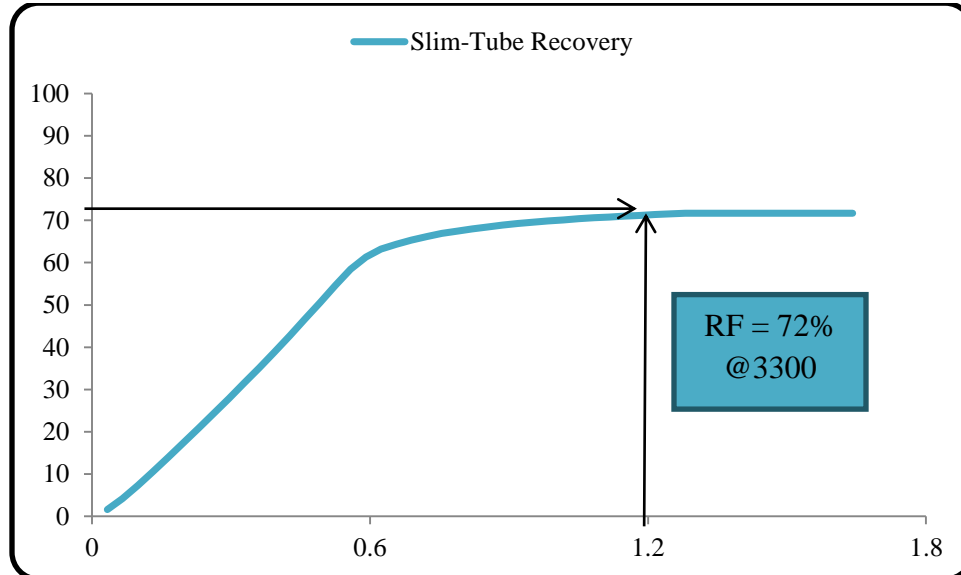


Figure 4.2: Oil Recovery From Slimtube at 3300

From these two results we can conclude the following:

- CO₂ is immiscible with Sarir Oil at reservoir temperature 225F and pressure 3300psig.
- Even when a higher pressure was tried the CO₂ is still immiscible with oil and this is due to the fact that the slim tube option in pvtp does not take into the account the chemical interaction between the CO₂ and the oil.
- The injected gas in the second case will be separator gas.

4.3.2 Case 2: Conducting Slim-tube Simulation Using Separator Gas

The same procedure that has been followed in the first case is repeated here again. The recovery obtained at pressure of 5300PSIG is shown in the Figure 4.3

- RF At pressure of 5300 psig

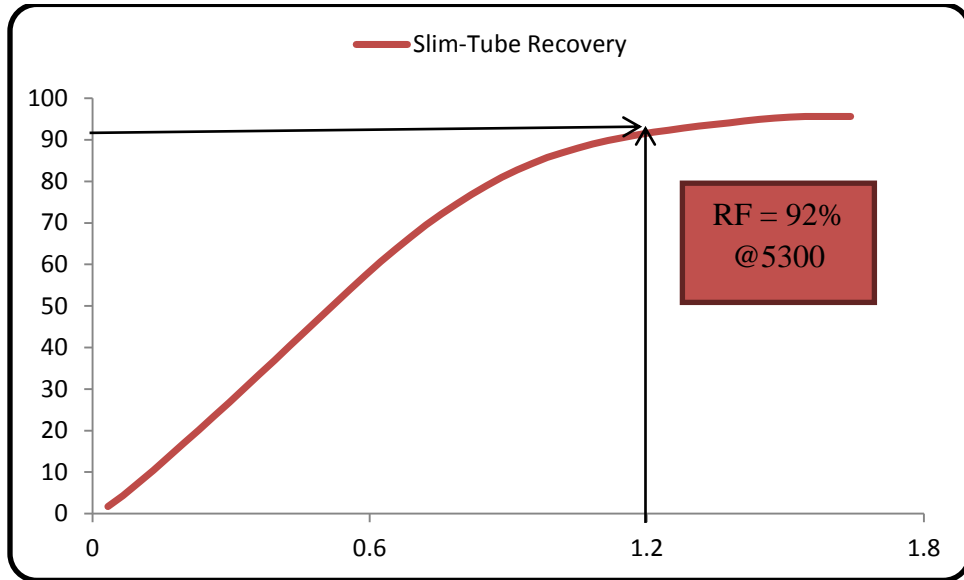


Figure 4.3: Oil Recovery From Slimtube at 5300

The recovery obtained at pressure of 3300PSIG is shown in the Figure 4.4

- RF At pressure of 3300 psig

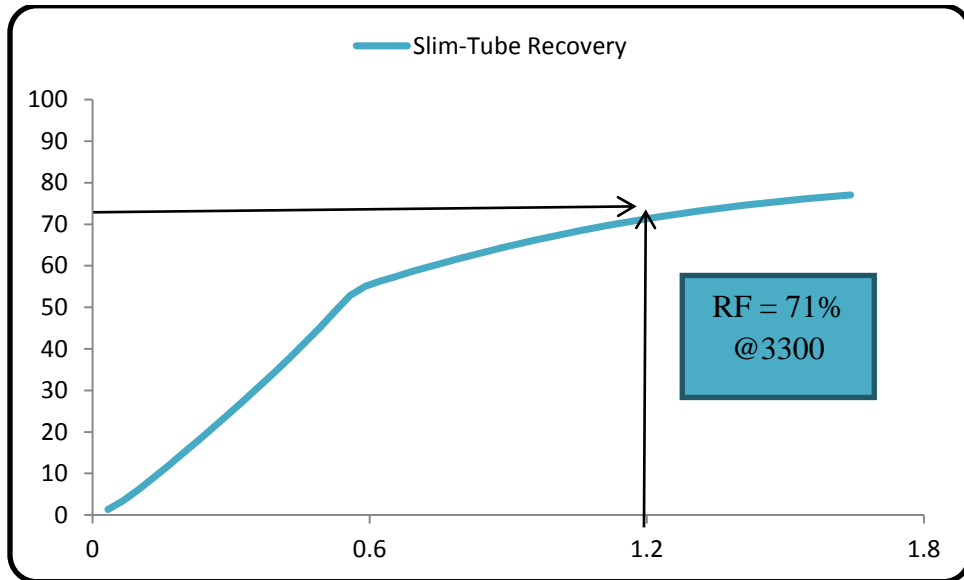


Figure 4.4 Oil Recovery From Slimtube at 3300

In this case we encounter a very strange behavior that the separator gas seems to be better than CO₂ in achieving the miscibility at lower pressure compared with CO₂.

For instance in the actual slim tube experiment the CO₂ gas and separator gas were found to be immiscible at pressure of 3300 psig also it is confirmed from the real slim tube experiment that the CO₂ was miscible at pressure of 3680 psig because the properties of the CO₂ allows it to achieve miscibility at lower pressure compared with separator gas.

In order to make a very fair comparison and before drawing the final conclusion we run a third case and this time by making the heavy end is much more lighter than it has to be. This has been done just to see how the CO₂ is going to behave when we have a lighter crude oil.

4.3.3 Case 3: Conducting Slimtube Simulation Using 100% CO₂ Solvent for Lighter Oil.

In this case the original composition of the fluid has been changed by making it light to see the effect of CO₂ injection.

The composition of the oil after making it much lighter than it used to be is presented in Table 4.2

Table 4.2 Oil with Lighter Composition

COMPONENT	MOL PERCENT
Hydrogen Sulphide	NTL
Carbon Dioxide	1.12
Nitrogen	1.05
Methane	10.82
Ethane	14.34
Propane	18.22
iso-Butane	12.22
n-Butane	6.41
iso-Pentane	2.86
n-Pentane	3.54
Hexanes	4.45
Heptanes plus	24.97

The recovery obtained at pressure of 5300PSIG is shown in the Figure 4.5

- RF At pressure of 5300 psig

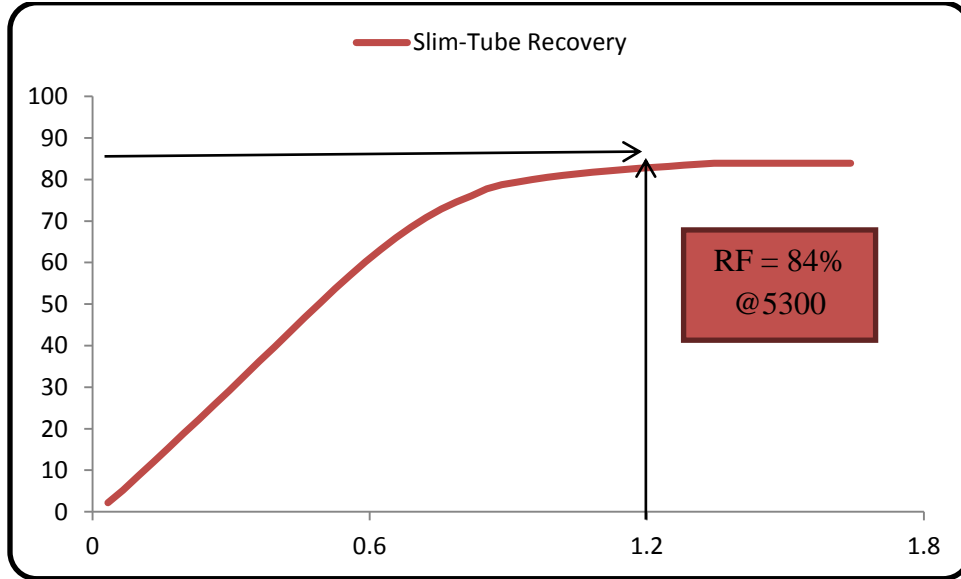


Figure 4.5: Oil Recovery From Slimtube at 5300

The recovery obtained at pressure of 3300PSIG is shown in the Figure 4.6

- RF At pressure of 3300 psig

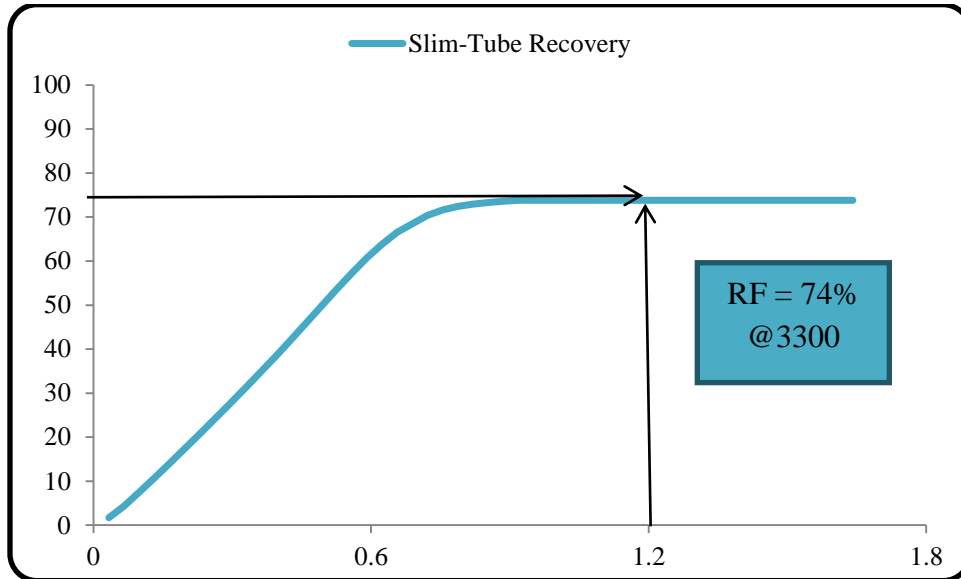


Figure 4.6: Oil Recovery From Slimtube at 3300

From these results we can say that the CO₂ still cannot achieve miscibility even by making the composition of the fluid lighter than it has to be , the reason behind that is because the slim tube option in pvtpr does not take into the account the chemical interaction between the Co₂ the oil. It is necessary now to build a 1-D model to verify the results obtained from MCM option CMG (winprop)

5. The 1-D Slimtube Simulation Model

5.1 Building the 1-D Slimtube Model by Using Reveal

In this section 1-D slimtube model will be constructed to simulate the MMP, Furthermore the deviation of the estimated MMP from the experimental value will be calculated. IPM suit “Reveal” is used to simulate the actual experiment.

The actual slim-tube experiment was conducted under the following conditions:

- Temperature of 225F
- Pressure of (3300 and 2500)Psig

The test was conducted under the following conditions

- Packing media: sand packed column
- Length : 40ft
- Internal diameter: 0.176 inches
- Porosity Percent : 37.5

The simulation model is built to capture and address all test conditions and properties of actual experimental test .The model will be built using Cartesian coordinates (I, J, K).

The model has 10 cells in the I direction each with length of 100 ft. summing up to 1000ft 1 cell in both J and K direction with length of 100 ft.

The injection well that simulate the CO₂ injection point in the actual experiment was defined in the program with 100% CO₂ solvent content by perforating the Cell (1,1,1) and The producing well was defined in the cell (10,1,1). Since there is no water saturation in the actual slim tube experiment the solubility of CO₂ in water has been neglected.

5.2 Steps followed to build the 1-D model

1- Control

a- The component model

The tuned EOS has been introduced to **Reveal** under this option

b- Grid geometry section

In this section the Cartesian coordinates have been specified as the following

- 10 grids in x direction
- 1 grid in both Y and Z direction (single layer)

The size has been specified as the following

	From	to	D (X,Y,Z) Ft
X	1	10	100
Y	1	1	100
Z	1	1	100

2- Reservoir section

a- The reference depth has been set to 10000ft

b- The porosity

The value has been set equivalent to the actual slim tube experiment value

$$\Phi=37.5\%$$

c- The Permeability with a value of 4 Darcy in all directions

d- Rock type definition

It is just a single region which covers all the blocks (Region1)

e- PVT Region

A single PVT file (EOS) for all the blocks

f- Equilibrium Region

Run a single rule of equilibrium for all blocks

g- Fluid in place (FIP)

A single definition for the whole reservoirs (in case of big reservoirs we might need to split it using different PVT files and different regions).

3- Physical Section

a- PVT file

Even though the EOS model has been specified from the beginning the software still requires the introduction of the PVT file because the software needs water data.

4- Relative Permeability Section

a- Three phase model

Linear model has been chosen with no hysteresis

b- Critical saturation has been set to the minimum values

c- Relative permeability data

Reveal does not support the simple Corey function for relative permeability thus the only available options are stones model (3-phase model with more complex system)

Relative permeability data that have been used are in the following tables

Table 5.1: Relative Permeability For Gas/Oil system

			Inputs in Reveal			
Sg	Krg	Krog	So	Krog	Sg	Krg.
0.0000	0.0000	0.9500	0.0000	0.0000	0.0000	0.0000
0.1000	0.0084	0.5700	0.1000	0.0000	0.1000	0.0084
0.2000	0.0496	0.3900	0.2000	0.0040	0.2000	0.0496
0.3000	0.1250	0.2750	0.3000	0.0390	0.3000	0.1250
0.4000	0.2347	0.1900	0.4000	0.0870	0.4000	0.2347
0.5000	0.3788	0.1300	0.5000	0.1300	0.5000	0.3788
0.6000	0.5349	0.0870	0.6000	0.1900	0.6000	0.5349
0.7000	0.6512	0.0390	0.7000	0.2750	0.7000	0.6512
0.8000	0.7674	0.0040	0.8000	0.3900	0.8000	0.7674
0.9000	0.8837	0.0000	0.9000	0.5700	0.9000	0.8837
1.0000	1.0000	0.0000	1.0000	0.9500	1.0000	1.0000

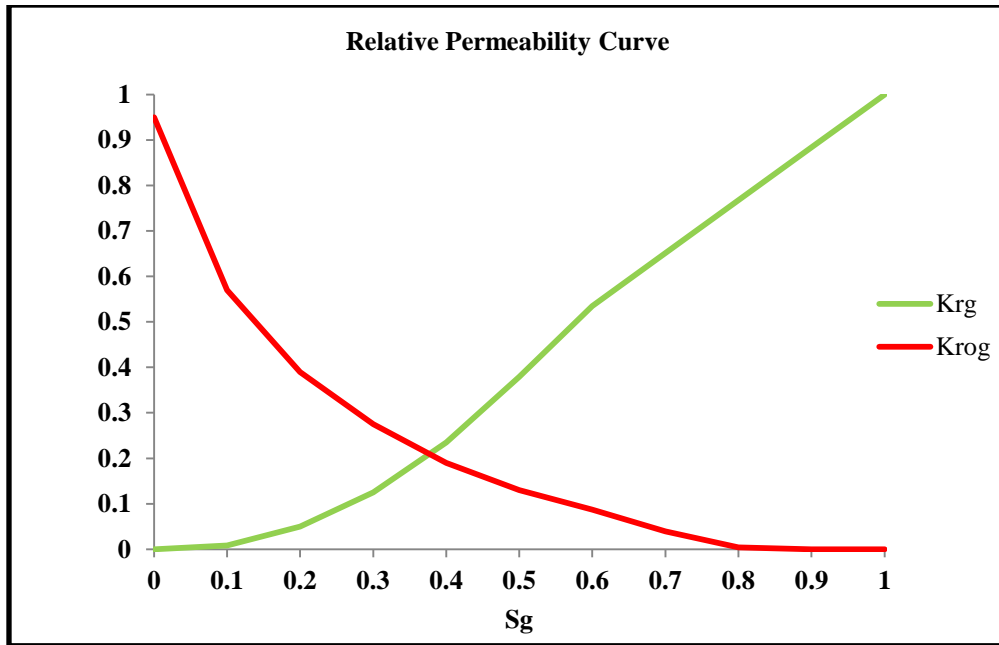


Figure 5.1: Relative Permeability Curves For Gas/Oil System

Table 5.2: Relative Permeability Values for Water /Oil System

Sw	Krw	Kro	Inputs in Reveal			
			Sw	Krw	so	krow
0	0	1	0	0	0	0
0.0001	0	0.999	0.0001	0	0.05	0.00001
0.05	0.00086	0.8478	0.05	0.00086	0.1	0.00012
0.1	0.00263	0.6975	0.1	0.00263	0.15	0.00051
0.15	0.00524	0.5572	0.15	0.00524	0.2	0.00149
0.2	0.00877	0.4329	0.2	0.00877	0.25	0.00346
0.25	0.01338	0.3276	0.25	0.01338	0.3	0.00699
0.3	0.01927	0.2418	0.3	0.01927	0.35	0.01284
0.35	0.02672	0.1742	0.35	0.02672	0.4	0.02199
0.4	0.03608	0.1224	0.4	0.03608	0.45	0.03572
0.45	0.04781	0.0837	0.45	0.04781	0.5	0.05565
0.5	0.0625	0.0557	0.5	0.0625	0.55	0.08374
0.55	0.0809	0.0357	0.55	0.0809	0.6	0.12237
0.6	0.10394	0.022	0.6	0.10394	0.65	0.17415
0.65	0.13277	0.0128	0.65	0.13277	0.7	0.24177
0.7	0.16869	0.007	0.7	0.16869	0.75	0.32757
0.75	0.21302	0.0035	0.75	0.21302	0.8	0.43286
0.8	0.26667	0.0015	0.8	0.26667	0.85	0.55717
0.85	0.32918	0.0005	0.85	0.32918	0.9	0.69746
0.9	0.39706	0.0001	0.9	0.39706	0.95	0.84782
0.95	0.46103	1E-05	0.95	0.46103	0.9999	0.999
1	0.5	0	1	0.5	1	1

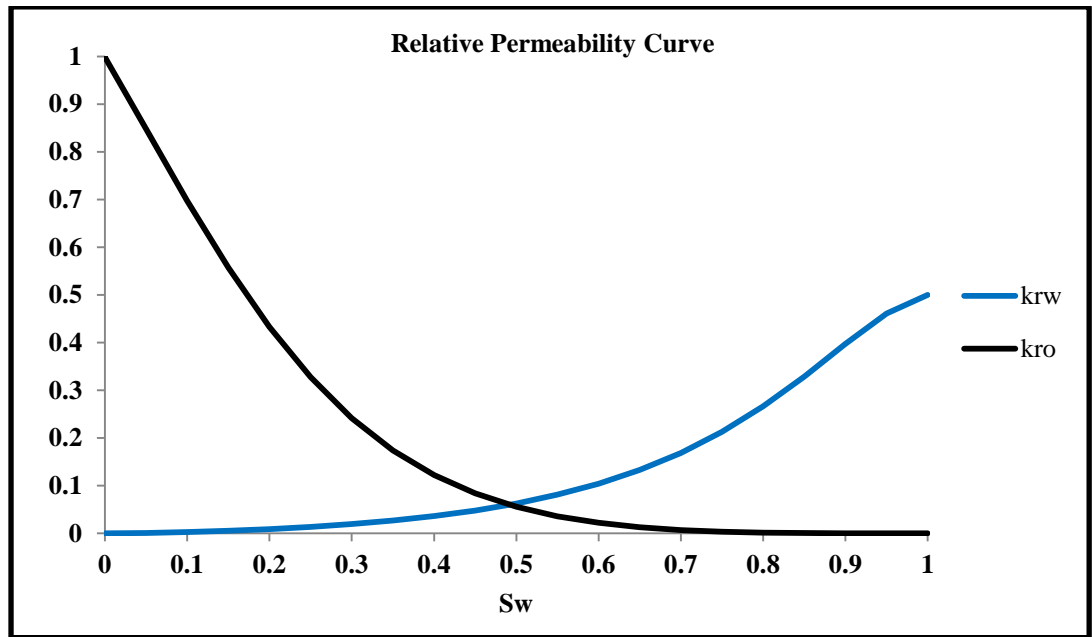


Figure 5.2: Relative Permeability Curves For Water/Oil System

5- Well Positions and properties

- a- The first well at the first block (injector)
- b- The second Well at the last block (Producer)
- c- The block is fully perforated
- d- The flowing radius (**rw**)

The software needs this value in order to compute the final dp between the block before the last Cell and the well (Darcy law cannot be used at that point).

rw: is set to the defaulted value of 0.354 ft.

The depth and initial reservoir pressure have to be set to the injection pressure

The production plan has been specified to be a pressure plan (steady state).

Since the aim of the study is to mimic the **MMP** so it is necessary to keep the pressure in the porous media as fixed as possible. This is done by arranging the outflow and inflow pressure so that the pressure stays more or less constant

In order to parameterize this we need to understand what they exactly do in the real slim tube experiment.

In the actual slim tube experiment we inject at specific rate but we focus more in the outlet pressure where we have a pack pressure valve which guarantee that the fluid will not come out from slim tube until the injection pressure is reached also the pack pressure regulator maintain any reduction in the pressure due to the production.

To simulate the function of pack pressure regulator valve a fixe bottom hole pressure in both producer and injector is selected with slightly higher pressure at injector so that to allow drawdown (flow).The 1-D model configuration is shown in Figure5.3

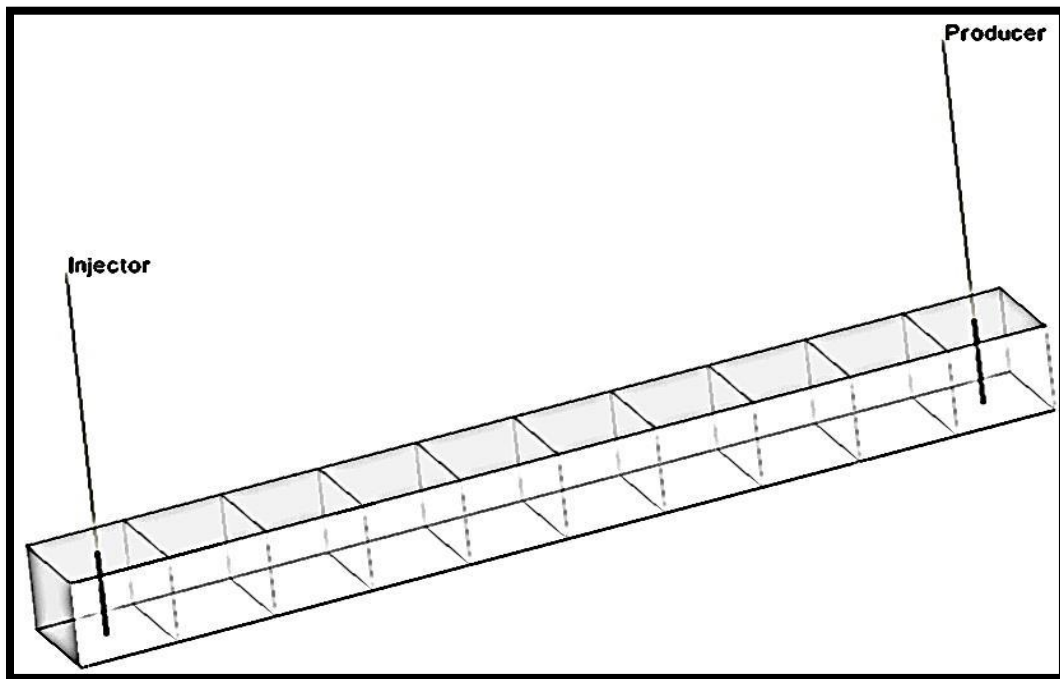


Figure 5.3: Slim-Tube 1-D Model

Running slim tube simulation with a small number of cells can give high uncertainty in the calculation due to the numerical dispersion effect however as the number of cells is increased, the effect of numerical dispersion is eliminated which in turns allows the solutions to stabilize and be more realistic. In our work, we verify this by choosing a different number of cells.

In order to select the optimum number of cells a set of oil recovery plots for a different number of cells has been constructed. See Figure5.4

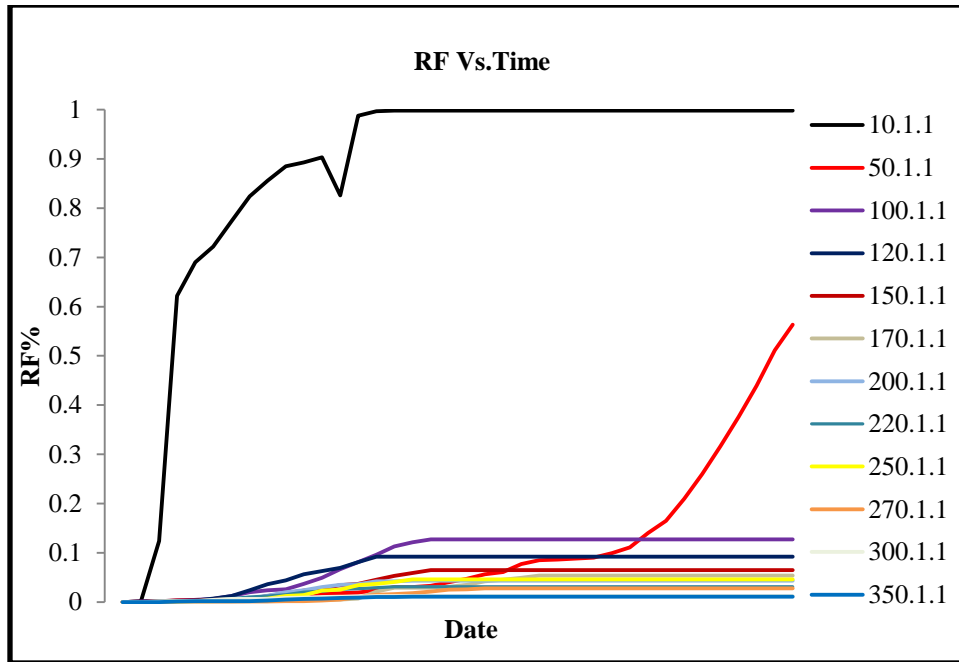


Figure 5.4: Optimizing the Cell Numbers

The numerical dispersion and solution stabilization effect can be seen in in Figure 5.4 in the models that have lower number of cells. For instance the deviation error in the oil recovery between the first models with 10 cells is about 50 percent from the second model. Also is the case between the second model and the third one .when the number of cells increased, the deviation in the oil recovery is reduced therefore the number of cells can strongly affect the overall calculation. A model with 150 cells has been chosen as the optimum model.

5.3 1-D model simulation Results

The simulation has been run at two different pressures:

- 1- The reservoir pressure 3300 psig
- 2- Pressure higher than the reservoir pressure MMP 4010 psig

An investigation of miscibility has been done at these pressures by tracking some oil properties that can give us an indication about the miscibility.

The Cell 75 in our model has been selected to monitor the effect of CO2 in the center of the slim tube Model.

5.3.1 Miscibility investigation at pressure of 3300 psig

- Oil Recovery

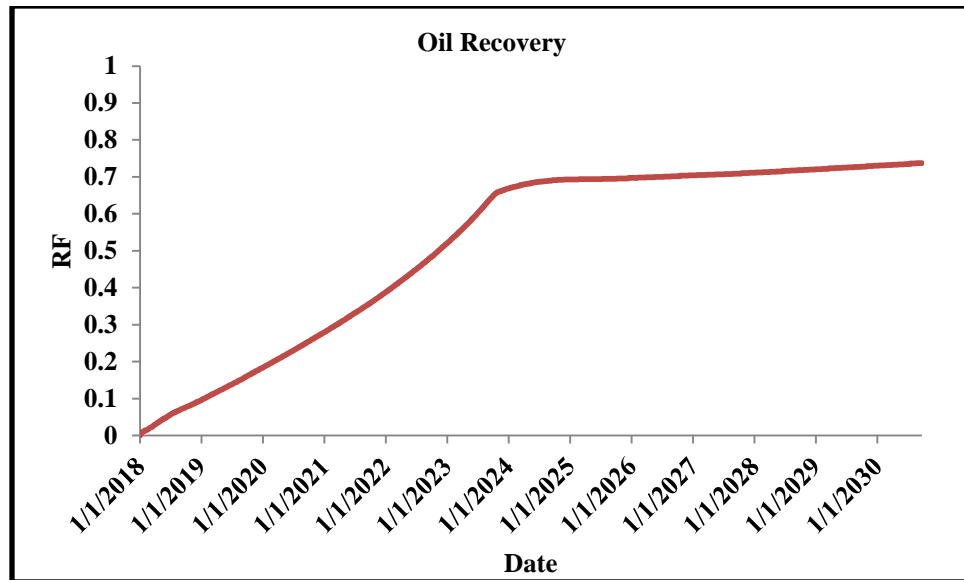


Figure 5.5: Oil Recovery at Pressure of 3300 psig

The **MMP** is estimated as the intersection of the two different trend line curves of oil recoveries versus the injected volume of CO₂ (PV of 1.2 intersect with oil recovery at 90 percent). It should be noted that the pore volume of 1.2 represents the time of the breakthrough. Simulation running time was selected to be enough for the CO₂ to reach the last cell.

Figure 5.5 shows that the breakthrough time occurred in the end of 2023 and oil recovery at that time estimated to be about 63%. From 2023 until the end of the simulation 2030 the recovery is increased slightly to 73%. This increment in oil recovery can be attributed to the vaporizing effect solely because as the gas breakthrough it will move faster than oil and the oil remained in place is continuously subjected to fresh CO₂ slugs

- Oil and Gas Saturation

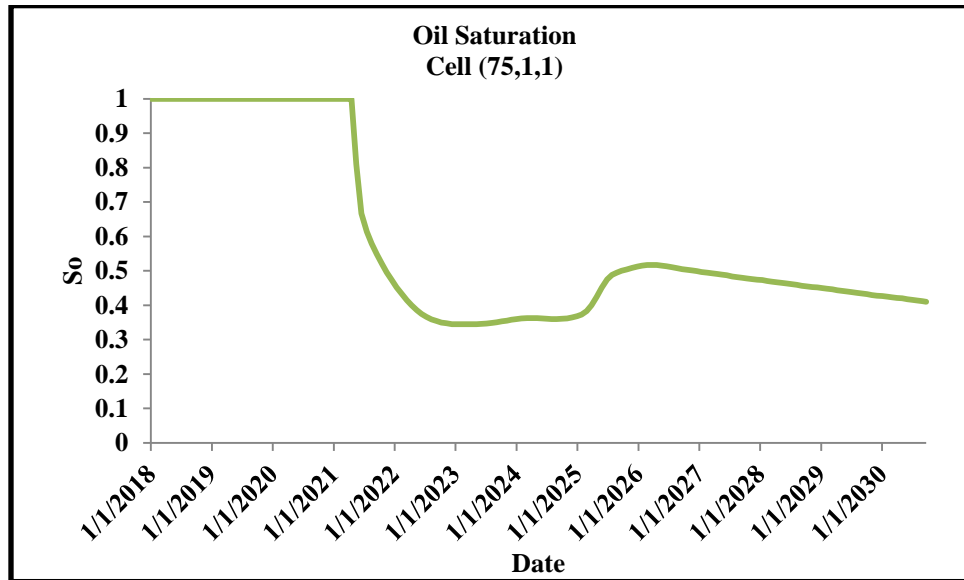


Figure 5.6: Oil Saturation at Pressure of 3300 psig

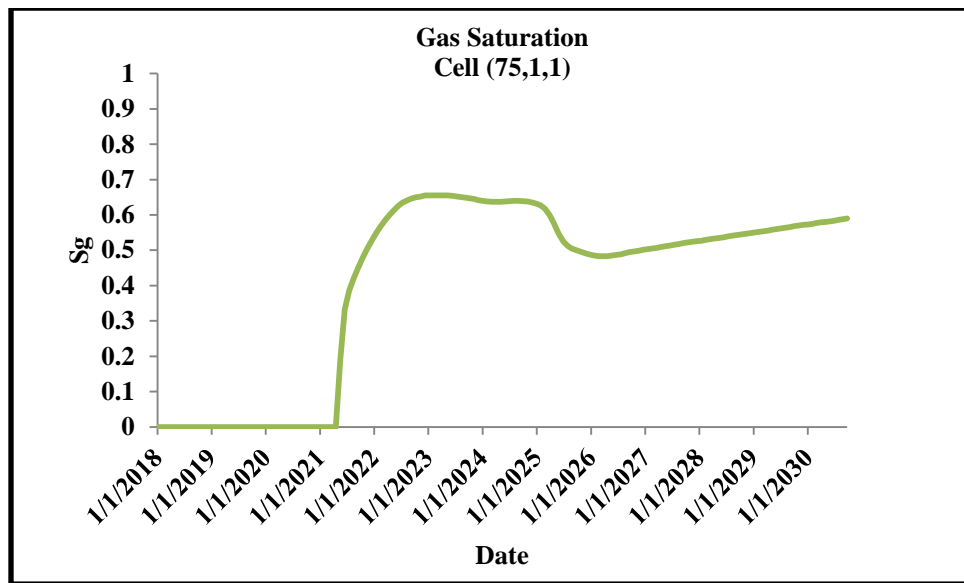


Figure 5.7: Gas Saturation at Pressure of 3300 psig

Figure 5.6 shows that the CO₂ has displaced the oil and reduced its saturation to about 40 % which means that about 60 percent of the oil has been displaced immiscibly by the end of the simulation while in Figure 5.7 the gas saturation has been increased to about 60% in 2030. The high residual oil saturation that is left behind is due the fact that the CO₂ has displaced the oil the immiscibly and slight the

increment in oil saturation after the breakthrough time can be attributed to the vaporizing effect solely.

- **The Oil and Gas Density**

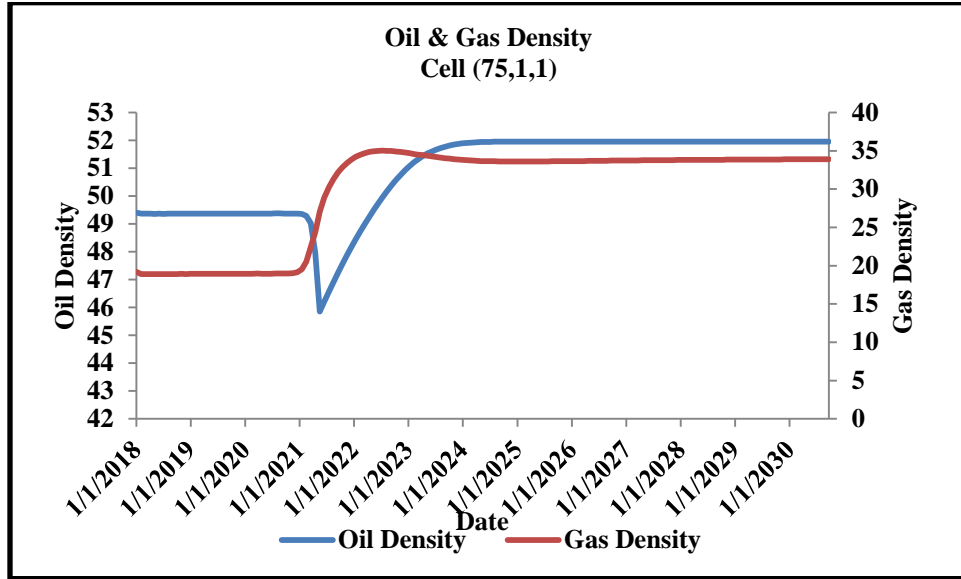


Figure 5.8: Oil and Gas Densities at Pressure of 3300 Psig

The partial vaporizing and condensing effect causes a reduction in oil density and increase gas density after some time only gas will move as a result of breakthrough due to immiscible displacement the gas will keep being enriched due to the vaporizing effect and the oil density will be high due to the fact that only a residual or heavy fractions of the oil is left.

- The Equilibrium Constant C1 (k-Value):

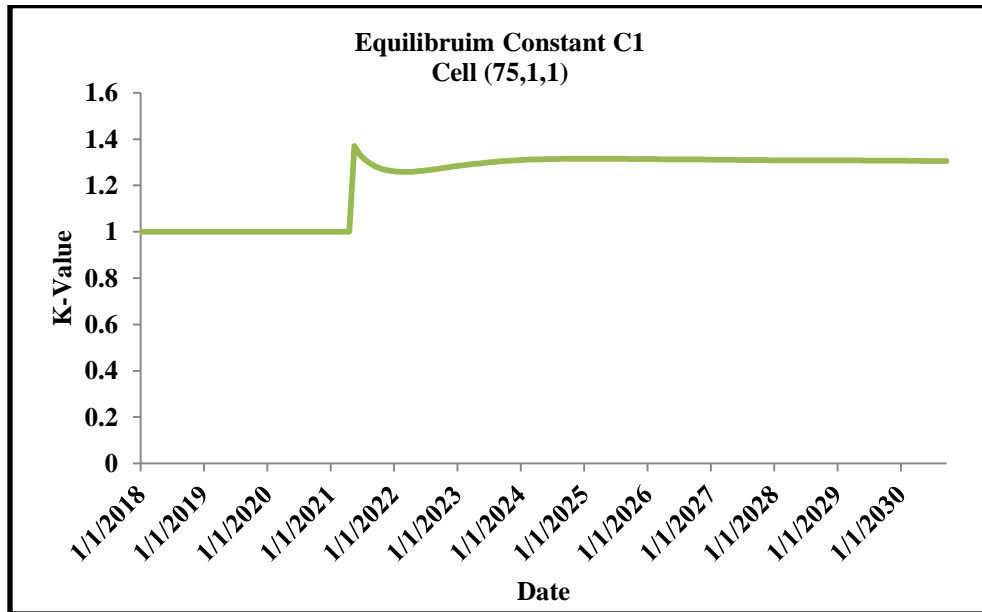


Figure 5.9 K-Value of C1 at Pressure of 3300 Psig

The equilibrium constant is the ($k=Y_i/X_i$) mole fraction of gas phase to the mole fraction of the liquid phase if this value approaches to the unity it can be a good indication of miscibility. From the figure above this value is higher than one which means that the miscibility is not possible at this pressure.

We should also notify that at pressure higher than bubble point pressure the K-value has to be equal to zero because all the vapor phase is dissolved in the oil. In fact Reveal does not take into the account vapor- liquid problem and assign a value of one to the oil phase whether if it is saturated oil or undersaturated one

5.3.2 Miscibility investigation at pressure of 4010Psig

- Oil Recovery

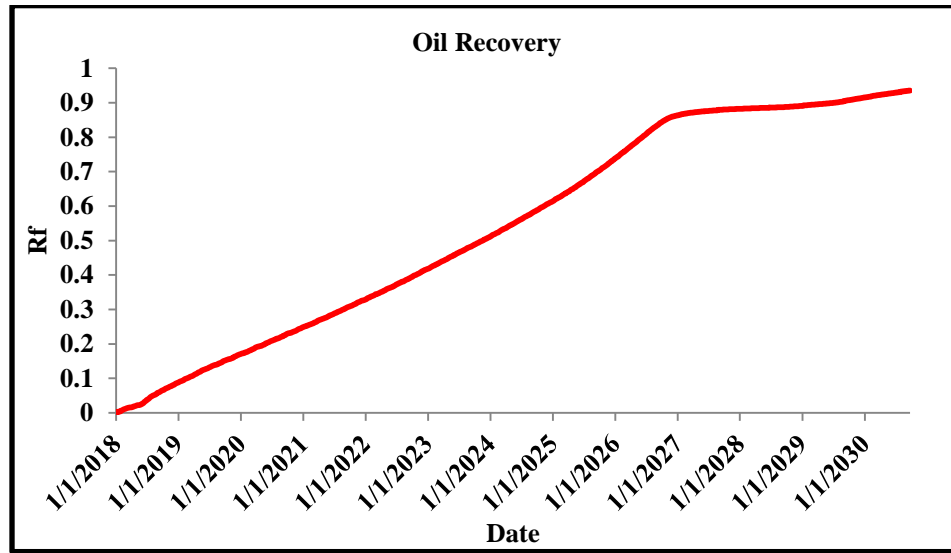


Figure 5.10: Oil Recovery at Pressure of 4010 Psig

At this pressure the recovery of oil has been increased to more than 90% which proves that the CO₂ is miscible with the oil pressure. In order to confirm this, we need to take a look at the other properties

- The oil and gas saturation

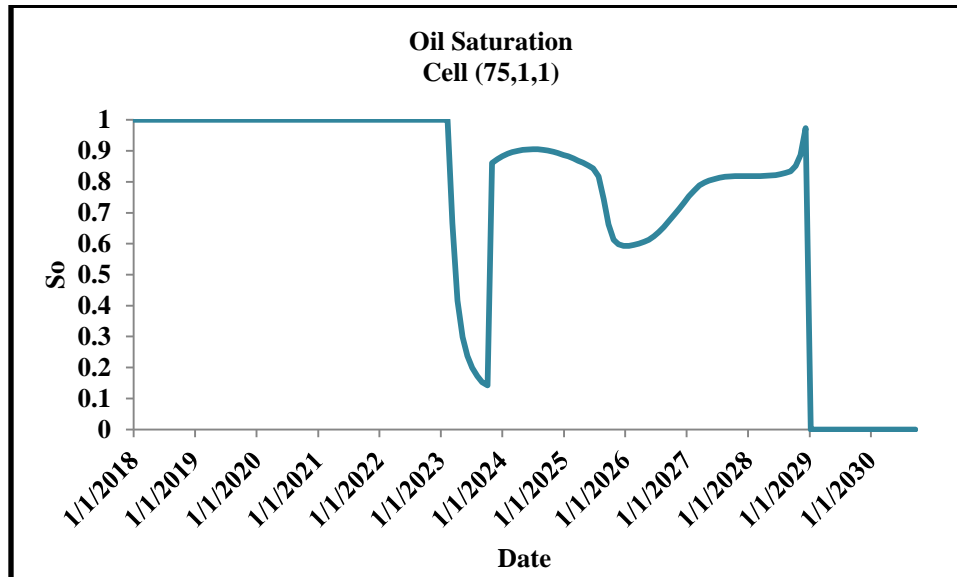


Figure 5.11: Oil Saturation at Pressure of 4010Psig

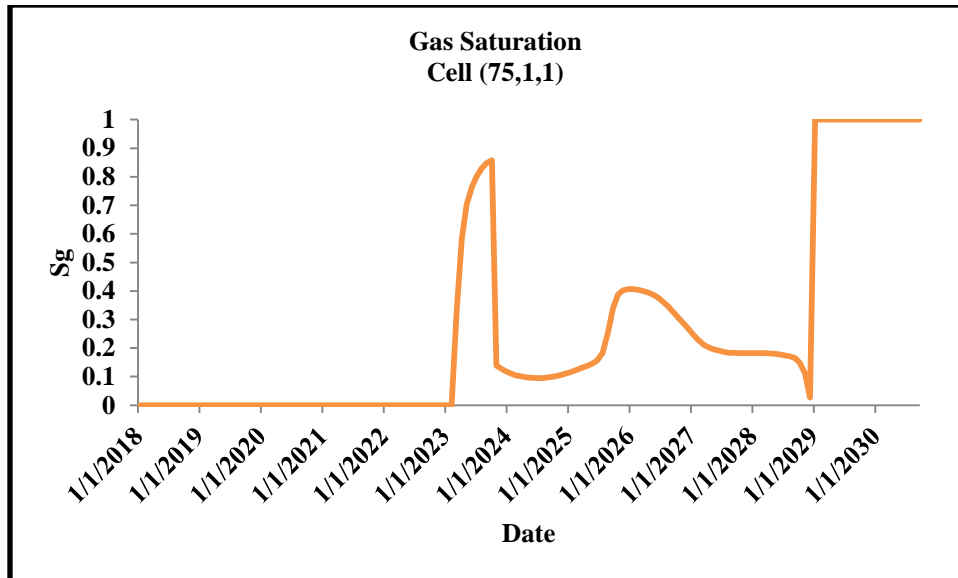


Figure 5.12: Gas Saturation at Pressure of 4010Psig

When we look at oil and gas saturation plots there is an abrupt change in both oil and gas saturation which is an indication of miscibility. The logical explanation to this abrupt change is that when the oil and gas are miscible. Reveal fail to distinguish between these two fluids and it will consider them as single fluid this is can be easily seen in the jump in the saturation in Figure 5.12&5.13

- The oil and gas density

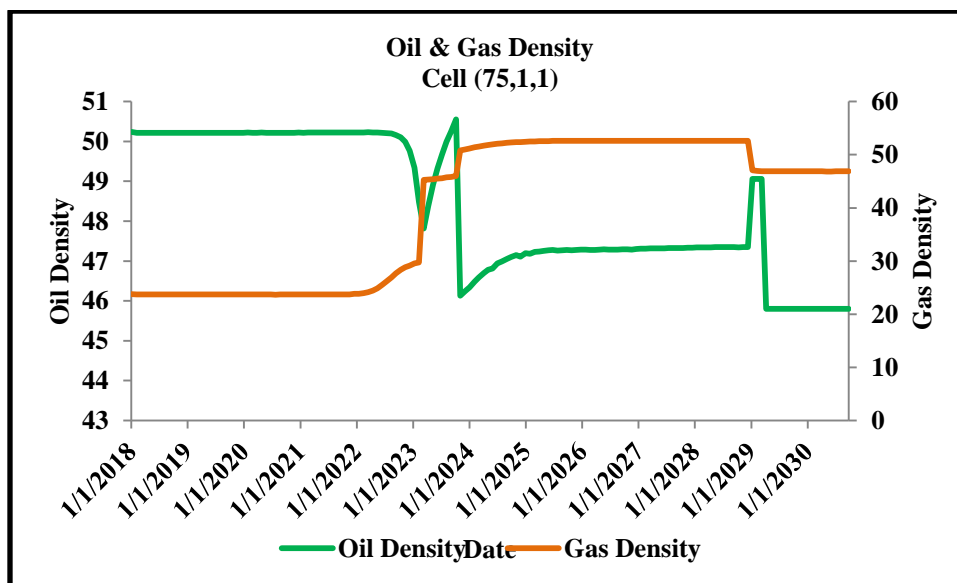


Figure 5.13: Oil and Gas Densities at Pressure of 4010 Psig

Oil is much denser than gas due to the miscibility effect and as we can see in Figure 5.14 the density of oil and gas are switched to the opposite direction.

- **The Equilibrium constant C1(k-value)**

At pressure of 4010 Psig the K value is approaching to the value of one (1) in other word the minimum miscibility pressure is encountered at this pressure and hence miscibility is developed.

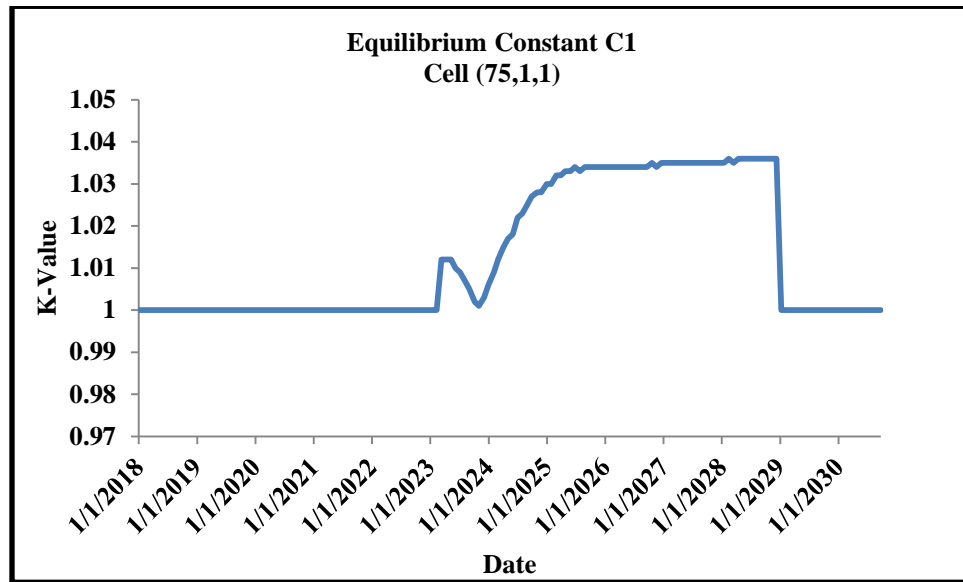


Figure 5.14: K-Value Of C1 at Pressure of 4010Psig

5.3.3 Comparison of the Estimation of MMP using two different methods

Table 5.3 shows the deviation in the calculation of MMP from the two different methods:

- The MCM option (cell to cell simulation in winprop)
- The 1-D slim tube simulation method

Table 5.3: the Predicted MMP by both EOS(MCM) and 1-D slimtube calculations:

MMP Calculations (Psig)		
MMP Experimental value	CMG WinProp (MCM option)	1-D Model
3680	5047	4010
Err%	37.15	8.97
Minimum Multiple Contact Miscibility Pressure (MMP) is achieved by	Vaporizing Drive	Combined Drive (vaporizing & Condensing)

6. Conclusion and Discussion

6.1 Equation of state Model

- Although the sample is collected with high level of contamination showing water content higher than 10% which might impact the validity of the sample's Representivity.
- last statement should be confirmed through a study of oil and gas composition equilibrium ratio from differential liberation questing the rate of light component transfer to gas phase a more analysis should be performed to judge on the sample validly, reliability (upward change in relative volume in low pressure is unexpected in this type of crude oil as low gas oil ratio suggest likely linear change of properties with pressure) and whether it is representative should be done which include trend analysis, data completeness, integrity of the sample with production and other PVT sample, compositional material balance cannot be performed in our case due to lack of information from distillation process, consistency of GOR, separator test Hoffman plot check, validity of CCE with extended Y function, Total formation volume factor check on CCE and DL, sample transportation information opening and closing pressure
- Before the regression took a place the original composition was changed with changing the Mw of heavy end C7+ however the changing In the composition did not improve the prediction of volumetric data significantly the method followed in changing the composition is as the one followed in (Aguar McCain and Meshari).
- The variation in the experimental MW+ was allowed up to $\pm 25\%$
- Because is difficult to adjust the Apparent mw with high accuracy the Solver option is introduced to give accurate value for each trail (the table of the method in the Appendix E).
- the critical properties of the heavy end PC,Tc,AC, MW+ and volume of shift were the best candidates for regression in our case
- more emphasis is put on the Separator Test data than Differential liberation test data Because the slim tube test is normally specified at single pressure and the results from this test are directly flashed to the surface therefore there is no need to consider the

change in volumetric properties under a range of pressures (depletion effect) is a priority.

The lack of the detailed data like distillation data forces us to use the built in correlation options in the software.

There are three splitting distributional functions available in CMG Winprop

- Exponential
- 2-Stage Exponential
- Gamma distribution

We tried to understand the difference between the three distributional functions used in winprop for Splitting the heavy end . According to the CMG manual we found out some suggestions concerning the distributional functions and these are:

- Exponential for gas
- Tow stage exponential for oils
- Gamma for both (Oil and Gas)

In fact the differences between these methods were insignificant with slightly better predication for volumetric data when the gamma distributional function was utilized.

The difference between the gamma distribution and the others is that the gamma has more accurate correlation for predicting the boiling temperature (Whitson correlation) which in turns affects the prediction of critical properties.

Alpha parameter in gamma distribution is another sensitive parameter which provides a high flexibility to this distribution.

The built method in CMG winprop for lumping and splitting is (Whitson's Method). We tried to stack to these methods to provide a consistency between our calculation and calculations done by winprop especially during the lumping Procedure.

The three EOS models are built as the following

- Original EOS C7+
- Splited EOS C31+
- Lumped EOS C15

The data exhibit a huge uncertainty but for an educational purpose it was worth to give it a try and see what we can get from it at our best.

6.2 Minimum Miscibility pressure MMP calculation

- **MCM calculation Cell to Cell Simulation**

- The Sarir oil is immiscible with both separator gas and CO₂ at the maximum operation pressure (Reservoir pressure).
- MMP is lower in the case of CO₂ than the case of separator gas this is what was expected before running the MCM calculation
- There is a weird shape in the liquid saturation line in liquid phase this shape has been found through all the calculation at different pressures.

This shape attributed to the limitation of MCM option to calculate MMP by using Cell to Cell calculation method .the behavior caused this shape is due to the so called "Bifurcation problem" this problem can happen for two reasons The physical explanation of the phase bifurcation is likely the result of CO₂ and Heavy hydrocarbon phase behavior at temperatures near the critical temperature of CO₂, and the formation of liquid-liquid (L1-L2) and liquid-vapor (L1-V) phases. The L2 phase is rich in CO₂. As a result, the two-phase region is separated into L1-V phases for a large C1 mole fraction and L1-L2 for a large CO₂ mole fraction.

The transition to and Separation of the L1-L2 phase region results in the hourglass-shaped two-phase region. Such phase behavior has been reported for a CO₂/C1/C16 system at temperatures of 70oF and 90°F (Larson et al. 1989; Orr and Jensen 1984).

The bifurcation can also occur even at temperatures above the critical temperature of CO₂ (Bryant and Monger 1988). Larson et al. (1989) suggested that the phase transition occurs when there are heavy oil fractions and CO₂ present, and oil is lean in intermediate extractable components.

Vaporization effect of CO₂ to the splitted/or lumped heavy end with Multiple carbon number (MCN) is much more easier than using than the case of a single carbon number for instance the CO₂ can vaporize the heavy end (C7-C10) much easier than vaporizing C7+ as one component .

In our case we only deal with the base model EOS C7+ because doing the same for all models requires more time.

- For the EOS C7+ the process has been judged as immiscible process at reservoir Condition
- There is a mistake in MCM option in winprop at which the value of *Equilibrium gas/original oil mixing ratio* is entered. This means the new mixture after the first contact has to be mixed with a ratio of 0.9 of equilibrated gas and 0.1 of the original oil. Knowing that if the value of 0.9 is entered for Equilibrated gas the calculation is reversed (0.9 will be assigned to oil and 0.1 will be assigned to the equilibrated gas). This option has to be adjusted so that when the value of 0.9 is entered to the software it will be assigned to equilibrated gas not the oil.
- We will try to contact the people of authority to eliminate this problem in the next generations
- Simulation of the slim tube experiment will be performed using slim tube calculation option in PVT P directly and also by constructing 1-D model in Reveal.

- **Slim-Tube calculation**

Introducing an EOS model tuned by using winprop to a PVTP is not an easy task.

- Both programs are using different units and thus these units have to be changed to make the EOS model Compatible with the PVTP However models cannot be identical by only changing the units.
- We found out that there is a different in the volume of shift calculation between the two pieces of software this differences affected the volumetric results.
- The viscosity is another property that has not been matched as both programs are using different type of correlations.

The base model EOS C7+ has been in this stage and the slim tube calculation for this model has been conducted at two different pressures using different solvents

- CO₂ recovery at pore volume of 1.2 and pressure of 5300 psig is about 77.4%
- CO₂ recovery at pore volume of 1.2 and reservoir pressure is about 71.4%
- Separator gas at pore volume of 1.2 and pressure of 5300 psig is about 92%
- Separator gas at pore volume of 1.2 and pressure of 3300 psig is about 71.5%

The calculations have shown that the separator gas is much more miscible in the Sarir oil than the CO₂. This is nonsense because the CO₂ has always an advantage over the other solvents of being miscible with hydrocarbons at lower pressure and this has been proved empirically.

The oil composition has been changed to be lighter than the original composition of Sarir oil. This has been done see the effect of CO₂ when we have oil with a light composition.

- CO₂ recovery at pore volume of 1.2 and pressure of 5300 psig is about 83%
- CO₂ recovery at pore volume of 1.2 and reservoir pressure is about 73.8%

There was no different between this case and the first case (where the co₂ is used with the original composition of Sarir oil).

From these results we can conclude that the calculations performed using slimtube option in PVTP are wrong and this option needs to be deeply investigated. There are also some limitations like the number of grids cannot be increased to more than 10 blocks. Most scientific papers recommended that the number of grids have to be enough to eliminate the so-called numerical dispersion which directly leads to inaccuracy in the calculated oil recovery.

Constructing 1D model to mimic the miscibility becomes necessary not only for our scope of work but also to evaluate the slim-tube option in PVT-P.

6.3 1-D Slimube Simulation Model

- The relative permeability values can have impact on the calculation with the displacement is immiscible or nearly miscible.
- the higher the number of the grids the lower the numerical dispersion effect
- Choosing the cell in center was just dedicated to make the comparison between the two scenarios much more clear in fact the injection cell is receiving fresh slugs of CO₂ continuously (it would not be a good idea to use it for making a comparison).
- the vaporizing effect can reduce the residual oil saturation to zero this is can be the case when large amount of fresh CO₂ is injected into the packed sand in the real experiment . This is also observed in our simulation that when CO₂ was injected for a long period time the Sor will be reduced to zero no matter what even if it has been specified as immobile.
- In our study we only focused on the thermodynamic behavior of the interaction between the oil and CO₂. In reality the Sor cannot be reduced to zero because as it had been identified previously that the slim tube experiment is conducted with neglecting some parameters like capillary and gravity and fingering caused by porous media and viscosity .
- The multiple contact miscibility was achieved by vaporizing gas drive in cell to cell calculation (winprop) while in the 1-D model the MCM was achieved by combined drive (vaporizing and condensing).
- at the highest reservoir pressure which is the highest possible injection pressure the CO₂ was nearly miscible with a recovery of about 75%
- Unlike the results from slim tube option in PVTP the slim-tube simulation using 1-D model proves that the CO₂ is indeed miscible with Sarir oil
- The computed value for MMP using 1-D slim tube is very close to the experimental value.

The determination of the MMP in most of slim tube simulation studies is done by finding the point of break-over in a plot of the recovery factor (RF1.2) at 1.2 PVI (pore volume injected) versus pressure .The MMP is claimed to be at Rf of 90%.We used a different approach to

judge the multiple contact miscibility pressure. This has been done by monitoring some fluid properties such as oil and gas densities saturation of oil and gas and the K values. For instance when the K-Value approach to the unity in the gas and oil phase it is strong evidence about the development of miscibility.

Recommendation

Collecting a new PVT data with high accuracy and without contamination is highly recommended, however the work that has been done in this thesis can be used for future screening as all the limitations and challenges encountered have been identified.

In Cell to Cell calculation in CMG the value of equilibrium gas to Oil ratio must be assigned to 0.9 and also the flash and the miscibility calculation must be adjusted based on this value.

Deep investigation must be done for understanding the compatibility between WINPROP and PVTP in term of tuning the equation of state.

The slimtube option in PVTP has to be reevaluated and deeply investigated as the results obtained from this option were nonsense.

In our work we used Reveal to simulate the slimtube experiment by constructing 1-D model. Most of the scientific papers encourage using Eclipse to construct 1-D slimtube simulation model therefore it is recommended to replicate this work by using Eclipse and compare its results with the results obtained from this study.

References

1. Green D, Willhite P. Enhanced Oil Recovery. 1998. 545 pp.
2. Lake LW. Enhanced Oil Recovery. Enhanced Oil Recovery. 1996. 600 p.
3. Alvarado V, Eduardo M. ENHANCED OIL Field Planning and Development. 2010. 209 p.
4. Moreno J, Gurpinar O, Liu Y, Al-kinani A, Cakir N. EOR Advisor System: A Comprehensive Approach to EOR Selection. 2014;1–15.
5. Stalkup FI. Status of Miscible Displacement. J Pet Technol [Internet]. 1983;35(4):815–26. Available from: <https://www.onepetro.org/journal-paper/SPE-9992-PA>
6. Craig, F. F., & Owens, W. W. (1960, April 1). Miscible Slug Flooding - A Review. Society of Petroleum Engineers. doi:10.2118/1391-G
7. Gao P, Towler BF, Pan G. Strategies for Evaluation of the CO₂ Miscible Flooding Process. Abu Dhabi Int Pet Exhib Conf [Internet]. 2010;(November):1–4. doi/10.2118/138786-MS
8. Dipietro P, Kuuskraa V, Malone T. Taking CO₂ Enhanced Oil Recovery to the Offshore Gulf of Mexico. Spe. 2014;
9. Bybee K. Successful Miscible-Gas Injection in Rhourde El Krouf Field, Algeria. J Pet Technol. 2006;(January):45–7.
10. Jethwa DJ, Rothkopf BW, Paulson CI, Company MO. Successful Miscible Gas Injection in a Mature U.K. North Sea Field. Soc Pet Eng. 2000;
11. Recovery P, Recovery O, Flow N, Lift A, Recovery S, Maintenance P, et al. Danny - EOR Potential in the Middle East - Current and Future Trends - SPE-0112-0070-JPT. 2012;(January):23–6.
12. Holm LW. Miscibility and Miscible Displacement. SPE J. 1986;(August):817–8.
13. Clark N.J., Shearin, H. M., Schultz, W. P., Garms, K., & Moore, J. L. (1958, June 1). Miscible Drive - Its Theory and Application. Society of Petroleum Engineers. doi:10.2118/1036-G

14. Ahmed T. Equations of State and PVT Analysis: Applications for Improved Reservoir Modeling: Second Edition. Equations of State and PVT Analysis: Applications for Improved Reservoir Modeling: Second Edition. 2016. 1-607 p.
15. Benham AL, Dowden WE, Kunzman WJ. Miscible Fluid Displacement--Prediction of Miscibility. Soc Pet Eng. 1960;219:229–37.
16. Stalkup, F. I. (1983, April 1). Status of Miscible Displacement. Society of Petroleum Engineers. doi:10.2118/9992-PA.
17. Cohen GS. Prediction of Conditions Necessary for Multiple-Contact Miscibility. 1983;(Figure 1).
18. Hutchison, C.A. Jr. and Braun, P.H.: “Phase Relations of Miscible Displacement in Oil Recovery,” *AIChE J.* (1961) 7, 64
19. Katz, D.L.: “Possibility of Cycling Deep Depleted Oil Reservoirs after Compression to a Single Phase,” *Trans., AIME* (1952) 195.175-82.
20. Wilson, J.F.: “Miscible Displacement-Flow Behavior and Phase Relationships for a Partially Depleted Reservoir,” *Trans., AIME* (1960) 219: 223-28.
21. Koch, H.A. Jr. and Hutchinson, C.A.: “Miscible Displacements of Reservoir Oil Using Flue Gas,” *J. Pet. Tech.* (Jan. 1958) 7-19; *Trans., AIME* (1958) 213
22. Rushing, M.D. et al.: “Miscible Displacement with Nitrogen,” *Pet. Eng.* (Nov. 1977) 26 30.
23. Zick, A. A. (1986, January 1). A Combined Condensing/Vaporizing Mechanism in the Displacement of Oil by Enriched Gases. Society of Petroleum Engineers. doi:10.2118/15493-MS
24. Stalkup, F. I. (1987, January 1). Displacement Behavior of the Condensing/Vaporizing Gas Drive Process. Society of Petroleum Engineers. doi:10.2118/16715-MS
25. Johns, R. T., Dindoruk, B., & Orr, F. M. (1993, July 1). Analytical Theory of Combined Condensing/Vaporizing Gas Drives. Society of Petroleum Engineers. doi:10.2118/24112 PA
26. Sage, B.H. and Lacey, W.N.: *Some Properties of the lighter Hydrocarbons, Hydrogen Sulfide, and Carbon Dioxide* Monograph, Research Project 37, API, Dallas (1955).

27. Helm. L.W. and Josendal, V.A.: "Mechanisms of Oil Displacement by Carbon Dioxide," *J. Per. Tech.* (Dec. 1974) 1427-35; *Trans.*, AIME, 257
28. Helm. L.W. and Josendal. V.A.: "Discussion of Determination and Prediction of CO2 Minimum Miscibility Pressure." *J. Per. Tech.* (May 1980) 870-71.
29. Orr. F.M. Jr. and Silva. M.K.: "equilibrium Phase Compositions of CO2 /Hydrocarbon Mixtures-Part 1: Mixtures Measurement by Continuous Multiple Contact Experiment," *Sot. Per. Eng. J.* (April 1983) 272-80:
30. Shelton, J.L. and Yarborough. L.: "Multiple Phase Behavior in Porous Media During CO, or Rich Gas Flooding," *J. Per. Tech.* (Sept. 1977) 1171-78.
31. Metcalfe, R. S., & Yarborough, L. (1979, August 1). The Effect of Phase Equilibrium on the CO2 Displacement Mechanism. Society of Petroleum Engineers. Doi:10.2018/7061-PA
32. Shelton, J. L., & Yarborough, L. (1977, September 1). Multiple Phase Behavior in Porous Media during CO2 or Rich-Gas Flooding. Society of Petroleum Engineers. doi:10.2118/5827-PA
33. Adyani, W. N., Wan Daud, W. A., Faisal, A. H., & Zakaria, N. A. (2009, January 1). Multi Component Mass Transfer in Multiple Contact Miscibility Test; Forward and Backward Method. Society of Petroleum Engineers. Doi: 10.2118/125219-MS
34. Lewis, C. J. (1976). Sarir Oilfield. Unpublished report written by the Exploration Staff of BP Exploration Company (Libya) Limited.
35. Qutob, H., Ubs, W., Shatwan, M. Ben, Gulf, A., Co, O., & Vieira, P. (2010). SPE 128876 Horizontal Underbalanced Drilling Technology Successfully Applied in Sarir C- Main Field - Libya : Case Study, 1–14.
36. Arabian Gulf Oil Company (AGOCO). (n.d.). Retrieved October 09, 2017, from <http://www.agoco.ly/index.php/agen/our-company/agocom-who-we-are>.
37. Belhaj H, Aljarwan A, Haroun M, Ghedan S. Increasing Oil Recovery with CO2 Miscible Injection: Thani Reservoir, Abu-Dhabi Giant Off-Shore Oil Field Case Study. Proc 2012 SPE Kuwait Int Pet Conf Exhib . 2012;
38. Christiansen, R. L., & Haines, H. K. (1987, November 1). Rapid Measurement of Minimum Miscibility Pressure with the Rising-Bubble Apparatus. Society of Petroleum Engineers. Doi: 10.2118/13114-PA

39. Christiansen, R. L., & Haines, H. K. (1987, November 1). Rapid Measurement of Minimum Miscibility Pressure with the Rising-Bubble Apparatus. Society of Petroleum Engineers.
40. Sibbald, L. R., Novosad, Z., & Costain, T. G. (1991, August 1). Methodology for the Specification of Solvent Blends for Miscible Enriched Gas Drives (includes associated papers 23836, 24319, 24471 and 24548). Society of Petroleum Engineers.
41. Ghedan, S. G. (2009, January 1). Global Laboratory Experience of CO₂-EOR Flooding. Society of Petroleum Engineers. doi:10.2118/125581-MS
42. Jean-Christophe Perrin, Michael Krause, Chia-Wei Kuo, Ljuba Miljkovic, Ethan Charob and Sally M. Benson Core-scale experimental study of relative permeability properties of CO₂ and brine in reservoir rocks. 2009; 1(1):3515–22.
43. Wang, Y.; Orr, F. M. Analytical Calculation of Minimum Miscibility Pressure. *Fluid Phase Equilibrium*. 1997, 139, 101-124.
44. A Very Simple Multiple Mixing Cell Calculation to Compute the Minimum Miscibility Pressure Whatever the Displacement Mechanism Jean-Noël Jaubert* and, Luc Wolff, Evelyne Neau, and Laurent Avaullee *Industrial & Engineering Chemistry Research* 1998 37 (12), 4854-4859 DOI: 10.1021/ie980348r
45. Spe.org. (2018). JPT Shale EOR Works, But Will It Make a Difference. Available at: <https://www.spe.org/en/jpt/jpt-article-detail/?art=3391> [Accessed 16 Jan. 2018].
46. Eia.gov. (2018). Available at <https://www.eia.gov/todayinenergy/detail.php?id=14431#> [Accessed 16 Jan. 2018].
47. Zhang, Hao, et al. "An improved Co₂-Crude oil minimum miscibility pressure correlation." *Journal of Chemistry*, vol. 2015, 2015. *Academic OneFile*, Accessed 31 Mar. 2018.
49. Jessen, K.; Michelsen, M. L. Minimum Miscibility Pressure Calculation. IFP seminar: Production of reservoir fluids in frontier conditions, Rueil-Malmaison, Dec 4-5, 1997.

Appendix A :(Sarir Oil Field Data)

Reservoir and Reservoir Performance Data based on study conducted in 2012

Reservoir Data as of 31 /12/2012

FIELD : SARIR C- MAIN		CONC: 65
RESERVOIR PROPERTIES		
Reservoir Properties	Value	
Productive Formation	SARIR	
Formation Type	Sandstone	
Datum Depth (ft-ss)	8200	
Original Oil Water Contact (ft-ss)	8466	
Average Porosity (%)	15.2	
Average Water Saturation (%)	37	
Average Net Pay (ft)	132	
Productive Area (acres)	87475	
Rock Compressibility (1/psi)	3.60E-06	
Drive Mechanism	Strong bottom water drive	

FIELD : SARIR C- MAIN		CONC: 65
FLUID PROPERTIES		
Fluid Properties	Values	
Oil FVF (RB/STB) @ B. Point Press	1.16	
Oil FVF (RB/STB) @ Current press	1.14	
Average Oil Gravity @ ST conditions (API)	37	
Saturation Pressure @ Reservoir Temp. (psi)	534	
Original Solution GOR (SCF/STB)	150	
Oil Viscosity (cp) @ Current Reservoir conditions (cp)	1.9	
Oil Compressibility (1/psi)	7.2E-06	
Water Salinity (ppm)	198000	
Water Viscosity (cp)	0.52	
Water Compressibility (1/psi)	3.3E-06	

FIELD : SARIR C- MAIN		CONC: 65
RESERVES		
Quantity	Values	
Original Oil in Place (MMSTB)*	7,528.50	
Recovery Factor (%)**	50.3	
Reserves (MMSTB)	3786.8	
Cum. Oil Production (MMSTB)	3,108.50	
Remaining Reserves (MMSTB)	678.4	

Reservoir Performance Data as of 31 /12/2012

FIELD : SARIR C- MAIN		CONC: 65
RESERVOIR PERFORMANCE		
WELL STATUS		Values
Total Wells Drilled		351*
Observation& Abandoned		54
Water Disposal Wells		6
Active Pumping Wells		220
Naturally Flowing Wells		0
Waiting on WO, ESP C/O, etc		16
Shut-in -Wellbore & F/L problems (stuck equip, corrosion, f/l plug etc.)		10
Waiting Completion		0
Shut-in due no flow		3
Shut-in due Casing leak		1
Shut-in under WO		4
Shut-in due Production Control.		37

(*) Wells up to C364 (excluding water source wells and initially abandoned wells due to drilling problems)

FIELD : SARIR C- MAIN		CONC: 65
RESERVOIR PERFORMANCE		
Production	Quantity	Values
	Cumulative Production (BSCF)	460.3
Gas	Produced during 2012 (BSCF)	6.9
	Daily Average Rate (MMSCF/D)	19
	Average GOR (SCF/STB)	141
	Cumulative Production (MMSTB)	3,108.50
Oil	Produced during 2012(MMSTB)	49.3
	Daily Average Rate (MSTB/D)	135
	Cumulative Production (MMSTB)	1,130
Water	Produced during 2012 (MMSTB)	52.2
	Daily Average Rate (MSTB/D)	143.1
	Average Water Cut (%)	51.4

FIELD : SARIR C- MAIN		CONC: 65
RESERVOIR PERFORMANCE		
Pressures		Values
Original Reservoir Pressure (psig)		3900
Current Reservoir Pressure (psig)		2600
Decline in Average Pressure (psi)		1300

Appendix B: (PVT Data)

Company	Arabian Gulf Company	Date Sampled	13th July 1983
WELL	C116	state	
Field	Sarir	country	S.P.L.A.J
FORMATION CHARACTERISTICS			
Formation name	Sarir Sandstone		
Date First well completed	19		
Original Reservoir Pressure	psig @ Ft		
Original Produced Gas to Oil Ratio	Scf/Bbl		
Production Rate	BB/Day		
Separator Pressure and Temperature	psig @ Ft		
Oil Gravity at 60° F .	API		
Datum			
Original Gas Cap			

WELL CHARACTERISTICS			
Elevation	Ft		
Total Depth	8888Ft		
Producing Interval	8662-8712 Ft		<u>50 ft</u>
Tubing Size and Depth	3-1/2 In, to 8572 Ft		
Productivity Index.	BBl/DAY/Psi	@BBl/Day	
Last Reservoir Pressure	3300*	Psig @	Ft
Date	19		
Reservoir Temperature	225 * ° F . @ Ft		
Status Of Well			
Pressure Gauge			
Normal Production Rate	Bbl/Day		
Gas-Oil Ratio	33 Scf/Bbl		
Separator Pressure and temperature	106 Psig, 136 ° F.		
Base Pressure	14.73		
Well Making Water	Cut%		
SAMPLING CONDITIONS			
Sampled at	8628 Ft		
Status Of Well	Flowing		
Gas-Oil Ratio	33Scf/BBL		
Separator Pressure and temperature	106 Psig, 136 ° F.		
Tubing Pressure	134 Psig		
Casing Pressure	Psig		
Sampled by	Flopetol		
Type Sampler	Flopetrol 11999		

HYDROCARBON ANALYSIS OF RESERVOIR FLUID SAMPLE					
COMPONENT	MOL PERCENT	WEIGHT PERCENT	DENSITY	API	MOLE WEIGHT
Hydrogen Sulphide	NTL	NTL			
Carbon Dioxide	1.12	0.27			
Nitrogen	1.05	0.16			
Methane	10.82	0.96			
Ethane	4.34	0.72			
Propane	8.22	2.01			
iso-Butane	2.22	0.72			
nButane	6.41	2.07			
iso-Pentane	2.86	1.14			
n-Pentane	3.54	1.42			
Hexancs	4.45	2.12			
Heptanes plus	54.97	88.41	0.8644	32	290
	100	100			

VOLUMETRIC DATA OF RESERVOIR FLUID SAMPLE					
1.	Saturation Pressure (bubble-point pressure)	PSIG	@225° F.		715
2.	Specific volume at saturation pressure	ft ³ /lb	@225° F.		0.0214
3.	Thermal expansion of saturated oil @	5000 PSIG =	Vol@225° F / Vol@59° F =		1.07895
4.	compressibility of saturated oil @reservoir temperature	Vol/Vol/PSI :			
	From	5000	PSIG to	3000	PSIG = 7.92×10-6
	From	3000	PSIG to	2000	PSIG = 8.81×10-6
	From	2000	PSIG to	1000	PSIG = 9.93×10-6
	From	1000	PSIG to	715	PSIG = 10.8×10-6

PRESSURE-VOLUME RELATION AT 225 ° F .		
Pressure	Relative	Y
PSIG	Volume(1)	Function(2)
5000	0.9628	
4000	0.9702	
3000	0.9783	
2000	0.987	
1500	0.9917	
1200	0.9948	
1100	0.9958	
1000	0.9969	
900	0.998	
800	0.9991	
715	<u>Psat</u>	1
708	1.0035	2.795
700	1.0076	2.772
680	1.0185	2.725
668	1.0255	2.7
652	1.0355	2.66
622	1.0564	2.59
582	1.0899	2.478
538	1.1344	2.382
463	1.2393	2.203
425	1.3116	2.115
373	1.4429	1.99
323	1.6215	1.866
287	1.8016	1.768
230	2.2157	1.628
180	2.841	1.489
136	3.8194	1.36

- (1) Relative Volume : V/Vsat is barrels at indicated pressure per barrel at saturation pressure
(2) Y function= ((Psatp)-(P))/((Pabs)(V/Vsat-1)).

DIFFERENTIAL VAPORISATION AT 225 ° F.							
Pressure (psig)	Solution GOR (scf/bbl*)	Relative Oil Volume (RB/bbl*)	Relative Total Volume (RB/bbl*)	Oil Density (g/cm3)	Deviation Factor Z	Gas FVF (FT3/SCF*)	Incremental Gas Gravity
715	192	1.232	1.232	0.7486			
600	171	1.223	1.332	0.7507	0.924	0.02915	0.914
500	155	1.215	1.446	0.7534	0.93	0.03504	0.867
400	135	1.205	1.651	0.7563	0.94	0.04395	0.88
300	113	1.195	2.019	0.7602	0.951	0.05858	0.957
200	90	1.182	2.764	0.7653	0.965	0.08709	1.121
137	74	1.175	3.788	0.7685	0.974	0.12434	1.309
103	63	1.17	4.866	0.7712	0.98	0.16088	1.472
83	57	1.163	6.701	0.7725	0.984	0.23034	1.563
0	0	1.083		0.8007			1.938
AT 60°F=		1					
gravity of residual oil =31.7 API @60 F							
(1) cubic feet of gas at 14.73 psig and 60 F.per barrel of residual oil at 60F.							
(2) barrels of oil at indicated pressure and temperature per barrels of residual oil at 60 F							
(3) barrels of oil plus liberated gas at indicated pressure and temperature per barrel of residual oil at 60 F.							
(4) cubic feet of gas at indicated pressure and temperature per cubic foot at 14.73 psig and 60 F.							

SEPARATOR TESTS OF RESERVOIR FLUID SAMPLE							
Separator Pressure (psig)	Separator Temperature(°F)	GOR(1) (ft3/STB)	GOR(2) (ft3/STB)	Stock-Tank Gravity (°API)@60F	FVF(3) (bbl/STB)	Separator Volume Factore(4) (bbl/STB)	Flashed-Gas Specific Gravity
150	123	70	76			1.083	0.694
to							
0	60	55	55	36.5	1.163	1	1.311
100	123	90	96			1.066	0.967
to							
0	60	36	36	36.5	1.162	1	1.334
50	123	119	125			1.05	1.092
to							
0	60	18	18	36.5	1.175	1	1.325

(1)In cubic feet of gas at 60°F and 14.73 psi absolute per barrel of oil at indicated pressure and temperature.

(2)In cubic feet of gas at 60°F and 14.73 psi absolute per barrel of stock-tank oil at 60°F.

(3)In barrels of saturated oil at 715 psi gauge and 225°F per barrel of stock-tank oil at 60°F.

(4)In barrels of oil at indicated pressure and temperature per barrel of stock-tank oil at 60°F.

VISCOSITY DATA AT 225° F.			
Pressure (psig)	Oil Viscosity (cp)	Calculated Gas Viscosity (cp)	Oil/Gas Viscosity Ratio
5000	1.76		
4000	1.61		
3000	1.46		
2000	1.31		
1000	1.16		
715	1.12		
600	1.15	0.0135	85.3
500	1.18	0.0134	87.9
400	1.23	0.0132	93.2
300	1.3	0.0127	102.1
200	1.41	0.012	117.8
137	1.52	0.0112	135.2
103	1.6	0.0107	149.5
83	1.69	0.0104	162.3
0	2.67		

SEPARATOR TESTS OF RESERVOIR FLUID SAMPLE							
Separator Pressure (PSI Gauge)	Separator Temperature(°F)	Separator GOR(1) (ft3/STB)	Stock Tank GOR(1) (ft3/STB)	Stock-Tank Gravity (°API)@60F	Shrinkage Factor Vsat/Vr(2) (STB/bbl)	FVF Vsat/Vr Volume Factore(4) (bbl/STB)	Flashed-Gas Specific Gravity
0	123	164		34.6	0.8326	1.201	1.342

1. In cubic feet of gas at 60°F and 14.73 psi absolute per barrel of oil at indicated pressure and temperature.

2. In barrel of stock-tank oil at 60°F per barrels of saturated oil at 715 psi gauge and 225°F per

3. In barrels of saturated oil at 715 psi gauge and 220°F per barrel of stock-tank oil at 60°F.

Appendix C: (Slim-Tube Data)

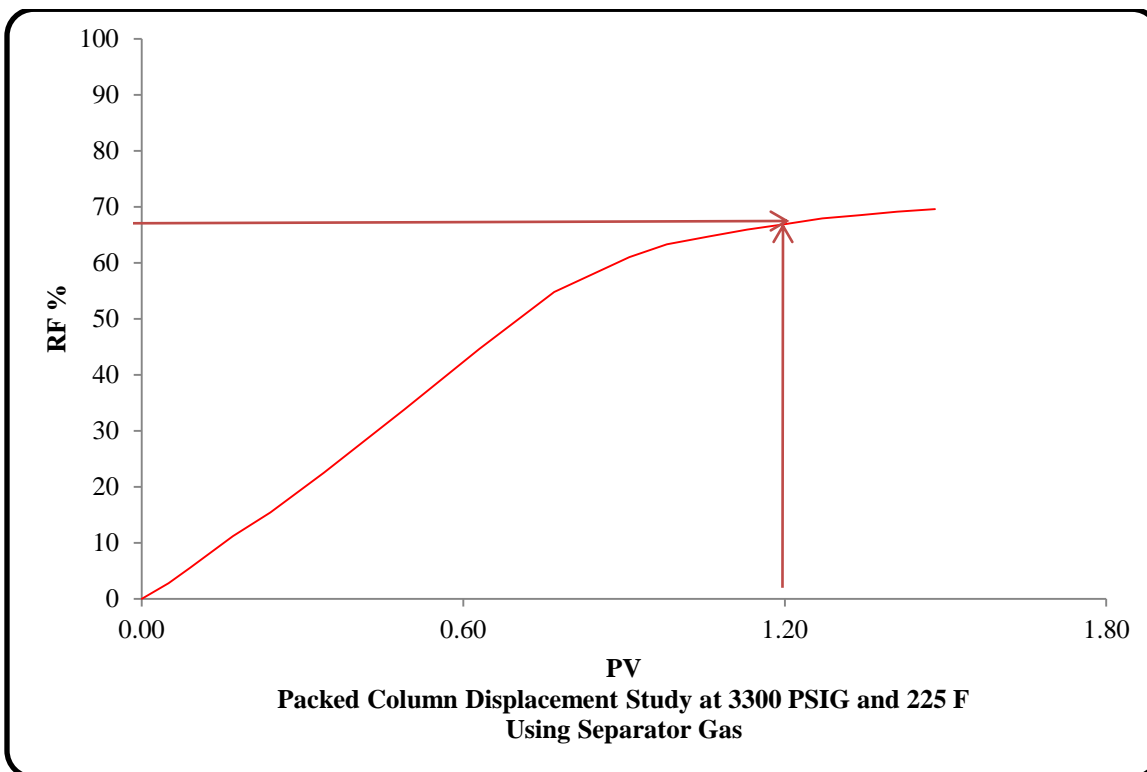
Packed Column Displacement Study Summary of Basic Data	
<i>Sand Packed Column Properties</i>	
length Feet	40
Internal diameter inches	0.176
porosity , percent	37.5
<i>Operating Condition</i>	
column temperature	225
separator pressure PSIG	0
separator temperature F	60
<i>Reservoir Fluid Properties</i>	
saturation pressure at 225 F.PSIG	715
Gas/Oil Ratio SCF/STB	162
formation volume factor ,bbl. at 715 Psig/STB	1.207
stock tank oil gravity API at 60 F.	36.1
Gas Gravity (air=1.000)	1.015

SEPARATOR TESTS OF RESERVOIR FLUID SAMPLE							
Separator Pressure (PSI Gauge)	Separator Temperature(°F)	Separator GOR(1) (ft3/STB)	Stock Tank GOR(1) (ft3/STB)	Stock-Tank Gravity (°API)@60F	Shrinkage Factor Vsat/Vr(2) (STB/bbl)	FVF Vsat/Vr Volume Factore(4) (bbl/STB)	Flashed-Gas Specific Gravity
0	123	164		34.6	0.8326	1.201	1.342

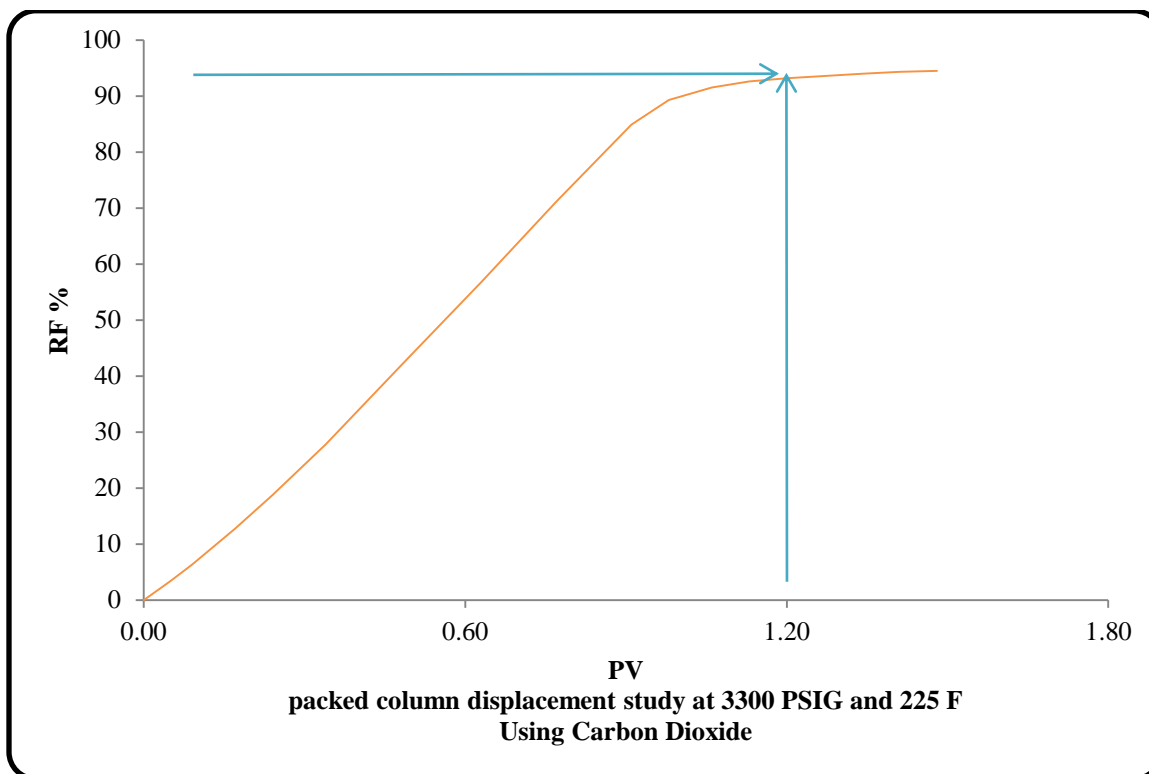
1. In cubic feet of gas at 60°F and 14.73 psi absolute per barrel of oil at indicated pressure and temperature.
2. In barrel of stock-tank oil at 60°F per barrels of saturated oil at 715 psi gauge and 225°F per
3. In barrels of saturated oil at 715 psi gauge and 220°F per barrel of stock-tank oil at 60°F.

HYDROCARBON ANALYSIS OF INJECTION GAS SAMPLE (Separator Gas)		
Component	Mol%	GPM
Hydrogen Sulphide	NTL	
Carbon Dioxide	4.16	
Nitrogen	9.94	
Methane	60.68	
Ethane	10.98	
Propane	9.2	2.531
iso-Butane	1.29	0.422
n-Butane	2.64	0.832
iso-Pentane	0.5	0.183
n-Pentane	0.46	0.167
Hexances	0.09	0.037
Heptanes plus	0.06	0.027
	<u>100.00</u>	<u>4.199</u>
calculated gas gravity (air=1.000)=		0.857

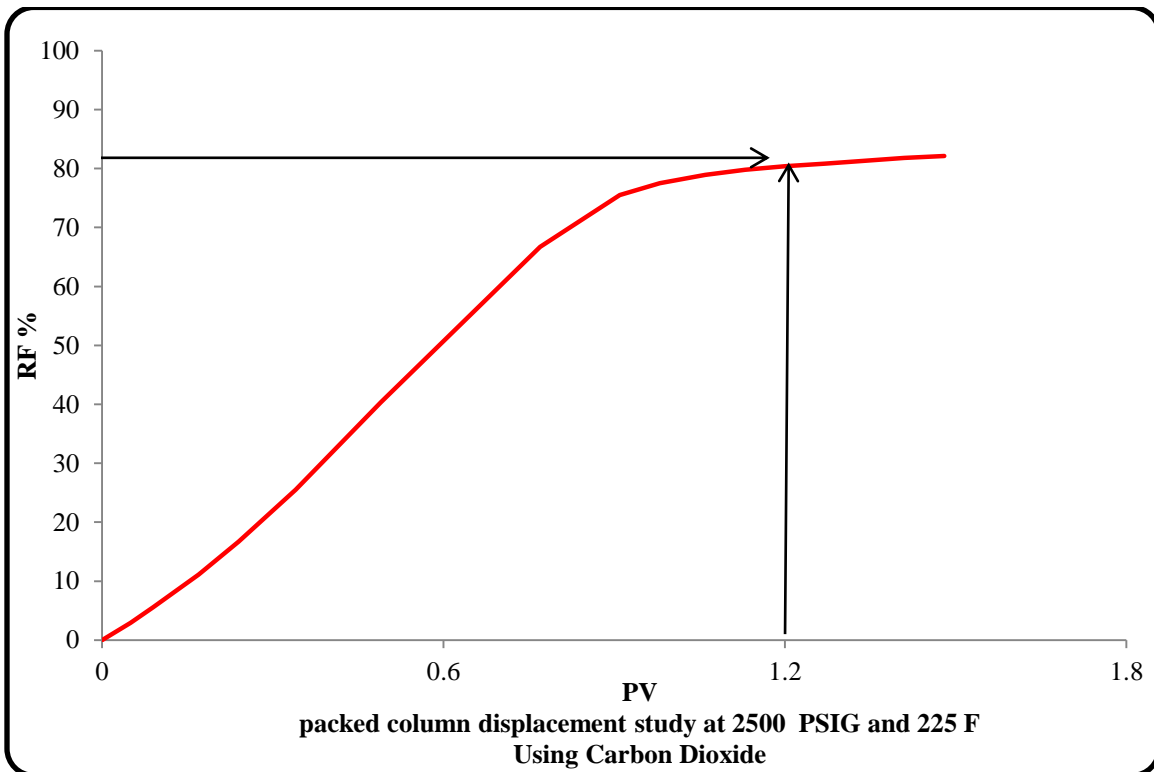
PACKED COLUMN DISPLACEMENT STUDY AT 3300 PSIG AND 225 F				
INJECTION GAS - SEPARATOR GAS				
Cumulative Gas Injected Pore Volume	Cumulative Oil Recovery %	Gas-Oil Ratio SCF/STB	Gas Gravity	Oil Gravity API at 60 F.
0.00	0			
0.05	2.8	155	1.013	37.1
0.09	5.5	161	1.018	37.4
0.17	11.2	154	1.019	37.4
0.24	15.4	160	1.016	37.5
0.34	22.5	155	1.057	37.7
0.49	33.8	146	1.005	37.3
0.63	44.6	206	0.975	37.3
0.77	54.8	554	0.931	37
0.91	61	1815	0.912	37
0.98	63.3	2301	0.906	
1.06	64.7	5493	0.909	
1.13	65.9	6779	0.906	
1.2	66.9	8413	0.936	39.4
1.27	67.9	9571	0.937	
1.34	68.5	10696	0.873	
1.41	69.1	13688	0.866	
1.48	69.6	17345	0.875	



PACKED COLUMN DISPLACEMENT STUDY AT 3300 PSIG AND 225 F				
INJECTION GAS - CARBON DIOXIDE				
Cumulative Gas Injected Pore Volume	Cumulative Oil Recovery %	Gas-Oil Ratio SCF/STB	Gas Gravity	Oil Gravity API at 60 F.
0.00	0			
0.05	3.4	154	1.016	36.2
0.09	6.3	155	1.02	36.4
0.17	12.7	141	1.095	36.4
0.24	18.7	160	1.119	36.5
0.34	27.8	151	1.144	36.3
0.49	42.9	149	1.135	36.4
0.63	56.8	155	1.139	36.3
0.77	71.1	154	1.142	36.4
0.91	84.9	158	1.153	36.2
0.98	89.3	367	1.19	37
1.06	91.5	1298	1.372	
1.13	92.6	8689	1.569	
1.2	93.2	18160	1.549	42
1.27	93.6	26741	1.534	
1.34	94	30440	1.548	
1.41	94.3	36953	1.492	
1.48	94.5	49715	1.501	



PACKED COLUMN DISPLACEMENT STUDY AT 2500 PSIG AND 225 F				
INJECTION GAS - CARBON DIOXIDE				
Cumulative Gas Injected Pore Volume	Cumulative Oil Recovery %	Gas-Oil Ratio SCF/STB	Gas Gravity	Oil Gravity API at 60 F.
0	0			
0.05	2.9	141	1.024	36.6
0.09	5.6	160	1.037	36.6
0.17	11.1	157	1.11	36.7
0.24	16.7	166	1.131	36.6
0.34	25.5	160	1.028	36.6
0.49	40.3	142	1.088	36.6
0.63	53.5	148	1.045	36.8
0.77	66.7	163	1.085	36.5
0.91	75.5	418	1.262	37.1
0.98	77.5	3341	1.482	
1.06	78.9	5557	1.553	
1.13	79.8	9157	1.568	39.8
1.2	80.4	13238	1.557	
1.27	80.8	17810	1.556	
1.34	81.3	18241	1.539	
1.41	81.8	19506	1.554	
1.48	82.1	22851	1.527	



Appendix D :(EOSs Tuning Results)

1- EOS C7+

CCE DATA			
Pressure (psia)	Relative Volume	Relative Volume	
Pressure	Exp. ROV	ROV	ERR%
5014.7	0.9628	0.9634	0.065
4014.7	0.9702	0.9696	0.058
3014.7	0.9783	0.9769	0.140
2014.7	0.987	0.9857	0.134
1514.7	0.9917	0.9908	0.095
1214.7	0.9948	0.9941	0.071
1114.7	0.9958	0.9953	0.055
1014.7	0.9969	0.9964	0.046
914.7	0.998	0.9977	0.034
814.7	0.9991	0.9989	0.019
729.7	1	1.0000	0.000
722.7	1.0035	1.0036	0.005
714.7	1.0076	1.0077	0.012
694.7	1.0185	1.0188	0.026
682.7	1.0255	1.0258	0.031
666.7	1.0355	1.0358	0.027
636.7	1.0564	1.0563	0.008
596.7	1.0899	1.0881	0.164
552.7	1.1344	1.1302	0.369
477.7	1.2393	1.2258	1.093
439.7	1.3116	1.2903	1.626
387.7	1.4429	1.4048	2.641
337.7	1.6215	1.5572	3.963
301.7	1.8016	1.7063	5.289
244.7	2.2157	2.0554	7.233
194.7	2.841	2.5730	9.433
150.7	3.8194	3.3793	11.522

DIFF. Liberation Test			
Pressure (psia)	Relative Oil Volume (rb/stb)	Relative Oil Volume (rb/stb)	
Pressure	Exp. ROV	ROV	ERR%
729.7	1.232	1.202	2.40
614.7	1.223	1.193	2.49
514.7	1.215	1.183	2.60
414.7	1.205	1.173	2.62
314.7	1.195	1.162	2.76
214.7	1.182	1.148	2.88
151.7	1.175	1.137	3.26
117.7	1.17	1.129	3.52
97.7	1.163	1.123	3.42
14.7	1.083	1.045	3.49

DIFF. Liberation Test			
Pressure (psia)	Gas-Oil Ratio (scf/stb)	Gas-Oil Ratio (scf/stb)	
Pressure	Exp. GOR	GOR	ERR%
729.7	192	224.212	16.78
614.7	171	205.385	20.11
514.7	155	188.393	21.54
414.7	135	170.423	26.24
314.7	113	150.85	33.50
214.7	90	128.067	42.30
151.7	74	110.775	49.70
117.7	63	99.5129	57.96
97.7	57	91.5901	60.68
14.7	0	0	0.00

DIFF. Liberation Test			
Pressure (psia)	Oil SG	Oil SG (Water = 1)	
Pressure	Exp. Oil SG	Oil SG	ERR%
729.7	0.7486	0.7702	2.88
614.7	0.7507	0.7735	3.04
514.7	0.7534	0.7766	3.08
414.7	0.7563	0.7800	3.13
314.7	0.7602	0.7839	3.11
214.7	0.7653	0.7885	3.04
151.7	0.7685	0.7922	3.08
117.7	0.7712	0.7947	3.04
97.7	0.7725	0.7964	3.10
14.7	0.8007	0.8176	2.10

DIFF. Liberation Test			
Pressure (psia)	Oil Viscosity (cp)	Oil Viscosity (cp)	
Pressure	Exp. Oil Visc.	Oil Visc.	ERR%
729.7	1.12	1.10	2.03
614.7	1.15	1.14	0.51
514.7	1.18	1.19	0.95
414.7	1.23	1.25	1.40
314.7	1.3	1.32	1.44
214.7	1.41	1.42	0.86
151.7	1.52	1.52	0.01
117.7	1.6	1.59	0.33
97.7	1.69	1.65	2.14
14.7	2.67	2.68	0.23

Psat.Exp	Psat.Pred	Err%
729.7	729.7	0

Separator Test Data			
	EXP.	PRE	Err%
GOR	132	133.26	0.95
BO	1.162	1.133	2.50
API	36.5	36.71	0.58

Lumped EOS C15

CCE Data			
Pressure (psia) Pressure	Relative Volume Exp. ROV	Relative Volume ROV	ERR%
5014.7	0.9628	0.96	0.11
4014.7	0.9702	0.97	0.20
3014.7	0.9783	0.98	0.25
2014.7	0.987	0.99	0.20
1514.7	0.9917	0.99	0.13
1214.7	0.9948	0.99	0.10
1114.7	0.9958	1.00	0.07
1014.7	0.9969	1.00	0.06
914.7	0.998	1.00	0.04
814.7	0.9991	1.00	0.02
729.7	1	1.00	0.00
722.7	1.0035	1.00	0.01
714.7	1.0076	1.01	0.02
694.7	1.0185	1.02	0.04
682.7	1.0255	1.03	0.06
666.7	1.0355	1.04	0.06
636.7	1.0564	1.06	0.04
596.7	1.0899	1.09	0.09
552.7	1.1344	1.13	0.27
477.7	1.2393	1.23	0.94
439.7	1.3116	1.29	1.43
387.7	1.4429	1.41	2.38
337.7	1.6215	1.56	3.61
301.7	1.8016	1.71	4.85
244.7	2.2157	2.07	6.60
194.7	2.841	2.60	8.55
150.7	3.8194	3.43	10.31

Diff. Liberation Test			
Pressure (psia) Pressure	Relative Oil Volume (rb/stb) Exp. ROV	Relative Oil Volume (rb/stb) ROV	ERR%
729.7	1.232	1.22	0.67
614.7	1.223	1.21	0.80
514.7	1.215	1.20	0.94
414.7	1.205	1.19	0.99
314.7	1.195	1.18	1.17
214.7	1.182	1.17	1.34
151.7	1.175	1.15	1.80
117.7	1.17	1.15	2.10
97.7	1.163	1.14	2.05
14.7	1.083	1.04	4.10

Diff. Liberation Test			
Pressure (psia) Pressure	Gas-Oil Ratio (scf/stb) Exp. GOR	Gas-Oil Ratio (scf/stb) GOR	ERR%
729.7	192	246.91	28.60
614.7	171	227.37	32.97
514.7	155	209.77	35.34
414.7	135	191.19	41.62
314.7	113	170.95	51.29
214.7	90	147.31	63.68
151.7	74	129.24	74.64
117.7	63	117.37	86.29
97.7	57	108.95	91.14
14.7	0	0.00	0.00

Diff. Liberation Test			
Pressure (Psia)	Exp. Oil SG	Pred. Oil SG	ERR%
729.7	0.7486	0.77	3.37
614.7	0.7507	0.78	3.53
514.7	0.7534	0.78	3.59
414.7	0.7563	0.78	3.65
314.7	0.7602	0.79	3.64
214.7	0.7653	0.79	3.59
151.7	0.7685	0.80	3.66
117.7	0.7712	0.80	3.64
97.7	0.7725	0.80	3.71
14.7	0.8007	0.83	3.15

Diff. Liberation Test			
Pressure (psia) Pressure	Oil Viscosity (cp) Exp. Oil Vis.	Oil Viscosity (cp) Oil Vis.	ERR%
729.7	1.12	1.1	1.8
614.7	1.15	1.1	0.6
514.7	1.18	1.2	0.7
414.7	1.23	1.2	1.3
314.7	1.3	1.3	1.6
214.7	1.41	1.4	1.3
151.7	1.52	1.5	0.4
117.7	1.6	1.6	0.0
97.7	1.69	1.7	1.9
14.7	2.67	2.7	0.1

Psat.Exp	Psat.Pred	Err%
729.7	729.7	0

Separator Test Data			
	EXP.	PRE	Err%
GOR	132	133.35	1.02
BO	1.162	1.128	2.93
API	36.5	36.75	0.68

EOS C31+

CCE Data			
Pressure (psia)	Relative Volume	Relative Volume	
Pressure	Exp. ROV	ROV	ERR%
5014.7	0.9628	0.9617	0.11
4014.7	0.9702	0.9683	0.20
3014.7	0.9783	0.9759	0.24
2014.7	0.987	0.9851	0.20
1514.7	0.9917	0.9904	0.13
1214.7	0.9948	0.9938	0.10
1114.7	0.9958	0.9951	0.07
1014.7	0.9969	0.9963	0.06
914.7	0.998	0.9976	0.04
814.7	0.9991	0.9989	0.02
729.7	1	1.0000	0.00
722.7	1.0035	1.0036	0.01
714.7	1.0076	1.0078	0.02
694.7	1.0185	1.0190	0.05
682.7	1.0255	1.0261	0.06
666.7	1.0355	1.0362	0.06
636.7	1.0564	1.0569	0.05
596.7	1.0899	1.0890	0.09
552.7	1.1344	1.1314	0.26
477.7	1.2393	1.2278	0.93
439.7	1.3116	1.2930	1.42
387.7	1.4429	1.4090	2.35
337.7	1.6215	1.5636	3.57
301.7	1.8016	1.7152	4.79
244.7	2.2157	2.0715	6.51
194.7	2.841	2.6025	8.40
150.7	3.8194	3.4349	10.07

Diff. Liberation Data			
Pressure (psia)	Relative Oil Volume (rb/stb)	Relative Oil Volume (rb/stb)	
Pressure	Exp. ROV	ROV	ERR%
729.7	1.232	1.227	0.42
614.7	1.223	1.216	0.55
514.7	1.215	1.207	0.70
414.7	1.205	1.196	0.75
314.7	1.195	1.184	0.93
214.7	1.182	1.169	1.12
151.7	1.175	1.156	1.58
117.7	1.17	1.148	1.90
97.7	1.163	1.142	1.85
14.7	1.083	1.038	4.14

Diff. Liberation Data			
Pressure (psia)	Gas-Oil Ratio (scf/stb)	Gas-Oil Ratio (scf/stb)	
Pressure	Exp. GOR	GOR	ERR%
729.7	192	250.7	30.6
614.7	171	231.1	35.1
514.7	155	213.4	37.7
414.7	135	194.7	44.2
314.7	113	174.4	54.3
214.7	90	150.6	67.4
151.7	74	132.4	79.0
117.7	63	120.4	91.2
97.7	57	111.9	96.3
14.7	0	0.0	0.0

Diff. Liberation Data			
Pressure (psia)	Oil SG	Oil SG (Water = 1)	
Pressure	Exp. Oil SG	Oil SG	ERR%
729.7	0.7486	0.7739	3.38
614.7	0.7507	0.7773	3.54
514.7	0.7534	0.7805	3.60
414.7	0.7563	0.7840	3.66
314.7	0.7602	0.7880	3.66
214.7	0.7653	0.7929	3.60
151.7	0.7685	0.7968	3.68
117.7	0.7712	0.7994	3.66
97.7	0.7725	0.8013	3.73
14.7	0.8007	0.8268	3.25

Diff. Liberation Data			
Pressure (psia)	Oil Viscosity (cp)	Oil Viscosity (cp)	
Pressure	Exp. Oil Visc.	Oil Visc.	ERR%
729.7	1.12	1.07	4.78
614.7	1.15	1.13	2.12
514.7	1.18	1.18	0.41
414.7	1.23	1.25	1.95
314.7	1.3	1.34	2.92
214.7	1.41	1.45	2.74
151.7	1.52	1.54	1.56
117.7	1.6	1.61	0.72
97.7	1.69	1.66	1.63
14.7	2.67	2.59	3.15

Psat.Exp	Psat.Pred	Err%
729.7	729.7	0

Separator Test Data			
	EXP.	PRE	Err%
GOR	132	133.35	1.023
BO	1.162	1.128	2.926
API	36.5	36.67	0.466

Appendix E

Changing the Composition Using Agualr McCain and Meshari Method				
components	mole frac	MW	wi	zi
CO2	0.0112	44.01	0.0027	0.0112
N2	0.0105	28.013	0.0016	0.0105
CH4	0.1082	16.043	0.0096	0.1082
C2H6	0.0434	30.07	0.0072	0.0434
C3H8	0.0822	44.097	0.0201	0.0822
IC4	0.0222	58.124	0.0072	0.0222
NC4	0.0641	58.124	0.0207	0.0641
IC5	0.0286	72.151	0.0114	0.0286
NC5	0.0354	72.151	0.0142	0.0354
FC6	0.0445	86	0.0212	0.0445
C7+	0.5497	290	0.8840	0.5497
Solver	MA of the fluid	180.3264777		
Changing Cell	Ma	180.3265		
	Mplus	290		

Experimental variation limit for Mw+ ($\pm 25\%$)	
Upper Limit	362
Exp . Value	290
Lower Limit	217.5